



# HHS Public Access

Author manuscript

*Chem Rev.* Author manuscript; available in PMC 2019 November 14.

Published in final edited form as:

*Chem Rev.* 2018 November 14; 118(21): 10659–10709. doi:10.1021/acs.chemrev.8b00163.

## Blue-Light Receptors for Optogenetics

**Aba Losi**<sup>1,\*,#</sup>, **Kevin H. Gardner**<sup>2,3,4,\*,#</sup>, and **Andreas Möglich**<sup>5,6,7,\*,#</sup>

<sup>1</sup>Department of Mathematical, Physical and Computer Sciences, University of Parma, Parco Area delle Scienze 7/A-43124 Parma, Italy.

<sup>2</sup>Structural Biology Initiative, CUNY Advanced Science Research Center, New York, NY 10031, USA.

<sup>3</sup>Department of Chemistry and Biochemistry, City College of New York, NY 10031, USA.

<sup>4</sup>Ph.D. Programs in Biochemistry, Chemistry and Biology, The Graduate Center of the City University of New York, New York, NY 10016, USA.

<sup>5</sup>Lehrstuhl für Biochemie, Universität Bayreuth, 95447 Bayreuth, Germany.

<sup>6</sup>Research Center for Bio-Macromolecules, Universität Bayreuth, 95447 Bayreuth, Germany.

<sup>7</sup>Bayreuth Center for Biochemistry & Molecular Biology, Universität Bayreuth, 95447 Bayreuth, Germany.

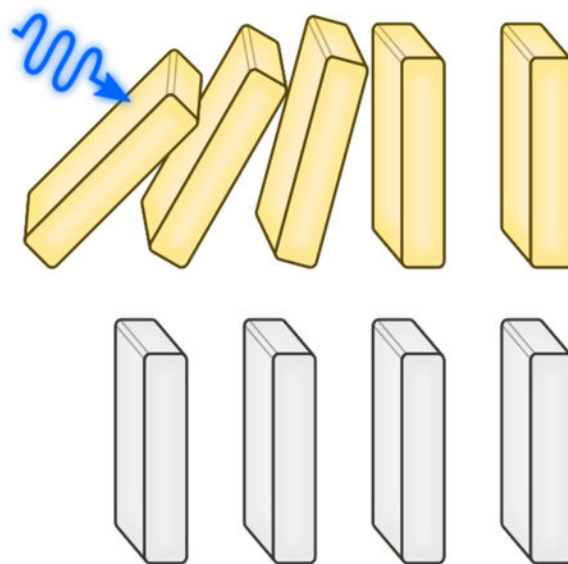
### Abstract

Sensory photoreceptors underpin light-dependent adaptations of organismal physiology, development and behavior in nature. Adapted for optogenetics, sensory photoreceptors become genetically-encoded actuators and reporters to enable the non-invasive, spatiotemporally accurate and reversible control by light of cellular processes. Rooted in a mechanistic understanding of natural photoreceptors, artificial photoreceptors with customized light-gated function have been engineered that greatly expand the scope of optogenetics beyond the original application of light-controlled ion flow. As we survey presently, UV/blue-light-sensitive photoreceptors have particularly allowed optogenetics to transcend its initial neuroscience applications by unlocking numerous additional cellular processes and parameters for optogenetic intervention, including gene expression, DNA recombination, subcellular localization, cytoskeleton dynamics, intracellular protein stability, signal transduction cascades, apoptosis and enzyme activity. The engineering of novel photoreceptors benefits from powerful and reusable design strategies, most importantly light-dependent protein association and (un)folding reactions. Additionally, modified versions of these same sensory photoreceptors serve as fluorescent proteins and generators of singlet oxygen, thereby further enriching the optogenetic toolkit. The available and upcoming UV/blue-light-sensitive actuators and reporters enable the detailed and quantitative interrogation of cellular signal networks and processes in increasingly more precise and illuminating manners.

### Graphical Abstract

\*to whom correspondence may be addressed: aba.losi@unipr.it, Kevin.Gardner@asrc.cuny.edu, andreas.moeglich@uni-bayreuth.de.

#ORCID identifiers: A.L. <http://orcid.org/0000-0003-0497-2723>, K.H.G. <http://orcid.org/0000-0002-8671-2556>, A.M. <http://orcid.org/0000-0002-7382-2772>



## 1. Introduction

The ability to sense and respond to stimuli is a basic hallmark of life. Light within the near-UV to near-infrared region of the electromagnetic spectrum represents a crucial environmental stimulus that is processed by a multitude of both sessile and motile organisms across all kingdoms of life. Beyond its role as the primary energy source in photosynthesis, light carries vital spatial and temporal information; light sensitivity thus bestows an evolutionary advantage on organisms by endowing them with a sense of where and when. Important and widespread physiological adaptations to light absorption include developmental and behavioral responses, entrainment of the diurnal rhythm and phototaxis. To utilize the information content of incident light for the regulation of biological processes, nature has evolved a plethora of so-called sensory photoreceptor proteins.<sup>1,2</sup> Notably, such sensory photoreceptors are distinct from the pigments in photosynthesis, e.g., light-harvesting complexes and photosynthetic reaction centers, and from photoenzymes,<sup>3</sup> which primarily absorb light for its energy content to drive demanding chemical reactions, e.g., the oxidative splitting of water. Sensory photoreceptors generally harbor an organic chromophore that is sensitive to certain bands within the electromagnetic spectrum. Photon absorption by the dark-adapted state of the photoreceptor initiates a series of photochemical reactions (“photocycle”) that couple the chromophore to the surrounding protein scaffold. These changes culminate in shifting the photoreceptor from the dark-adapted to the light-adapted (or, “signaling”) states, which differ in their structures, dynamics and biological activity. These conformations are often simply referred to as the ‘dark state’ and ‘lit state’. (However, we discourage denoting these as “ground” and “excited” states as these terms also refer to the electronic configuration of molecular orbitals, and it is important to note that both the dark- and light-adapted states feature chromophores that are generally electronic ground states). Usually, the photocycle is fully reversible, with the metastable signaling state spontaneously decaying in a thermal reaction back to the dark-adapted state. Based on chromophore identity and photocycle, sensory photoreceptors divide into approximately ten

different classes. Taken together, one can consider sensory photoreceptors as signal processors or transducers that convert one type of signal (light) into another (a biological response). Photoreceptors can be functionally dissected into a photosensor (“input”) module that harbors the chromophore and mediates light absorption, and an effector (“output”) module that elicits downstream physiological responses. Often, photosensor and effector moieties localize to distinct domains of the photoreceptor and can hence be physically separated into distinct parts.

The light-dependent adaptations in nature mediated by sensory photoreceptors display key desirable properties: genetic encoding, reversibility, and exquisite resolution in time and space. These benefits have made sensory photoreceptors versatile and powerful actuators for the targeted control of cellular processes and parameters. In an approach dubbed “optogenetics”,<sup>4</sup> targeted cells (or, tissues, organs or organisms) are rendered light-sensitive via the heterologous expression of suitable sensory photoreceptors. Light can then be used as a perturbatory stimulus to trigger defined physiological responses. Compared to other stimuli, e.g., addition of chemical compounds, the optogenetic approach excels in its reversibility, genetic encodability, spatiotemporal acuity and non-invasiveness. Optogenetics originated in the neurosciences, as reviewed by Bamberg, and at first solely relied on microalgal and bacterial rhodopsin photoreceptors that function as light-driven ion pumps and light-gated ion channels.<sup>5–8</sup> With these actuators in hand, ion flux across the plasma membrane either against or along the electrochemical gradient has been controlled by light, and action potentials have been elicited at will. While light-regulated ion pumps and channels continue to serve as extremely versatile and powerful actuators, the past several years have readily demonstrated the broader generality of optogenetics to many other kinds of light-regulated tools and applications.

Such advances have been enabled by protein engineering strategies that have been particularly successful for several classes of soluble photoreceptors sensitive to near-UV and blue light (BL). In this article, we chiefly consider pertinent approaches based on three types of flavin-binding, blue-light-sensitive photoreceptors that have proven most versatile for optogenetics: the Light-Oxygen-Voltage (LOV) domains,<sup>9,10</sup> the Blue Light sensors Utilizing Flavin adenine dinucleotide (BLUF) domains<sup>11,12</sup> and cryptochromes.<sup>13</sup> We will also discuss applications derived from the BL-sensitive photoactive yellow protein<sup>14</sup> (PYP, and the broader group of xanthopsins) and the UV-B-sensitive photoreceptor UVR8.<sup>15</sup> By contrast, photoreceptors from other classes are treated in the accompanying reviews by Gärtner, Bamberg, Engelhard, and Kandori on phytochromes and rhodopsins. We begin by reviewing the photochemistry, the molecular architectures and the predominant signaling strategies used by the listed UV-light/BL receptors in section 2. The mechanistic elucidation of light-dependent allostery in natural photoreceptors and their constituent modules directly informs the rational engineering of novel photoreceptors that translate desired light stimuli into customized cellular output. Although the so-far implemented photoreceptor engineering studies are diverse, a small set of particularly successful design strategies emerge, as discussed in section 3. Using naturally occurring and engineered UV-light/BL-sensitive photoreceptors, many cellular activities and parameters have been subjected to optogenetic control including gene expression, cellular cytoskeleton and motility, and signal transduction (cf. section 4.). The applications of these photoreceptors can be further expanded by

abrogating their normal photochemistry while retaining their ability to specifically incorporate their chromophores (cf. section 5.). By doing so, novel fluorescent proteins and blue-light-driven generators of singlet oxygen have been devised that further enrich the optogenetic toolkit as versatile reporters and actuators.

## 2. Blue-Light-Responsive Photoreceptors

### 2.1. Classes of Blue-light-responsive Photoreceptors

Our focus here is on photoreceptors which sense light in the UV and blue regions of the electromagnetic spectrum, roughly spanning 250-500 nm. While such proteins have very diverse origins – including disparate host organisms, kinds of biology they control, and methods used to originally identify them – they share several common themes:

- *modularity*: these photoreceptors are relatively small proteins or protein domains, often under 20 kDa in size (all except the cryptochromes and UVR8 in this chapter). These can be found in a wide variety of settings with other enzymatic and non-enzymatic effectors, either *in cis* in the same polypeptide or *in trans* with other components. While the *in cis* combinations are obviously easier to identify by sequence analyses, a substantial number of standalone “short” proteins which contain only photosensor domains suggest that many *in trans* sensor/effector pairs remain to be identified.
- *chromophores*: fundamental to photoreception are chromophores which absorb electromagnetic radiation in the appropriate section of the spectrum, using photochemical reactions of different kinds to initiate signaling processes. The bulk of the systems described in this chapter are blue-light-sensitive through the binding of flavin chromophores – flavin mononucleotide (FMN), flavin adenine dinucleotide (FAD) and riboflavin (Fig. 1) – to take advantage of their maximal absorption near 440-450 nm (and substantial absorbance across a broader range, ca. 390-490 nm) in the oxidized state. UVR8, which absorbs much shorter wavelength (UV-B, 280-315 nm) utilizes tryptophan sidechains instead of small ligands.
- *allosteric signal transmission*: the photochemical initiation of the photosensory process leads to a variety of changes in protein/chromophore interactions, sometimes including substantial configurational changes to the chromophore itself (e.g., the formation of novel covalent protein/chromophore adducts or double bond *Z/E* isomerization). These conformational transitions in the protein structure immediately surrounding the chromophores are subsequently amplified by allosteric networks within the photoreceptors. The resulting changes in protein dynamics and structure – which can be as dramatic as light-driven protein (un)folding events, protein/peptide binding interactions, and changes in quaternary structure – provide the molecular foundation of signaling in biological and engineered systems.
- *thermal reversion*: post-excitation, the light-adapted conformations of all systems detailed here will spontaneously revert back to the initial resting state upon the

cessation of illumination. The relaxation times for these processes vary widely among the different photoreceptor systems, and within specific proteins among the different families. These structure/function variations have been fruitful at both revealing insights into the mechanisms of the reversion process and enabling the rational tuning of the kinetics of such processes. Notably, the light-adapted state of certain photoreceptors can be catalyzed to revert to the dark-adapted state by illumination at wavelengths absorbed by the light-adapted state chromophores, making them photochromic switches.

**2.1.1. Light-Oxygen-Voltage (LOV) Proteins**—LOV domains were initially identified in the phototropins,<sup>9,10</sup> a group of plant and algal serine/threonine kinases activated by blue light, giving them the primary sensory role in the process of phototropism (Fig. 2). Soon afterwards, these LOV domains were discovered in fungal and bacterial systems, including transcription factors, histidine kinases and standalone “short” LOV proteins containing only the photosensor domain itself. Continuing large-scale sequencing efforts of genomic and metagenomics samples have led to over 7,000 LOV domains being identified to date.<sup>16</sup> Most of these proteins contain effectors C-terminally attached of the LOV sensor itself.

At a molecular level, LOV domains are a subset of the broader family of PAS (Period-ARNT-Single-minded) domains of environmental sensory domains.<sup>17,18</sup> All of these domains are approximately 110 amino acid residues long in their minimal forms and adopt a mixed  $\alpha/\beta$  protein fold, with several  $\alpha$ -helices located on one face of an antiparallel  $\beta$ -sheet. Many PAS domains are involved in protein/protein interactions, often regulating the strength of these interactions via the presence of small, internally-bound cofactors or ligands which have environmentally-sensitive concentrations or configurations. Different subsets of PAS domains are capable of preferentially interacting with different ligands, thus giving rise to collections of sensors specific for diverse stimuli.<sup>18</sup>

Within this broader context, LOV domains achieve their photosensory functionality via their specific binding to flavin chromophores. While FMN most commonly serves in this role, FAD and riboflavin-bound forms have also been reported in the literature.<sup>22</sup> The oxidized quinone forms of these cofactors non-covalently bind within LOV domains in the dark, nestled within the helices mentioned above. Photochemically-triggered radical chemistry<sup>23</sup> leads to the specific formation of a novel covalent adduct between the  $\gamma$  sulfur atom of a conserved cysteine residue (Cys 450 in the widely-studied *Avena sativa* phototropin 1 LOV2 domain, often referred to as “AsLOV2”) and the C4a position of the flavin isoalloxazine ring. This modification can be trivially followed by visible absorption spectroscopy, as it leads to the elimination of substantial absorption in the blue around 450 nm with a simultaneous increase in near-UV absorption around 390 nm. Coupled with the concomitant protonation of the adjacent N5 position, this change effectively serves as the photochemical trigger for a range of subsequent structural transitions. Most importantly, this includes a reversal of hydrogen bonding activity of a conserved Gln residue (Gln 513 in AsLOV2) in the LOV  $\beta$  sheet, switching it from donating an H-bond to a deprotonated N5 to accepting an H-bond from the protonated N5. In combination with other structural modifications, a wider range of larger allosteric changes are triggered. In the arguably best-known case of AsLOV2,

these changes culminate in the reversible unfolding of a C-terminal  $\alpha$  helix, termed Ja.<sup>19</sup> Subsequent work also implicated an N-terminal helix, A'  $\alpha$ , in the light-induced signal transduction process.<sup>20,24</sup> Notwithstanding the widespread use of AsLOV2 in photoreceptor engineering (detailed in section 4.), signaling in the parental plant phototropin receptor remains incompletely understood, as different experimental approaches suggest different reliance on Ja unfolding for activation of the intact receptor.<sup>25,26</sup> The photoadduct spontaneously (i.e. thermally) decays to regenerate the dark-adapted, non-covalently-bound state over a timescale of seconds to hours, depending on protein sequence and structure surrounding the chromophore.

Notably, the ample mechanistic information available for LOV domains has led to the collection of a wide range of useful point mutations that work across many comparable systems. These include residue exchanges that lock the photoreceptor in its dark-adapted state. In the corresponding “constitutively dark” variants the critical cysteine is replaced by an alanine or serine residue that is incapable of progressing through adduct formation. Of note, recent reports have shown that reduced flavins can bind into some cysteine-free LOV domains, activating these systems via a redox process rather than via light-induced formation of the covalent thioether bond.<sup>27</sup> Complementing such variants are “constitutively lit” variants that are locked in their light-adapted state, many of which replace the Gln 513 residue with an asparagine or directly perturb LOV-effector interactions. Finally, a suite of mutations is available for controlling the kinetics of the spontaneous dark-state reversion process by up to three orders of magnitude, many of which were initially inspired by variations in such rates evident in natural LOV domains.<sup>28</sup> We underscore that such mutations provide a starting point for regulating the signaling properties of any new LOV receptor, but their efficacy in doing so must be checked in each setting.

### 2.1.2. Sensors of Blue Light Using Flavin Adenine Dinucleotide (BLUF)—

Similar to the LOV receptors, BLUF domains sense blue light through flavin chromophores non-covalently bound within a mixed  $\alpha/\beta$  fold, but with substantial differences in origin and mechanism worth noting (Fig. 3). The vast majority of the presently-known ca. 900 BLUF domains are from proteobacteria, with a few notable exceptions from eukaryotic fungi and flagellates.<sup>29</sup> Most BLUF-containing proteins are “short” BLUF-only photoreceptors, although a number contain covalently attached effectors that are either enzymatic (typically involved in cyclic-nucleotide biosynthesis or degradation) or non-enzymatic (including DNA-binding).

Structurally, BLUF domains adopt a ferredoxin-type fold of about 100 amino acids, placing two  $\alpha$ - helices on one face of an antiparallel  $\beta$ -sheet.<sup>30–33</sup> Within the gap between these two helices, the isoalloxazine ring of an oxidized FAD chromophore is non-covalently bound. In contrast to the photochemistry of either the LOV domains or cryptochromes, blue light illumination near the absorption maximum at 450 nm does not elicit a change in oxidation state of the flavin. Instead, a relatively subtle electronic change is triggered, accompanied by a 10-nm red shift seen by visible absorption spectroscopy upon the dark to lit state conversion.<sup>34–36</sup> The precise nature of the BLUF signaling state is still under debate. In one model, a conserved glutamine residue is thought to undergo tautomerization of its amide side chain, thereby triggering subsequent allosteric transitions that culminate in changes

across the  $\beta$ -sheet (including a conserved Trp residue which interconverts between inward- and outward-pointing states).<sup>37–39</sup> In a competing view, the same glutamine residue is proposed to undergo a 180° flip of its sidechain and to thus elicit the described allosteric changes.<sup>35,40</sup> Given the limited light-induced structural changes that either model proposes, the relatively long persistence of the signaling state (between seconds and minutes depending upon BLUF protein) is puzzling. Regardless of the precise mechanism, the light-induced changes appear to alter flavin/protein hydrogen-bonding patterns and trigger conformational shifts across the central  $\beta$ -sheet that propagate to moderately conserved  $\alpha$ -helices on the far side and onwards to effector modules.

**2.1.3. Cryptochromes (CRYs)**—The third and final class of flavin-containing photoreceptors we cover here are the cryptochromes (Fig. 4). First postulated as a class of blue-light sensors controlling plant growth, they were subsequently found as regulators of circadian processes in mammals and insects.<sup>41</sup> While this broad group of proteins has evolved into several different phylogenetic families, all maintain a homology to the photolyase class of DNA-repair enzymes. Whereas most cryptochromes are incapable of catalyzing DNA repair, at least some representatives retain this ability.<sup>42</sup> The cryptochrome/photolyase homology displays a similar two-domain structural organization, including N-terminal  $\alpha/\beta$  and C-terminal all-helical domains, together constituting a “photolyase homology region” (PHR).<sup>43</sup> Fundamental to blue light sensing is a FAD chromophore bound within the C-terminal domain of the PHR.

Cryptochrome photochemistry is an area of active research, and some debate, at the time of this review. This contrasts with the photolyases, where three photochemical excitation mechanisms are well understood: a photophysical energy transfer from an antenna pigment to FADH<sup>-</sup>, electron transfer from the flavin to the DNA damage, and photochemical activation involving three conserved Trp residues (“Trp triad”). The applicability of either route to cryptochromes remain somewhat in question, given the apparent utilization of a flavin semiquinone in Cry signaling along with the differential effects of Trp triad mutations in signaling.<sup>46–49</sup>

Regardless of the precise activation mechanism, converting these photochemical changes to altered protein/protein interactions requires the involvement of C-terminal extensions (CRY C-termini, or “CCTs”) which vary among the cryptochromes. For the optogenetic uses detailed below, these lead to light-controlled heterotypic interactions of the cryptochromes – usually constructs of *A. thaliana* CRY2 (“AtCRY2”) encoding the PHR alone or with short CCTs – with the cryptochrome-interacting basic-helix-loop-helix proteins (“CIBs”)<sup>50</sup> involving Cry N-terminal regions or homotypic CRY:CRY interactions via CCTs.<sup>45,51–53</sup> In both cases, the dark-adapted state does not participate in these interactions while the light-adapted state does.

**2.1.4. Non-Flavin Alternatives: Xanthopsins and UVR8**—Two additional classes of soluble biological photosensors detect electromagnetic radiation in the blue and UV regions of the spectrum without using flavin chromophores: the xanthopsins, including their best-known member photoactive yellow protein (PYP),<sup>14</sup> and the plant photoreceptor UVR8.<sup>15</sup> Like the LOV domains, xanthopsins are members of the PAS domain family of

environmental sensors. While LOV and xanthopsin receptors also share the sensing of blue-light stimuli, they do so with substantially different chromophores and mechanisms. PYP and the other xanthopsins rely on 4-hydroxycinnamic acid (4-HCA, also termed *p*-coumaric acid) chromophores, attached to the photoreceptor through a thioester linkage to a conserved cysteine. Notably, this chromophore is not routinely available in most heterologous systems, necessitating either the expression of biosynthetic enzymes or feeding of precursor compounds to enable the use of PYP-based optogenetic tools in living cells. In the dark-adapted state, this covalently-tethered chromophore exhibits a *trans* configuration of the C7-C8 double bond and establishes a series of hydrogen-bond interactions to stabilize the phenolate state which absorbs in the blue (ca. 430-460 nm). Illumination with BL leads to protonation of 4-HCA and isomerization about the double bond, producing a *cis* configuration and substantial change in the structure and dynamics of the protein.<sup>54-58</sup> These principles have been best examined in PYP, a standalone photoreceptor approximately 17 kDa in size, originally isolated from halophilic bacteria and believed to be involved in a negative phototactic response to blue light.<sup>14,59</sup> As with most of the other photoreceptor types here, other xanthopsin domains have been found in a handful more complex proteins with different sensory and effector domains.

The last component we review here is UVR8, part of the UV-B (280-320 nm) response pathway in *Arabidopsis thaliana* and other plants. Initial biochemical identification of a light-dependent interaction of UVR8 with the COP1 protein in the same signaling pathway led to further biophysical characterization.<sup>15,60</sup> These studies revealed that UVR8 interconverts between a dark-adapted homodimeric state and a light-adapted monomeric state which interacts with COP1 – all strikingly without the use of any small-molecule chromophores like the flavins or hydroxycinnamic acid described above. The mechanistic basis of this phenomenon was revealed by a crystal structure of a UVR8 dark-state dimer, showing a collection of aromatic sidechains arranged in close proximity to each other at the protein/protein interface and facilitating an excitonic coupling excitation mechanism.<sup>61-63</sup> In addition, the rest of the interface involves a network of salt bridges which laid the foundation for point mutations which can be used to generate constitutively monomerized (= “constitutively lit state”) UVR8.

We note that numerous members of the rhodopsin photoreceptor family also serve as blue-light-sensitive receptors. However, as the focus of the present treatise is on the soluble classes of UV-B/BL-sensitive photoreceptors, we refer to the accompanying reviews on rhodopsin photoreceptors by Bamberg, Engelhard, and Kandori.

## 2.2. Allostery and Signal Transduction by Blue-Light-Responsive Photoreceptors

To exert control over biological function, the photochemical changes initiated at chromophores and immediately-surrounding protein residues must be relayed via allosteric pathways to affect protein conformation more globally. While a comprehensive discussion of these processes is outside the scope of this review, we can broadly categorize them into four groups:

- *Intramolecular effector release*: Light induces the release of an intramolecular interaction between the photosensory and effector domains, often converting an



autoinhibited dark state into an activated lit state. Examples include the *AsLOV2* domain mentioned above, where N- and C-terminal helices (A' $\alpha$  and J $\alpha$ ) are freed from interactions with the LOV core domain upon illumination,<sup>19</sup> thus allowing them to freely interact with other partners.

- *Rearrangement of preformed dimer/oligomer:* Commonly seen among LOV and BLUF domains, these proteins undergo light-triggered conformational changes in a dimer which exists regardless of illumination state. In these cases, rotations and/or translations between the subunits are utilized to move effectors between different functional states, as exhibited by the engineered YF1 LOV-histidine kinase system.<sup>64</sup>
- *Change in oligomerization state:* Most commonly, this involves a light-dependent change from monomer to dimer, or dimer to monomer, as observed in UVR8.<sup>60,61</sup> However, higher-order changes have also been observed in natural systems (e.g., in BLUF PixD,<sup>33</sup> and in cryptochrome photobody formation<sup>50,65</sup>), to the point that light-dependent phase separation can occur.<sup>66</sup>
- *Recruitment of heterologous partner:* A number of blue-light receptors bind to other proteins selectively in either dark- or light-adapted states. The blue-light-activated interaction observed between plant cryptochromes and the CIB1 interacting partner has been most actively used for optogenetic applications,<sup>51</sup> but other examples exist as well. A similar concept is realized in the red-light-sensitive plant phytochromes (reviewed in this issue by Gärtner) with the light-dependent recruitment of phytochrome-interacting factors (PIFs).

Notably, photoreceptors using the first two mechanisms maintain their oligomeric states upon illumination, while those using the latter two undergo substantial changes. Hence, photoreceptors can alternatively be grouped into “non-associating” and “associating” types (Fig. 5).<sup>67</sup> We underscore that several of these elementary mechanisms are often combined with each other, rather than acting individually. The UVR8 UV-B plant photoreceptor mentioned above provides an excellent example of this principle, with illumination triggering the dissociation of a dark-adapted dimer into light-adapted monomers capable of recruiting the heterotypic partner COP1;<sup>15,60,61</sup> analogously, the BLUF PixD system interacts in similarly-controlled manner with PixE.<sup>33,68</sup> Likewise, BL-induced rearrangements in the LOV proteins Vivid and EL222 lead to dimerization via the unmasking of protein segments (an N-terminal cap segment for Vivid,<sup>22,69</sup> a C-terminal helix-turn-helix DNA-binding effector for EL222<sup>21,70</sup>) from the surface of the photosensory LOV domain.

More broadly, it is important to appreciate that different members of the same family of photosensory domain can use different mechanisms from among these four groups. Similarly, different variants of the same system – such as truncations – can exhibit differences as well.<sup>25,71</sup> These idiosyncrasies stem in large part from the relatively small changes in protein structure needed to switch structural and functional states, where “off” and “on” states exhibit slightly different sets of non-covalent interactions within or between proteins. As reflected by the moderate 10- to 100-fold switches in function seen in many blue-light photoreceptor systems,<sup>67</sup> these differences translate into small energetic

differences on the order of 5-10 kJ mol<sup>-1</sup> which can be easily modulated by differences in domain context, sequence or point mutations. While this feature opens up opportunities for rational structure-based tuning of important functional parameters like background activation and dynamic range,<sup>72</sup> it also underscores the importance of validating signaling mechanisms within full-length native proteins and engineered optogenetic systems.

### 3. Photoreceptor Engineering

At a phenomenological level, biological processes responsive to light have long been known, e.g., flowering onset and tropic growth in plants, as well as diurnal rhythmicity and vision in diverse organisms. Although these and related light-dependent responses in nature already display the pertinent traits we now cherish in optogenetics, that is, genetic encoding, precision in time and space, non-invasiveness, and often reversibility (cf. sec. 1.), an analysis of the underlying light-sensitive cellular circuits, let alone their rational construction and practical application, had long been precluded. This situation changed dramatically with the molecular identification of the sensory photoreceptors underpinning many of these responses (cf. sec. 2.), which enabled more detailed study and eventual application. In a parallel key development, researchers pinpointed light as the ideal perturbatory stimulus for the acute and precise control and monitoring of living systems,<sup>73</sup> thus laying the conceptual groundwork for the later implementation of optogenetics.<sup>74</sup> Certain sensory photoreceptors, exemplified by the channelrhodopsins<sup>75,76</sup> and photoactivated adenylyl cyclases<sup>11</sup>, proved of immediate optogenetic utility upon expression in heterologous cells and organisms.<sup>5-8</sup> Not only did these naturally-occurring photoreceptors facilitate the interrogation of biological systems in unprecedented ways, but they also validated the principal concept and feasibility of optogenetics. At the same time, the molecular description of the structure of the archetypical phototropin LOV photosensor module<sup>77,78</sup> and the light-dependent allosteric transition it undergoes<sup>19</sup> constituted key events towards the engineering of novel UV-light- and BL-sensitive photoreceptors. Aside from earlier work on PYP,<sup>56</sup> these studies provided the first atomic view of how light signals are detected by a soluble, autonomously assembling photoreceptor and translated into protein structural transitions, here the reversible unfolding of the ancillary J $\alpha$  helix of the LOV photosensor. In combination with the ongoing revolutionary success of optogenetics in the neurosciences,<sup>79,80</sup> these findings provided the impetus for researchers to explore how other protein activities might be subjected to light control in genetically encodable fashion.<sup>67,81-89</sup> As we illustrate in this and the ensuing section 4., the engineering of light-regulated protein actuators that serve as tools in optogenetics has been nothing but amazingly successful. Section 3.1. considers the principal and most successful design strategies which have spawned the plethora of optogenetic actuators now available for controlling cellular metabolism and parameters (cf. sec. 4.). In the subsequent section 3.2., we discuss attributes of light-regulated actuators that are relevant for optogenetic application and that are hence often optimized during the engineering of novel photoreceptors.

#### 3.1. Optogenetic Application of Photoreceptors

**3.1.1. Applications of Natural Photoreceptors**—As a manifestation of their intrinsic modularity,<sup>16,90</sup> the photoreceptors of the BL-sensitive classes BLUF and LOV

occur in conjunction with a diverse set of effector modules, certain of which can be exploited as optogenetic actuators essentially in their naturally occurring forms. Prominent examples of this approach are LOV- and BLUF-based nucleotide cyclases (cf. sec. 4.6.1.),<sup>91</sup> and the transcriptional regulator EL222 (cf. sec. 4.1.1.).<sup>92</sup> These and a limited number of related receptors can often be optogenetically deployed in heterologous hosts with minimal prior engineering or modification. For example, the bacterial light-activated adenylate cyclase bPAC is readily expressed in animal host cells where it regulates by light cAMP-dependent processes such as the opening of cyclic-nucleotide-gated ion channels in neurons.<sup>93,94</sup> Certain properties of naturally occurring photoreceptors, e.g., photocycle dynamics or substrate specificity,<sup>94</sup> can be modified as dictated by application via the introduction of appropriate residue modifications. The considerable potential of natural BL-sensing systems has only been tapped to limited extent, often on account of practical issues such as low dynamic range (e.g., LOV-EAL and BLUF-EAL enzymes that regulate the turnover of the second messenger c-di-GMP, cf. sec. 4.6.1.), large size and unwieldy architecture (e.g., the fungal WC-1:WC-2 complex, cf. sec. 4.1.2.), or complications of using the effector output in a heterologous setting. As the number of known BL receptors continues to steadily increase, additional protein architectures and functions are likely to emerge and find application in optogenetics.<sup>16,95</sup>

**3.1.2. Engineering Novel Photoreceptors**—As diverse and ingenious as the design approaches are that underlie novel light-regulated protein actuators (detailed in section 4.), they share a common foundation in the mechanistic knowledge on naturally occurring photoreceptors. Perplexingly, this knowledge is often incomplete, a prime example being plant phototropins where the light-dependent signal transduction mechanism still awaits full elucidation.<sup>96</sup> That notwithstanding, the allosteric principles realized in natural receptors and laid out above (cf. sec. 2.), have been employed in numerous creative ways for the construction of novel photoreceptors. Despite the rich versatility of engineered optogenetic actuators now available, we identify in the following recurring themes which span natural and artificial systems (Fig. 5). Surveying these systems, we see the two broad categories of non-associating and associating forms proposed by Ziegler & Möglich<sup>67</sup> which can be further branched into detailed molecular mechanisms (Fig. 5). All of these mechanisms rely on light-triggered conformational changes that affect the activity of tethered effector domains, binding to other macromolecules, hetero- and homo-oligomerization, or compartmentalization within cells. This principle is general for the UV-light- and BL-responsive optogenetic tools treated here, with the exceptions described in section 5., e.g., derivative LOV photosensors for use as fluorophores or for production of reactive oxygen species (ROS). To enable the light-dependent control of cellular activity in scenarios where no suitable naturally-evolved photoreceptor already exists, a cohort of artificial photoreceptors has been engineered as section 4. discusses in depth. Specifically, the intrinsic modularity and mechanistic versatility of BL-sensitive photoreceptors, together with the ubiquitous availability of flavins *in vivo*, make these photoreceptors invaluable tools for a growing number of applications, including light-controlled gene expression, gene modification, protein activity and localization, and regulation of signaling networks.<sup>67,81–89</sup> Compared to the membrane-embedded rhodopsins, soluble photoreceptors necessitate different engineering strategies for optogenetics (Fig. 5),<sup>67,81,85</sup> on account of differences in

their modular organization<sup>16</sup> and allosteric signaling mechanisms.<sup>97</sup> As mentioned in section 2.2., BL-regulated actuators can be broadly classed into associating and non-associating forms. Associating photoreceptors such as *AtCRY2:AtCIB1*<sup>51</sup> usually offer predictable and successful engineering strategies when target proteins and processes are regulated via oligomerization (i.e. light-dependent recruitment and colocalization). This concept can be extended to the reconstitution of split proteins or functions relying on a two-hybrid strategy by linking one polypeptide to a photosensing module and the second one to its interacting partner.<sup>67,86,87</sup> As illustrated in section 2., physiological modes of action for associating photoreceptors are often well understood and at hand. Generally, there are minimal requirements for the linker between photosensing and effector domain(s), in that protein-protein interactions themselves drive the process. As a potential disadvantage, such association/dissociation equilibria strongly depend on several factors that may require optimization, including local concentration, self-association and limited dynamic range of the *off*-kinetics. By contrast, nonassociating photoreceptors keep their oligomeric state upon light activation, generally monomeric (e.g., *AsLOV2*)<sup>20</sup> or dimeric (e.g., *Bacillus subtilis* YtvA [*BsYtvA*]).<sup>98,99</sup> Notably, the oligomeric state that a photosensor assumes may depend on protein fragment size; for example, a construct of *A. thaliana* phototropin 1 LOV2 that included a more extended A'α helix than previously used in *AsLOV2*<sup>19,20</sup> crystallized as a homodimer.<sup>100</sup> Non-associating photoreceptors form the basis of chimeric proteins where a molecular or cellular function is put under light control by fusing light-sensing modules to various effectors. The design is in many cases inspired by the natural and variegate architecture of BL receptors, with particular emphasis on LOV proteins.<sup>16</sup> In this category, many applications explore and exploit the order-disorder transitions induced by BL-triggered detachment and unfolding of the Jα-linker in *AsLOV2*.<sup>101</sup>

Despite reasonably mature engineering strategies and many case studies to draw upon, the construction of novel light-gated actuators for optogenetic application remains challenging. To help surmount such challenges, efficient experimental and computational protocols have been devised. Whereas an exhaustive survey is beyond the current scope, we present several vignettes. At the experimental level, eventual success of photoreceptor engineering often depends on being able to create and then screen sizeable collections (or, libraries) of candidate construct variants. Techniques for generating libraries of desired size and diversity are well established in the protein-design field.<sup>102</sup> A classic approach that pertains to both associating and non-associating photoreceptors is provided by random mutagenesis, followed by efficient functional *in vitro* and *in vivo* screening, cf. below.<sup>67</sup> In particular for non-associating photoreceptors, the linker segment connecting photosensor and effector modules can severely impact on photoreceptor activity and degree of regulation by light.<sup>103–106</sup> To aid evaluation of the best length and sequence for such linkers, a strategy was designed for the construction of hybrid-gene libraries with defined linker distributions.<sup>106,107</sup> Regardless of the strategy by which candidate photoreceptor libraries are obtained, these libraries must be efficiently screened to identify the (few) variants displaying the desired property of robustly light-regulated function. Again, the protein design field has developed efficient approaches for this purpose.<sup>102,108</sup> The best-suited strategy differs on a case-by-case basis, but generally speaking, screening is most efficient if light-dependent

photoreceptor activity can be tied to cell survival, to a colorimetric or fluorogenic output, or to binding of a substrate molecule (e.g., another protein, a small molecule, or nucleic acids).

In addition to experimental protocols, new computational methods for the rational design of photoactivatable proteins can provide a solid base for the construction of optimized BL-sensitive actuators.<sup>72,86</sup> A prominent example of computationally aided design has been recently provided by Dagliyan *et al.*<sup>109</sup> Informed by molecular dynamics simulations, the *AsLOV2* photosensor was inserted into non-conserved surface loops of target proteins that are allosterically coupled to the active site of these proteins (e.g., kinases, phosphatases, guanine exchange factors). The idea was prompted by the fact that the N- and C-terminal parts of *AsLOV2* are close in space<sup>19,20</sup> and therefore suited for insertion into surface loops: light-triggered undocking of  $\text{J}\alpha$  hence imposes a larger flexibility in the spacing between the *AsLOV2* N- and C-termini, thus disordering portions of host proteins and inducing functional inhibition. With this powerful and generalizable approach, diverse photo-inhibited (PI) proteins were designed, as covered in more detail in sections 4.4. and 4.9.<sup>109</sup> We note that a related approach was proposed based on a circular permutant of PYP, obtained by linking its N- and C-termini via a short peptide. Given that this BL sensor partially unfolds at its N terminus when forming the signaling state,<sup>110</sup> this “circularization” system was proposed as a general approach to control conformation and activity of host proteins, albeit somewhat limited by the fact that PYP has a chromophore foreign to most organisms.

Other computational methods used to date include large-scale molecular dynamics simulations aimed at improving the dynamic range of BL-gated actuators by identifying key residues,<sup>111</sup> and differential network analysis.<sup>16</sup> This latter approach correctly identified several residues within the LOV core which affect a large number of distant nodes (single amino acids) and edges (connections). Importantly, this network-like behavior continues during signal transmission, in which linker regions flanking the LOV core (and particularly, connecting it to effectors) play a pivotal role. Moreover, the detailed bioinformatics analysis of more than 6,700 proteins exhibited clusters of conserved linker lengths, to some extent related to a common ancestry and to the type of effector.<sup>112</sup> The important parameter required for maintaining intact signaling is the preservation of heptad repeats in helical linkers, rendering the distribution of linker lengths in nature highly discretized, at least for some effectors.<sup>16,17,105,113</sup>

**3.1.3. Pioneering Examples of Engineered Photoreceptors**—Prior to comprehensively surveying in section 4. the UV-light- and BL-sensitive optogenetic actuators available for manipulation of cellular physiology, we start by highlighting pioneering examples of photoreceptor engineering and the general principles they exhibit. By exploiting the intrinsic modularity of LOV receptors and their light-controlled changes in protein structure or oligomerization, several useful types of chimeric proteins were devised. The first example linked the *AsLOV2* domain to the *E. coli* Trp repressor protein (TrpR) to build a light-regulated DNA-binding protein (cf. sec. 4.1.1.), thereby making use of the light-induced undocking of the  $\text{J}\alpha$  helix as an allosteric photoswitch.<sup>104</sup> Initially, the degree of light activation in the *AsLOV2*-TrpR hybrid protein was modest due to the docked-undocked equilibrium of  $\text{J}\alpha$  being shifted towards the undocked state, thus rendering the protein mostly functionally active even in the dark. Subsequent introduction of residue

exchanges which increased LOV2–J $\alpha$  affinity in the dark led to a considerable improvement in dynamic range of light regulation, thereby paving the general way to enhanced LOV-based actuators.<sup>72</sup> The light-induced unfolding of the *As*LOV2 J $\alpha$  helix also provided the foundation for a photo-activatable form of the small GTPase Rac1 that served to control cytoskeletal dynamics by BL (cf. sec. 4.4.1.).<sup>103</sup> To subject Rac1 activity to BL control, the GTPase was linked to *As*LOV2 such that steric occlusion resulted in the dark but could be relieved upon illumination. Another LOV protein, FKF1 from *A. thaliana*, was used to develop the light-activated-dimerization (LAD) technology which capitalizes on the light-activated binding of *A*tFKF1 to its interacting protein GIGANTEA (*A*tGI).<sup>114</sup> Using LAD, Rac1 could be recruited to the cell membrane via a membrane-anchored GI, thus eliciting cytoskeletal rearrangements upon BL (cf. sec. 4.4.1.). The LAD system was also adapted to generate a light-activated transcription factor (cf. sec. 4.1.2.).<sup>114</sup> A major drawback of the *A*tFKF1:*A*tGI dimerizing system was the slow kinetics of association (tens of minutes) and, especially, of dissociation (tens of hours). This latter aspect rendered the interaction effectively irreversible on most physiologically relevant timescales, underscoring the importance of *off*-kinetics.<sup>28</sup> In another early application, the LOV domain of *Bs*YtvA replaced the O<sub>2</sub>-sensing PAS-B domain of the histidine kinase FixL from *Bradyrhizobium japonicum*, thus generating the hybrid YF1 protein (cf. sec. 4.1.1.).<sup>105</sup> BL regulation of histidine-kinase activity in the constitutively dimeric YF1<sup>115</sup> apparently relies on left-handed supercoiling of a coiled-coil linker between photosensor and effector, which in turn induces internal repositioning within the effector unit.<sup>64</sup>

CRYs came into optogenetics as an alternative option for BL-induced dimerization (cf. sec. 4., esp. sec. 4.1.2.). By fusing proteins of interest (or, parts of split proteins) to either *A*tCRY2 or its partner *A*tCIB1, it was possible to control gene expression and subcellular protein localization.<sup>51</sup> Heterodimerization of *A*tCRY2:*A*tCIB1 occurred significantly faster (in seconds) than with *A*tFKF1:*A*tGI, whereas dissociation was in the minutes range. Importantly it was demonstrated that the PHR domain of *A*tCRY2 suffices for forming heterodimers with full-length CIB1 or a truncated version lacking the basic helix-loop-helix DNA-binding domain, and that the system could also be triggered with two-photon excitation at 860 nm.<sup>51</sup> Beyond heterodimerization with *A*tCIB1, the *A*tCRY2-PHR domain can also independently homooligomerize to give large clusters, within a few seconds after illumination.<sup>65</sup> PYP was first fused to the basic-zipper protein GCN4, in an attempt to put under light control the binding of GCN4-PYP to DNA (cf. sec. 4.1.2.).<sup>116</sup> The weak, two-fold increase in DNA affinity induced by BL was later improved to some extent by mutations.<sup>117</sup> In a further application the N- and C-terminal ends of PYP were linked by means of a short peptide, introducing into BL-regulated actuators the concept of caging by circularization as a strategy for light-dependent control (cf. sec. 3.1.2.).<sup>110</sup>

### 3.2. Traits in Photoreceptor Engineering

The performance and eventual success of UV-light-/BL-sensitive actuators within a specific application setting depend on several aspects including genetic encoding, spatial and temporal resolution, light sensitivity and magnitude of light-induced effect,<sup>67,81</sup> as summarized below. The photoreceptor engineering (cf. sec. 3.1.) and implementation stages commonly strive to optimize performance regarding these parameters. Because these

considerations generally apply to optogenetics, they have been recently discussed in detail.<sup>67,81</sup> In the present article, we mainly focus on sensory photoreceptors themselves and their engineering, and hence only touch upon these practical aspects.

**3.2.1. Genetic Encoding and Spatial Resolution**—Genetic encodability is usually a given for the three flavin-based photoreceptor classes (LOV, BLUF, CRY) because upon expression and folding *in situ* they autonomously incorporate their flavin chromophores which universally occur as essential metabolic cofactors. A quantitative analysis revealed riboflavin, FMN and FAD to be present in mammalian cell lines in attomole quantities per cell.<sup>118</sup> The ready tissue availability of flavin chromophores contrasts with the situation for several other photoreceptor families, specifically the xanthopsin and many bilin-based photoreceptors, which require chromophores that are specific to certain organisms and that hence need be added exogenously to assemble the functional holo receptor in a heterologous cell context.

Spatial control in optogenetics is commonly exerted at the levels of gene expression and illumination protocols. For the former, tailored gene-delivery methods and specific promoters can target the expression of photoreceptors (and hence, light sensitivity) to specific cells, cell types, tissues or organs. Moreover, flavin-based photoreceptors have been successfully directed to different cellular compartments<sup>119</sup> and organelles to achieve subcellular spatial resolution. An additional layer of spatial control can be achieved by using spatially confined light (as opposed to wide-field illumination) to specifically actuate photoreceptors within a given region of interest. Depending upon photoreceptor, the targeted cellular process and the timeframe of the experiment, diffusive events post illumination can degrade the attainable spatial resolution. In contrast to chemical means of controlling cellular metabolism, optogenetics at least offers the benefit of using a trigger, i.e. light, which is not diffusive itself, although light scattering may limit the achievable spatial resolution.

**3.2.2. Light Sensitivity**—Compared to other photoreceptor classes, UV-light/BL receptors are generally sensitive to relatively short wavelengths and feature low absorption cross sections, e.g.,  $\epsilon_{450} = 12,500 \text{ M}^{-1} \text{ cm}^{-1}$  for FMN in water<sup>120</sup>, or  $\epsilon_{280} \approx 5,500 \text{ M}^{-1} \text{ cm}^{-1}$  for the tryptophan indole group. A potential impediment to optogenetic application stems from light of short wavelengths not penetrating living tissue as deeply as red/near-infrared light does.<sup>67,121,122</sup> Moreover, UV and blue light are potentially phototoxic because of absorption by endogenous photosensitizers for reactive oxygen species, such as flavins themselves (cf. sec. 5.) and iron-free porphyrins.<sup>123</sup> In some studies, the shallow tissue penetration and phototoxicity of BL was bypassed by two-photon excitation or by using upconverting nanoparticles to convert near-infrared light into visible light, but the latter approach suffers from the need of delivering the particles to target sites.<sup>87,124,125</sup> On the other hand, BL-responsive optogenetic circuits are largely insensitive to wavelengths larger than 500 nm and can hence be readily combined with fluorescent reporters with more red-shifted absorption spectra. This offers a particular advantage if an experiment requires just a short perturbation via BL excitation, while long-term effects can be probed with a red-absorbing reporter.

Short of introducing chemically-modified chromophores,<sup>126</sup> the tuning of the spectral sensitivity of flavin-binding photoreceptors has proven to be a very difficult task.<sup>123</sup> As a case in point, in the *BsYtvA* LOV receptor, the absorption maxima of the dark-adapted state ranged between 445 and 448 nm across a wide range of protein variants bearing different residue exchanges near the chromophore.<sup>127</sup> Owing to the rigid scaffold of the flavin isoalloxazine ring, the tuning of absorption of flavin chromophores in their oxidized quinone state to substantially longer wavelengths, let alone to the attractive near-infrared ‘transparent’ window (650–900 nm) where light readily penetrates mammalian tissue,<sup>121,122</sup> is likely impossible.<sup>123,128,129</sup> By contrast, the partially reduced semiquinone radical states of flavin chromophores are known to absorb at longer wavelengths.<sup>130</sup> Recently, an animal-type cryptochrome from *Chlamydomonas reinhardtii* has extended the spectral range of BL receptors to yellow and red light, given that its dark-adapted state contains the neutral semiquinone radical form of FAD.<sup>131–133</sup> It is currently unclear if this is a rare exception and whether flavin-binding photoreceptors can be deliberately modified to assume a partially reduced flavin in their dark-adapted states, cf. sec. 5.

**3.2.3. In Situ Activity and Dynamic Range**—The *in situ* activity of an optogenetic actuator and accordingly the response of the system under study will depend on the applied light dose, as well as on the expression levels, the spatiotemporal distribution and the specific activity of the underlying photoreceptor.<sup>67</sup> As cellular circuits often display threshold and amplification effects, the system response to optogenetic perturbation may be highly nonlinear and hence its quantitative prediction challenging. This particularly applies to actuators embedded in signaling cascades that amplify the response, e.g., for enzymes engaged in second-messenger signaling, cf. sec. 4.6. Likewise, this is true for associating photoreceptors, e.g., in case of BL-induced clustering of *AiCRY2*, the response of which is expected to display a strong dependence on the spatiotemporal concentration of activated receptor.<sup>67</sup>

Beyond the overall activity, the difference in activity between the dark-adapted and light-adapted states of photoreceptors and derived optogenetic circuits is of prime interest. Commonly, the ratio of activities in these two states is referred to as the dynamic range, and photoreceptor engineering often attempts to maximize this quantity. The maximally achievable dynamic range is strongly governed by how well activity can be suspended in the low-activity state of a receptor, i.e. in darkness for light-activated actuators, or under light for light-repressed receptors.<sup>67</sup> Whereas the membrane-integral rhodopsin photoreceptors often feature exquisitely low dark-state activities and accordingly high dynamic ranges, e.g., references<sup>75,134,135</sup>, the soluble BL-sensitive photoreceptors frequently display substantial residual activity in their low-activity state and correspondingly smaller dynamic ranges. As previously discussed in a thermodynamic framework,<sup>67</sup> these soluble photoreceptors fundamentally rely on equilibria between low-activity and high-activity conformations<sup>136</sup> which are modulated by illumination.<sup>101</sup> Put another way, BL receptors usually do not behave as digital on/off switches but as analog switches. Non-binary switching of optogenetic circuits may incur high dark-state (background) activity and limited extent of activation by illumination. Potentially, the energy content in visible light, e.g., ca. 250–300 kJ mol<sup>-1</sup> for BL in the range of 480 to 400 nm, suffices to substantially shift the equilibrium



between low- and high-activity states and to thereby achieve much larger dynamic range. However, to the extent it is known, only a fraction of the photon energy is converted into useable free energy changes ( $G$ ). For example, the unfolding of the Ja helix in the widely-used AsLOV2 photosensor is associated with a  $G$  of only around  $16 \text{ kJ mol}^{-1}$ , and accordingly the maximally achievable dynamic range is inherently limited.<sup>67,101</sup> Notably, judiciously-chosen residue exchanges within the photosensor can shift the equilibrium between low- and high-activity states and hence the attainable dynamic range.<sup>67,72,101</sup> In addition, dynamic range may be enhanced by embedding photoreceptors into signaling cascades or by exploiting cooperativity effects in oligomeric receptors.<sup>105,137</sup>

**3.2.4. Temporal Resolution**—Depending on the timescale of biological processes one desires to interrogate, the kinetics of activation and deactivation of optogenetic circuits are relevant. Generally, photoreceptor activation occurs well under a second, making it fast compared to many cellular events (excepting the millisecond and faster timescale processes common in the neurosciences). For example, the detachment and unfolding of Ja in AsLOV2 is complete within 0.3-1.0 ms.<sup>138-141</sup> Comparable structural perturbations in associating photoreceptor systems are equally fast, occurring on the sub-millisecond timescale in plant cryptochromes.<sup>142-144</sup> Similarly, the photodissociation of multimeric BLUF proteins takes place within 4 to 45 ms,<sup>145-147</sup> and the light-induced dimerization of *Neurospora crassa* Vivid (*NcVivid*) is complete within 20 ms, compatible with a diffusion-limited process under the conditions tested.<sup>148</sup> As such, aspects other than the inherent photochemical mechanisms typically limit the *on*-kinetics with which an optogenetic response can be triggered. For example, light is strongly absorbed and scattered by tissue, cf. sec. 3.2.2., and hence in some scenarios only a relatively low dose may effectively be delivered to the target site. As a corollary, the accumulation of sufficient amounts of activated photoreceptor molecules in time and space to trigger the desired physiological response, cf. threshold effects mentioned above, can become time-limiting. Furthermore, the triggered cellular function may be inherently slow, e.g., gene expression, thus limiting response dynamics.

In addition to the activation kinetics, the *off*-kinetics with which an optogenetic circuit deactivates once illumination ceases greatly bear on optogenetic application. As detailed in section 2., photoexcitation of BL-sensitive and UV-sensitive photoreceptors leads to population of a metastable signaling state that thermally (i.e. passively) decays back to the dark-adapted state with kinetics that are governed by receptor identity, solvent accessibility and environment of the chromophore, oxygen concentrations and temperature.<sup>28,97,123,149-153</sup> A range of residue exchanges modulating these dark-recovery kinetics have been identified, especially for LOV proteins.<sup>28</sup> To a considerable extent, such exchanges are transferable between related photoreceptors and thus provide a ready means of adjusting recovery kinetics for a given optogenetic application. As a word of caution, we note that such exchanges can potentially impair proper signal transduction within the photoreceptor,<sup>154</sup> as is the case for a conserved glutamine in LOV domains<sup>152,155</sup> or for hydrogen-bond forming histidines in cryptochromes.<sup>156</sup> Faster *off*-kinetics and resultant enhancement of the temporal resolution can be effected by photochromic photoreceptors that are toggled back and forth between two photochemical and activity states by light of different colors.

Photochromicity is a general feature of bilin-based photoreceptors (reviewed by Gärtner) and frequently occurs among rhodopsins. By contrast, BL-sensitive photoreceptors are usually not photochromic. However, we note that the covalent thioether bond formed in LOV receptors upon BL absorption (cf. sec. 2.) can be photolyzed by UV-A/violet radiation.<sup>157–159</sup> Due to the low quantum yield for this process and the requirement for potentially phototoxic UV-A/violet illumination, this effect has to date not been taken up in optogenetic applications. In cryptochrome photoreceptors, BL absorption leads to population of the partially reduced semiquinone radical state of the flavin chromophore (cf. sec. 2.1.3.). At least in certain cases,<sup>131,160</sup> secondary absorption of photons between 450 and 600 nm promotes complete reduction to the hydroquinone state and thereby toggles the effector output of the photoreceptor.

Optogenetic experiments often resort to prolonged illumination, such that photoreceptors undergo repeated cycles of photoactivation to their light-adapted states and thermal recovery to their dark-adapted states. As a consequence, a photostationary state is assumed in which on average a constant fraction of the photoreceptor ensemble resides in its dark-adapted state and the remainder in the signaling state. While the absolute light sensitivity of a photoreceptor (cf. sec. 3.2.2.) cannot be modified much, the effective light sensitivity at photostationary state can be conveniently modified by altering recovery kinetics via the above strategies.<sup>67</sup> Knowledge of the recovery kinetics of a given optogenetic circuit can be exploited for the optimization of illumination protocols and for the parallel deployment of actuators that respond to the same light color but differ in their sensitivity.<sup>161</sup>

#### 4. Photoreceptors as Actuators in Optogenetics

Galvanized by the ready and far-reaching impact of the initial optogenetic applications in the neurosciences<sup>5–8</sup> that employed rhodopsin photoreceptors to act on membrane potential,<sup>75,76</sup> researchers also explored the suitability of other photoreceptor classes for optogenetics. To this end, a small set of naturally-occurring photoreceptors with immediate optogenetic applicability have been complemented by a much larger suite of engineered photoreceptors devised by the strategies covered in section 3.<sup>67,81–89</sup> To date, these engineering efforts have been most successful with blue-light-sensitive photoreceptors, particularly in the cryptochrome and LOV classes. As discussed in this section, natural and engineered UV- and BL-sensitive photoreceptors together have now unlocked numerous cellular parameters and processes for optogenetic intervention, including protein-protein interactions, transcription (sec. 4.1.), recombination and epigenetic modification (sec. 4.2.), subcellular localization (sec. 4.3.), cytoskeleton dynamics (sec. 4.4.), protein stability (sec. 4.5.), signaling by second messengers (sec. 4.6.), receptor signaling (sec. 4.7.), apoptosis (sec. 4.8.), enzyme activity (sec. 4.9.), and membrane potential (sec. 4.10.) (Fig. 6).

Moreover, as we illustrate in section 5., photoreceptor proteins, once suitably conditioned, are not only restricted to their conventional role of regulating effector output in response to light, but can also serve other purposes. Pertinent applications generally exploit the genetic encodability of photoreceptor proteins and their ability to autonomously and specifically bind their respective chromophores, even within living cells. In this manner, several flavin-based photoreceptor variants have been developed that function as fluorescent proteins or as

light-driven generators of reactive oxygen species. Among the UV-B/BL-sensitive receptors, these ‘off-label’ applications have to date been realized for LOV receptors, but conceptually they should extend to at least the other flavin-based photoreceptors, too. Moreover, there is mounting evidence that flavin-based photoreceptors can double as sensors of intracellular oxygen and redox potential under physiological conditions, and we discuss both the intended and the unintended implications of these properties.

In the following, we survey cellular processes and parameters which have been controlled by light via optogenetic actuators based on the UV-/blue-light-sensitive photoreceptors introduced in section 2. (Fig. 6). We loosely group these applications and photoreceptors based on the cellular process targeted. In doing so, we focus on the original development and initial optogenetic application(s) of a given photoreceptor, as a comprehensive treatise of each subsequent application of each tool is beyond the scope of the current review. For an up-to-date overview, we refer to a web resource that records available optogenetic actuators in incremental manner.<sup>162</sup> On the whole, the optogenetic deployment of blue-light-sensitive photoreceptors displays impressive versatility and ingenuity of the approaches chosen. As perhaps best exemplified by the recurring use of the *AsLOV2* domain, even a single photosensor unit can be configured such that it regulates by light the activity of a broad palette of highly disparate effectors. Evidently, the underlying allosteric principles of light-dependent signal transduction, treated in sections 2. and 3., far transcend sensor-effector combinations realized in nature and can be extended to even completely unrelated effector moieties.

#### 4.1. Transcription

Going by the sheer number of different examples, the regulation of gene expression by light represents one of the most successful optogenetic application areas afforded by BL-sensitive photoreceptors. Most often, control over gene expression is exerted at the level of transcription initiation, but select photoreceptors intervene in later stages as well. There are at least three principal reasons for the relative popularity of light-regulated transcription: first, gene expression is of profound biological significance and lends itself as a highly versatile leverage point for optogenetic intervention; second, the biological process of transcription is well understood and many transcription factors (TF) are inherently modular which benefits photoreceptor engineering (cf. sec. 3.); third, expression of (fluorescent) reporter genes provides a ready means for engineering and optimizing novel photoreceptors, cf. sec. 3.1.2. Light-gated actuators have been constructed for the regulation of transcription initiation in both prokaryotes and eukaryotes, and we will cover them in turn. Certain representatives straddle this divide in that they are of optogenetic utility in both domains of life.

**4.1.1. Prokaryotic Transcription**—In one of the earliest examples of photoreceptor engineering, the activity of the *E. coli* Trp repressor (TrpR) was put under light control by fusing its N-terminal helix with the C-terminal J $\alpha$  helix of the *AsLOV2* module<sup>104</sup> such that steric overlap would result between the two entities (Fig. 7), cf. sec. 3.1.3. Within such fusions, the TrpR and *AsLOV2* domains thus engage in a tug-of-war for the intervening J $\alpha$  linker helix. As the J $\alpha$  conformation and its affinity for the *AsLOV2* core are modulated by

light, the correct folding and function of TrpR is thus regulated. Fusion constructs between TrpR and *AsLOV2* were prepared according to this rationale and tested for light-regulated binding to the TrpR DNA operator sequence in nuclease-protection assays. In one variant, denoted LOVTAP, DNA affinity was enhanced by ~6-fold by BL. While subsequent stabilization of the *AsLOV2:Ja* interface by site-directed mutagenesis<sup>72</sup> improved the dark/light difference in DNA affinity to around 65-fold, LOVTAP has not been widely deployed, arguably because its DNA affinity is much weaker than that of wild-type (wt) TrpR.

Complementing this fusion approach, domain-exchange strategies into existing transcriptional control systems have also been successful. In the most highly used application of this approach, the YF1 light-regulated sensor histidine kinase (SHK) was generated<sup>105</sup> by replacing the oxygen-sensitive PAS-B sensor domain of the *B. japonicum* FixL SHK by the structurally homologous LOV photosensor of *B. subtilis* YtvA (Fig. 7).<sup>168</sup> Notably, SHKs form part of two-component systems (TCS)<sup>169</sup> that mediate transcriptional responses to cognate stimuli in bacteria and in certain plants and fungi, and the architecture of YF1 closely corresponds to that of naturally occurring LOV-SHKs.<sup>16,170–172</sup> Net phosphorylation of the cognate response regulator *BjFixJ* by YF1 was repressed by more than 1000-fold in blue light compared to in darkness. Two portable plasmids, denoted pDusk and pDawn, assembled on the basis of YF1 and *BjFixJ*, afford BL-activated and BL-repressed gene expression, respectively, and have been widely used.<sup>107,173–176</sup> A derivative version of YF1, that combined the original PAS-B domain of *BjFixL* with *BsYtvA*-LOV rather than replacing it, integrated the signals blue light and molecular oxygen in positive cooperative manner.<sup>137</sup> Catalytic activity and response to light of YF1 variants crucially depended on the length of the linker that connects sensor and effector moieties and that adopts parallel  $\alpha$ -helical coiled-coil conformation in the dimeric receptor.<sup>105,106</sup> This dependence on linker length hinted at the structural mechanism for signal transduction in YF1 which was recently borne out in biophysical measurements.<sup>64,177,178</sup> BL absorption evidently promotes left-handed supercoiling of the coiled-coil linker, thereby triggering reconfiguration of the effector module. Insertion of single residues in said linker sufficed for inversion of the response to light,<sup>105,106</sup> as did certain residue exchanges within the LOV sensor.<sup>115,179</sup> Whereas canonical SHKs, such as YF1, adopt homodimeric structure, a *bona fide* monomeric LOV-SHK, denoted EL346, was discovered in the marine bacterium *Erythrobacter litoralis* (Fig. 7).<sup>163</sup> In EL346, a LOV photosensor forms an intramolecular complex with the effector moiety; upon light absorption, this complex dissociates, the effector is liberated and its activity increased for both autophosphorylation and phosphotransfer to cognate response regulators.<sup>163,170,180,181</sup> EL346 represents an important paradigm for SHKs and LOV receptors alike and could be used as a light-gated actuator in optogenetics, but to date it has not been deployed in this manner.

Two other BL-sensitive photoreceptor systems afford a simpler architecture than the above TCSs in that they are realized as single protein entities. First, in the EL222 receptor, also from *E. litoralis*, a LOV photosensor associates intramolecularly with a helix-turn-helix effector via a helical connector (Fig. 7).<sup>21</sup> Light absorption promotes dissociation of the effector from the LOV sensor and allows receptor dimerization. In its dimeric state, EL222 binds to a cognate operator sequence to activate transcription from the corresponding genetic loci.<sup>182</sup> As discussed below, EL222 underpins an efficient system for light-activated gene

expression in eukaryotes,<sup>92</sup> but more recently it was also deployed in *E. coli*.<sup>183</sup> By placing the cognate operator sequence at different positions relative to the –35 and –10 regions of bacterial promoters, EL222 either served as a light-activated transcriptional activator or repressor. This approach recently provided the basis for a cell-free optogenetic expression system.<sup>184</sup> Second, a light-regulated transcriptional repressor, termed LEVI, was generated through fusion of the *E. coli* LexA repressor with the *NcVivid* LOV sensor,<sup>164</sup> conceptually similar to the LightON system (cf. below) which affords light-activated gene expression in eukaryotes (Fig. 7).<sup>185</sup> In LEVI, the LexA effector was truncated such that it lost its ability to dimerize and to bind to DNA; light-promoted association of *NcVivid* rescued dimerization, DNA binding and transcriptional repression. The LEVI system excelled in its compact architecture and highly stringent response to blue light.

Recently, bacterial expression was also optogenetically regulated at the level of the RNA polymerase itself. In two closely similar approaches,<sup>166,167</sup> the phage T7 polymerase was split into two fragments which could be reconstituted in BL-activated manner by linking the split parts to the LOV-based Magnets photoreceptors for heterodimerization (Fig. 7).<sup>165</sup> By varying the split site within the T7 polymerase and the (relative) abundancies of the resultant fragments, expression of target genes could be induced by BL by up to several hundredfold. As the wild-type T7 polymerase can be functionally expressed in mammalian cells,<sup>186</sup> the split, BL-regulated variants may also unlock optogenetic control of transcription in eukaryotic cells.

**4.1.2. Eukaryotic Transcription**—Natural BL-regulated transcription factors have been identified in several eukaryotic organisms, most prominently the fungal white-collar (WC) proteins, e.g., from *N. crassa*,<sup>187</sup> and the aureochromes, first identified in stramenopile algae<sup>188</sup> but later also in diatoms. The fungal WC system is involved in regulating circadian rhythm in response to BL and consists of several components. One protein, WC-1, comprises a LOV sensor and a zinc finger DNA-binding domain (DBD). Upon light absorption, WC-1 forms a heterodimeric complex with WC-2 which also contains a zinc finger but lacks a LOV photosensor. The WC-1:WC-2 complex can then bind to cognate operator sequences and activate transcription from associated promoters.<sup>187</sup> Activation of the WC complex drives the expression of several genes, including one encoding another LOV receptor (*NcVivid*) that also contributes to light adaptation. Despite its relatively early discovery and functional annotation, the WC system has not been widely deployed in optogenetics, presumably because of the heterodimeric nature of the system and the considerable size of its constitutive components. By contrast, aureochromes<sup>188</sup> feature a more compact architecture with a basic-zipper DNA-binding module succeeded by a LOV photosensor domain. In the alga *Vaucheria frigida*, two aureochrome receptors regulate development and morphogenesis in response to BL. Although no endogenous operators/promoters have been reported, an artificially-selected DNA consensus sequence was identified from a random pool of DNA fragments that the aureochromes bind to. Sequence homology searches also identified aureochrome receptors in diatoms, e.g., in *Phaeodactylum tricoratum* and *Thalassiosira pseudonana*.<sup>188</sup> The isolated LOV photosensors of several aureochromes have been shown to undergo light-regulated homodimerization,<sup>189</sup> prompting their subsequent use as building blocks in photoreceptor engineering.<sup>190</sup> By contrast, intact

aureochromes themselves have not yet played a significant role in optogenetic applications despite their small size (perhaps due to the limited degree of light-dependent switching of DNA binding affinity<sup>191,192</sup>).

To address the need for efficient light-regulated gene expression in eukaryotes, a cohort of photoreceptor systems, many of which respond to blue light, have been engineered. Following its original characterization<sup>21</sup> and identification of its DNA target sequences,<sup>182</sup> the prokaryotic LOV receptor EL222 has been converted into an eukaryotic transcription factor via C-terminal appendage of a viral *trans*-activating domain (*tAD*) (Fig. 8A).<sup>92</sup> The expression of transgenes from promoters that contained several repeats of the EL222 target operator sequence could be upregulated by more than 100-fold by BL illumination. For applications in zebrafish, an optimized version of the system with lower cytotoxicity was developed by exchanging the *tAD* for another.<sup>197</sup> Recently, light-regulated gene expression via EL222-*tAD* in yeast was deployed in single cells<sup>453</sup> or to optogenetically control metabolic flux in bulk culture.<sup>198</sup> Application of BL induced yeast cells to switch from growth to production phase at desired time points and thus enabled the overall increase of biosynthesis yields by several folds. While EL222 has essentially been used as an intact protein as provided by nature, other systems for light-regulated gene expression generally recombine photosensor, *tAD* and DNA-binding modules. As a case in point, in the LightON approach a truncated Gal4 DBD, the *NcVivid* LOV photosensor and a *tAD* were fused to yield a monomeric chimera, denoted GAVPO, that in darkness had low affinity for the Gal operator sequence (Fig. 8A). BL absorption by the *NcVivid* photosensor domain triggered dimerization of the chimeric receptor and thereby restored DNA affinity. Using GAVPO, transgenes could be expressed in strongly BL-regulated manner from promoters that contained several copies of the Gal operator sequence. In mammalian cell culture, upregulation of luminescent reporters by several hundredfold was achieved, and the LightON system also showed good performance in a mouse model. Introduction of a mutation in the *NcVivid* LOV domain that increases dimerization propensity yielded a variant of GAVPO that supported higher absolute transgene expression levels, albeit at the cost of a reduced dynamic range by increased dark-state binding.<sup>199</sup> Whereas EL222 and GAVPO are single polypeptide chain designs, several other systems for light-regulated gene expression rely on a two-hybrid strategy, employing split transcription factors that are composed of two separate polypeptide components. Although details differ, these systems generally utilize photoreceptor pairs that undergo light-driven association/dissociation reactions involving separate DNA-binding and transcriptional-activation components (Fig. 8B). Light prompts association of the two components and thereby recruits the *tAD* to the DNA site specified by the DBD, and transcription is initiated. An early implementation, denoted light-activated dimerization (LAD), of this concept was achieved on the basis of the LOV receptor FKF1 from *Arabidopsis thaliana* that associates with its partner protein GIGANTEA (*AtGI*), or N-terminal fragments thereof, under blue light,<sup>114</sup> cf. sec. 3.1.3. When fused to the Gal4 DBD and a viral *tAD*, respectively, the *AtGI:AtFKF1* pair enabled expression of transgenes in mammalian cells that could be enhanced by BL by up to around 5-fold. Of note, this BL-induced activation of expression was essentially irreversible on physiologically relevant time scales due to the exceedingly slow dark-recovery reaction of the *AtFKF1* LOV receptor.<sup>200</sup> Recently, the performance of this system for light-regulated

gene expression was significantly enhanced by random mutagenesis of *A $\alpha$ FKF1* and construct optimization. The improved setup enabled transgene expression in cell culture and in mice that could be upregulated under BL by around two orders of magnitude.<sup>201</sup> In a different LOV-based strategy, Lungu *et al.*<sup>202</sup> interwove short peptide epitopes in the Ja helix of *AsLOV2* such that upon light-induced unfolding of Ja, they become more accessible and able to specifically bind to partner proteins. The modified *AsLOV2* sensor and the partner protein were connected to the DBD and *tAD* of Gal4, respectively, to furnish a system that achieved around 10-fold upregulation of a reporter gene in yeast under BL. Although not implemented yet, the performance of the gene-expression system could conceivably be improved by resorting to enhanced versions of the *AsLOV2*-based, photo-associating protein pair that were developed in a later study.<sup>203</sup>

Other systems for light-regulated gene expression have been based on cryptochromes, most notably cryptochrome 2 from *Arabidopsis thaliana* (*AtCRY2*). As discussed in section 3., *AtCRY2* undergoes light-dependent association with the full-length *AtCIB1* protein or N-terminal parts of it.<sup>50</sup> (Unless explicitly stated otherwise, in the following the abbreviation *AtCIB1* refers to the N-terminal fragment of the protein. Likewise, the abbreviation *AtCRY2* denotes the N-terminal PHR portion rather than the entire protein.) Early on,<sup>51</sup> the *AtCRY2:AtCIB1* pair was linked with the DBD and *tAD* of Gal4, respectively, to drive gene expression of transgenes in yeast that could be strongly upregulated by blue light (Fig. 8B). Unexpectedly, the same system failed to achieve meaningful degrees of light-regulated gene expression when applied in mammalian cells.<sup>196</sup> A careful investigation revealed that blue light promotes clearing from the nucleus of the *AtCRY2*-DBD that could eventually be pinpointed to the presence of a dimerization motif within the DBD. Removal of this dimerization motif abolished BL-induced nuclear export of *AtCRY2*-DBD and, in combination with *AtCIB1-tAD*, enabled robust BL-activated gene expression; variation of the *tAD* further enhanced the system up to more than 100-fold induction by BL. In addition, Tucker and colleagues realized that the phenomenon of BL-induced nuclear clearing can be capitalized on and devised a single-chain transcription factor that comprised DBD, *AtCRY2* and *tAD* modules (Fig. 8C). In the dark, this TF predominantly resided in the nucleus and drove expression of transgenes, but upon illumination with blue light, it translocated to the cytosol, and expression could hence be repressed by up to 50-fold. Similar to the original approach by Kennedy *et al.*,<sup>51</sup> a system for light-regulated gene expression in zebrafish was established by connecting *AtCRY2* and *AtCIB1* to the DBD and *tAD* of Gal4, respectively.<sup>193</sup> Interestingly and in line with the above work, the performance of the system in zebrafish lagged behind that in yeast. In a related setup,<sup>204</sup> *AtCIB1* and *AtCRY2* were fused to the LexA-DBD and a *tAD*, respectively, to allow BL-induced expression of transgenes in *Drosophila*. In a similar vein, *AtCIB1* was combined with the widely used TetR-DBD to enable BL-induced recruitment of *AtCRY2* connected to a strong *tAD* that enabled transcriptional activation of target transgenes.<sup>205</sup> Because the TetR-DBD has been widely employed in cell biology, this implementation of the *AtCIB1:AtCRY2* system unlocks scores of additional systems for optogenetic intervention.

As these examples compellingly illustrate, the performance and function of light-regulated gene expression systems may drastically vary between hosts and contexts, often for (initially) poorly understood reasons. As it is challenging to systematically compare the

various systems, let alone in a number of heterologous host systems, only few efforts have been undertaken to this end.<sup>206,207</sup> Against this backdrop, we regard it an advantage that several systems are now in place from which can be selected the best suited for a given application.

Photoreceptors other than LOV and cryptochromes have also provided building blocks for light-regulated gene expression. In two related studies,<sup>194,195</sup> the UV-light induced dissociation of the *AtUVR8* homodimer into monomers and their subsequent association with the *AtCOP1* protein was harnessed (Fig. 8B). In one report,<sup>194</sup> *AtCOP1* was fused with the Gal4-DBD, and *AtUVR8* with a *tAD* to drive expression of transgenes in mammalian cells in strongly UV-B-dependent manner. In the other study,<sup>195</sup> *AtUVR8* was covalently linked to the DBD of the macrolide-responsive repressor E, and the WD40 domain of *AtCOP1* was linked with a *tAD* to achieve expression of transgenes in mammalian cells that could be up-regulated by up to several-hundredfold by UV-B light. Notably, the combination of the UV-sensitive *AtUVR8:AtCOP1* systems with a BL-sensitive and a red/far-red-light-sensitive system enabled the sequential light-triggered expression of three separate transgenes.<sup>195</sup> In a different approach,<sup>116,117</sup> PYP was employed to control the GCN4 TF. The DNA affinity could be modestly upregulated by BL via linkage of the C terminus of GCN4 to an N-terminally truncated variant of PYP. A biophysical characterization indicated that in the dark the GCN4 moiety folds back onto PYP, and a monomeric protein results. Light-induced refolding of the PYP N terminus liberates GCN4 and thus promotes dimerization and DNA binding. Arguably, due to the limited enhancement of DNA affinity by light and due to the requirement for the specific chromophore *p*-coumaric acid, the system has to date not been applied in optogenetics.

The combination of split transcription factors with photoassociating photoreceptors that underpins many of the above strategies is not limited to regulating transcriptional initiation alone, but instead extends to other processes. As demonstrated by Cao *et al.*,<sup>208</sup> *AtCIB1* can be linked to the  $\lambda$ N RNA-binding domain that binds to a specific motif embedded in the 5'-untranslated region of a target mRNA; blue light allowed recruitment of a fusion protein between *AtCRY2* and the eukaryotic translation initiation factor eIF4E. In turn, other components of the translational machinery could be assembled, and expression of a transgene was upregulated by BL by up to around threefold. An alternative means of regulating gene expression is provided by BL-controlled nuclear import and export, discussed in detail in section 4.3.1. Briefly, in pertinent setups,<sup>209–212</sup> the transcriptional activity of target TFs is regulated by sequestering them in the cytosol in BL-dependent manner.

**4.1.3. Eukaryotic Transcription from Endogenous Promoters**—The above approaches have in common that they permit light-regulated expression of transgenes from synthetic promoters. As versatile and powerful these approaches are, they suffer from the requirement of delivering to host cells a suitable promoter-transgene cassette in addition to the photoreceptor setup *per se*. As such, the copy number and expression strength of the transgene may substantially differ from the corresponding endogenous genes. Moreover, depending upon the research question pursued, the host system may need to be configured beforehand, e.g., by attenuating or suspending expression of certain endogenous genes.



These potential problems may be circumvented by a set of optogenetic actuators that operate on the cellular expression machinery in a dominant way, thus obviating delivery of transgene cassettes or prior modification of the host cell.

In the PICCORO approach,<sup>213</sup> a dominant-negative version of the zebrafish transcriptional repressor Ntl was constructed and linked to the N-terminal portion of the *SsPixE* protein from *Synechocystis sp.* PCC6803 (Fig. 9A). The chimeric Ntl-*SsPixE* protein was expressed in zebrafish alongside the BLUF photoreceptor *SsPixD*. Notably, in the dark, *SsPixD* formed a homodecamer capable of strongly interacting with *SsPixE*, but BL promoted dissociation of *SsPixD* into homodimers and concomitant dissociation from *SsPixE*. Complex formation between *SsPixD* and Ntl-*SsPixE* in the dark lowered the DNA affinity of Ntl and relieved transcriptional repression of endogenous genes involved in tail development of zebrafish. The authors suggested that PICCORO may be a widely applicable strategy to regulate expression from endogenous promoters.<sup>216</sup> A recent study<sup>217</sup> achieved light-dependent regulation of the so-called ‘repressor element 1-silencing transcription factor’ (REST) and downstream genes. REST naturally acts in concert with co-repressory factors, among them mSin3a, to repress expression of target genes. A two-pronged strategy was chosen to interfere with function of endogenous REST in light-dependent manner. First, a REST epitope that mediates interaction with mSin3a was fused to the C terminus of *AsLOV2* such that its affinity to mSin3a was subject to BL. Following illumination, the resultant *AsLOV2*-PAH1 construct competed with REST for mSin3a binding and thereby relieved transcriptional repression. Second, in the construct *AsLOV2*-RILP, *AsLOV2* was C-terminally fused with the interaction domain of a REST inhibitor such that BL absorption allowed inhibition of DNA binding by REST and relief of transcriptional repression. Both approaches succeeded in upregulating REST-target genes in response to BL in both neuronal cell culture and primary neurons. In a recent approach,<sup>218</sup> the *Drosophila* morphogen Bicoid that acts as a transcription factor and key regulator of development was fused with *AiCRY2* such that BL attenuated Bicoid activity, presumably due to *AiCRY2*-mediated protein clustering. Interestingly, the Bicoid-*AiCRY2* chimera acted in dominant-negative manner, and BL also suspended the transcriptional activity of endogenous Bicoid. Fly development could hence be precisely studied in time and space. Another group of optogenetic actuators combine photoassociating photoreceptors with DNA-binding proteins that can be programmed to specifically bind (almost) arbitrary unique target sequences within eukaryotic genomes. Polstein and Gersbach<sup>219</sup> introduced the LITEZ system by connecting a zinc-finger DNA-binding protein to *AiGI*, and a *tAD* to the *AiFKF1*-LOV module.<sup>114</sup> BL stimulated recruitment of the *tAD* to the DBD and allowed expression of a reporter gene in mammalian cells to be strongly up-regulated under blue light. Although the proof-of-concept was achieved for a transgene, zinc fingers<sup>220</sup> can be reprogrammed to target diverse, defined DNA sequences, and therefore light-regulated expression of endogenous genes appears feasible with the LITEZ system as well. In the conceptually similar LITE approach,<sup>221</sup> the ‘transcription activator like effectors’ (TALE)<sup>220</sup> served as a programmable DNA-binding platform to which *AiCRY2* was covalently linked. Light-triggered association with *AiCIB1* allowed the recruitment of a palette of effectors to the target DNA site specified by the TALE. By using transcriptional activators and repressors as effectors, the expression of endogenous genes could be up- or downregulated in response to blue light.

The DNA sequence specificity of both zinc fingers and TALEs is rooted in modular protein domains, and reprogramming to different DNA targets therefore entails laborious production of new protein variants. By contrast, the DNA endonuclease Cas9 from *Streptococcus pyogenes* encodes its DNA specificity in one of two bound RNA molecules, which can easily be adapted to new targets. For practical applications, the two RNAs are routinely combined into a so-called single guide RNA or sgRNA (Fig. 9B)<sup>222</sup>. *Sp*Cas9 belongs to the CRISPR-Cas (clustered regularly interspaced short palindromic repeats-CRISPR associated) system that mediates adaptive immunity.<sup>223,224</sup> A cleavage-deficient variant, denoted dCas9, that harbors two mutations serves as an inert, programmable DNA-binding platform that has been exploited for the construction of systems for BL-regulated expression of endogenous genes.<sup>225</sup> In the LACE setup,<sup>214</sup> dCas9 was linked to two copies of the N-terminal part of *At*CIB1, whereas *At*CRY2 was fused with a strong *tAD*. Directed to the promoter regions of different endogenous genes via suitable sgRNAs, the LACE system enabled upregulation by BL of expression by up to several hundredfold in mammalian cells. In a closely similar approach, Sato and coworkers fused dCas9 with one copy of *At*CIB1 to which an *At*CRY2-*tAD* fusion protein could be recruited under blue light.<sup>215</sup> As in the LACE system, strong upregulation of endogenous genes by BL was achieved in mammalian cells. Compared side-by-side, the degree of light regulation appears slightly higher in LACE which could be due to the fusion of two *At*CIB1 copies to dCas9.<sup>214</sup> In a related recent approach,<sup>226</sup> unmodified dCas9 was combined with an extended sgRNA that harbored MS2 aptamers at its 3' end. *At*CIB1 was fused with the MS2 phage coat protein which strongly binds to these aptamers; *At*CRY2-linked effectors could hence be recruited upon BL exposure, and transcription could be strongly activated. Sato also pursued an orthogonal strategy by which dCas9 activity could be subjected to light control.<sup>227</sup> To this end, dCas9 was split into two fragments which were connected to derivatives of *Nc*Vivid, denoted Magnets, that afford BL-stimulated heterodimerization.<sup>165</sup> The split halves of dCas9, denoted pa-dCas9, could thus be reassembled in light-dependent manner and DNA-binding be restored. When one dCas9 fragment was linked with a *tAD*, strong upregulation of endogenous genes was achieved under BL. In a strategy inspired by the CRISPRi concept for transcriptional regulation in bacteria,<sup>228</sup> pa-dCas9 could also be directed to the coding region of target genes such that the expression was attenuated as a function of BL. As in the approach by Konermann *et al.*,<sup>221</sup> the degree of light-induced downregulation was relatively modest, much lower than that achievable with CRISPRi in bacteria.<sup>228</sup> As is also evident in the LACE method,<sup>214</sup> the degree of regulating gene expression by dCas9-dependent approaches can be significantly improved by recruiting to the same site and by thereby multiplexing several DNA effectors.<sup>229</sup> The underlying rationale principally applies to optogenetic applications as well and should help to further improve their efficiency.

#### 4.2. Epigenetics & Recombination

Given the modularity of the above dCas9-based recruitment strategies, these approaches are also suited for facilitating BL-regulated addition or removal of epigenetic markers (Fig. 10). Employing this rationale, different effector functionalities could be recruited to specific genomic sites to induce, for example, histone (de)acetylation, histone and DNA (de)methylation, or chromatin remodeling.<sup>221</sup> This strategy was recently implemented by using as locus-specific DNA-binding proteins TALEs to which *At*CIB1 was fused.<sup>230</sup> Via

covalent linkage to *A*CRY2, either a CpG DNA methylase or a methylation-editing enzyme could be recruited to the specified DNA target site in BL-activated manner. Resultant changes in DNA methylation were confined to the immediate genomic vicinity of the TALE binding site and elicited changes in the expression of a nearby gene. Regulation of epigenetic modifications was also achieved with a BL-induced nuclear export system,<sup>212</sup> described in section 4.3.1., that enabled optogenetic control of the subcellular localization of histone-modifying enzymes.

In addition to the cleavage-deficient dCas9 variant (cf. above), the original cleavage-competent Cas9 form has also been the subject of photoreceptor engineering (Fig. 11A). Current approaches towards regulating Cas9 cleavage activity by external trigger signals are generally realized at the levels of DNA and sgRNA binding, rather than at the level of DNA cleavage *per se*.<sup>225</sup> As a corollary, strategies that put Cas9 activity under control of an external trigger should directly apply to dCas9-based applications as well but the opposite is not necessarily true. As a case in point, the above split-Cas9 approach by Sato<sup>227</sup> not only enabled light-regulated gene expression but also supported BL-activated generation of double-strand breaks (DSBs) at target DNA sites. In turn, DSBs trigger cellular repair mechanisms,<sup>231</sup> principally non-homologous end joining and homology-directed repair, to promote deletions/insertions and recombination, respectively, at specified genomic loci. In another study,<sup>232</sup> (d)Cas9 was put under light control by inserting in its sequence at varying positions the homodimeric LOV sensor from *Rhodobacter sphaeroides* (*Rs*LOV) that undergoes light-induced subunit dissociation.<sup>233</sup> In one of the resultant chimeric proteins, denoted paRC9, in the dark the (d)Cas9 enzyme was presumably sequestered in a homodimeric complex such that binding to the DNA target sequence was sterically hindered.<sup>232</sup> Light absorption enhanced DNA affinity of paRC9 and increased site-specific cleavage activity, albeit to relatively modest extent. Unexpectedly, insertion of the *Rs*LOV sensor conferred a pronounced temperature sensitivity to (d)Cas9; whereas robust activity was observed at 29°C, almost none was detected at 37°C.

Light-regulated DNA recombination has also been accomplished via photosensitive variants of the Cre recombinase (Fig. 11B).<sup>51</sup> Earlier work had shown that Cre can be split in two fragments that have little mutual affinity and thus very low catalytic activity.<sup>235</sup> By linking the two fragments to the FKBP protein and the FRB domain, respectively, they could be reconstituted upon rapamycin addition, and recombinase activity was restored. To render activity of the split Cre BL-sensitive, the FKBP:FRB pair was replaced by the photoassociating *A*CRY2:*A*CIB1 pair<sup>51</sup> and a photoactivatable Cre (PA-Cre) was obtained. In mammalian cells, DNA recombination by PA-Cre could be activated by BL by more than hundredfold with low dark activity. PA-Cre and derived variants were also deployed *in vivo*, e.g., to achieve BL-induced recombination for the regulation of angiogenesis in mice.<sup>236</sup> Another study employed PA-Cre for BL-activated recombination and concomitant activation of a reporter gene in mice brain.<sup>237</sup> To achieve high frequencies of recombination events, BL had to be applied for extended periods of time, up to several hours. Tucker and colleagues<sup>53</sup> reasoned that a PA-Cre variant with a longer-lived signaling state of the *A*CRY2 photoreceptor would be more light-sensitive at photostationary state and might hence support efficient recombination at lower light doses. Using a screening assay based on light-regulated gene expression in yeast, a longer-lived variant of *A*CRY2 was identified and

implemented in the second generation of PA-Cre. Consistent with the design rationale, PA-Cre 2.0 indeed required lower BL doses for activation; unexpectedly, PA-Cre 2.0 also displayed lower recombination activity in the dark than observed for the original PA-Cre, and thus PA-Cre 2.0 had a higher dynamic range than its predecessor. A split Cre was also established using the Magnets LOV receptors (cf. above) that heterodimerize upon BL exposure.<sup>234</sup> The resultant light-regulated Cre recombinase, confusingly also denoted PA-Cre, supported DNA recombination in mammalian cells that could be enhanced by BL by up to several hundredfold. Notably, the Magnet-based split Cre showed enhanced light sensitivity and accompanying efficient activation by comparatively low BL doses to the point that Cre recombination could be activated within the internal organs of mice.

### 4.3. SUBCELLULAR LOCALIZATION

Numerous biological processes, e.g., transport into or out of organelles, cell polarization and motility, require the precisely orchestrated localization of cellular constituents to specific compartments or sites within cells. Optogenetics is well suited to perturb and study such processes because many photoreceptors, especially BL-sensitive ones, grant ready control over the subcellular localization of near-arbitrary target proteins. The most common, and arguably most easily implementable approach, relies on photoreceptors that undergo light-dependent protein-protein interactions (PPI) with partner proteins, cf. sections 2 and 3. To this end, one component of the interacting photoreceptor:partner pair is constitutively directed to the cellular location of interest, often via immobilization, e.g., by a membrane anchor. Passive diffusion or active transport mechanisms bring into spatial vicinity the other component and allow it to be retained, provided the photoreceptor is in its binding-component state (depending on photoreceptor, either in the presence or absence of light). For example, this design principle of light-modulated PPIs underpins many optogenetic approaches for controlling cytoskeleton dynamics, cf. section 4.4. To a first approximation, every photoreceptor that undergoes light-dependent PPIs lends itself to control subcellular localization. An alternative strategy capitalizes on trafficking signal epitopes that the cell uses to control localization, e.g., nuclear import and export signals. By modulating as a function of light the exposure of these epitopes, optogenetic control over subcellular localization was achieved as well.

**4.3.1. Nuclear Import & Export**—The control by blue light of the exposure and hence the activity of trafficking epitopes underpins BL-regulated systems for nuclear import and export (Fig. 12).<sup>209–212</sup> In the LINuS system,<sup>209</sup> a nuclear localization signal (NLS) peptide was embedded in or appended to the J $\alpha$  helix of the AsLOV2 photosensor to regulate by BL epitope accessibility and cellular activity. In darkness, the NLS was predominantly masked and the target protein of interest (POI) preferentially resided in the cytosol but upon BL application, J $\alpha$  unfolded, the NLS was exposed and the POI distributed to the nucleus. In this manner, the nuclear localization of fluorescent reporters could be controlled by BL in mammalian cells. A suite of LINuS variants offered different degrees of BL regulation and NLS versions of varying strengths which benefits the coupling of LINuS to arbitrary POIs with different intrinsic propensities of residing in the nucleus or the cytosol. The nucleocytoplasmic distribution can further be modulated by including constitutive NLS and nuclear export signals (NES). Using LINuS, mitotic entry and gene expression in

mammalian cells was controlled by BL. The LANS approach<sup>211</sup> is related to LINuS in that it is also based on interleaving the *AsLOV2* J $\alpha$  helix with NLS peptides. BL-induced nuclear translocation by LANS was demonstrated for mammalian cells, yeast and in *Caenorhabditis elegans* embryos. Based on LANS, a light-inducible transcription factor was devised and expressed in transgenic *C. elegans* to control by BL development. Recently, the dynamic range of the LANS system was improved by combining it with the LOVTRAP<sup>238</sup> strategy (cf. sec. 4.4.1.1.).<sup>239</sup> Moreover, employing the same general strategy underpinning LINuS and LANS, two systems were engineered that mediate BL-induced nuclear export.<sup>210,212</sup> In LEXY,<sup>210</sup> an NES peptide was embedded in the *AsLOV2* J $\alpha$  helix to allow BL-activated depletion of target POIs from the nucleus of mammalian cells. The technique was used to regulate by BL gene expression and activity of the tumor suppressor protein p53. LINX<sup>212</sup> realized a similar setup to achieve BL-induced nuclear export in mammalian cells, yeast and *C. elegans*. Using LINX, gene expression and epigenetic modifications in yeast were optogenetically controlled. As an alternative discussed in section 4.1.2., the versatile *AtCRY2* photoreceptor can also respond to BL exposure by nuclear clearing.<sup>196</sup> Hence, *AtCRY2* may provide another means for light-induced nuclear export of POIs.

**4.3.2. Peroxisomal Import**—A strategy similar to that for the BL-induced nuclear import and export<sup>209–212</sup> gave rise to the LOV-PTS1 system for optogenetic control of peroxisomal import (Fig. 13).<sup>240</sup> A pertinent trafficking signal peptide was appended to J $\alpha$  of *AsLOV2* and thereby caged in BL-dependent fashion. In mammalian cells, LOV-PTS1 mediated the peroxisomal import of fluorescent reporter proteins upon BL exposure.

**4.3.3. Optically Induced Compartments**—Several optogenetic actuators exploit the propensity of *AtCRY2* to associate with *AtCIB1*<sup>51</sup> or to form higher-order oligomers under BL (Fig. 14).<sup>65,241</sup> Via conjugation to *AtCRY2*, target effector proteins of interest can hence be assembled into clusters upon BL, and protein-based microcompartments can be formed inside the cell. For improved efficiency, often the E490G variant of *AtCRY2*, denoted Cry2olig,<sup>52</sup> is employed as it shows enhanced clustering propensity. The protein-based compartments were used to analyze PPIs between proteins of interest inside of cells,<sup>52</sup> and to modulate by BL the activity of target effectors.<sup>52,242</sup> In the LINC setup,<sup>52</sup> the interaction between two fluorescently labeled proteins of interest was assessed by connecting one of them to *AtCRY2*. BL induced *AtCRY2*-mediated cluster formation of this protein, and a possible interaction with a second POI could be detected by coclustering of the two interacting proteins. The LARIAT method<sup>242</sup> pursued a slightly different strategy in that protein clusters were formed via the BL-induced heterodimerization of *AtCRY2:AtCIB1* instead of the homooligomerization of *AtCRY2* (Fig. 14A). In this approach, *AtCIB1* was fused with a multimeric scaffold protein that assumes a homododecamer. BL induced the association of *AtCRY2* and the multimeric *AtCIB1* conjugate such that clusters were formed. While little BL-induced clustering was observed with *AtCRY2* alone, it is conceivable that robust clusters would be obtained if using Cry2olig. By conjugating *AtCRY2* with a GFP-specific nanobody, GFP-tagged target proteins were sequestered into the BL-induced clusters formed by *AtCRY2* and the multimeric *AtCIB1*. In principle, the LARIAT technique could be adapted to target for BL-induced sequestration and concomitant attenuation other endogenous proteins via substitution of the GFP-specific nanobody for

another one. Similar to the applications of LARIAT, LINC<sup>52</sup> was used to disrupt via BL-induced *AiCRY2* clustering endocytosis, cf. section 4.4.3.

In recent years, it has become increasingly evident that membrane-less organelles formed by assemblies of ribonucleoproteins (RNP) are engaged in important biological processes,<sup>243</sup> prominent examples being the Cajal bodies and nucleoli. At sufficiently high local concentration, the RNP complexes display liquid-liquid phase separation to form distinct RNP droplets that are dynamic and in constant flux with the surroundings. The formation and size of RNP droplets inside mammalian cells was optogenetically controlled by connecting to *AiCRY2* the intrinsically disordered protein FUS known to bind RNA and capable of forming droplets (Fig. 14B).<sup>66</sup> Upon BL exposure, *AiCRY2* assembled into clusters, leading to an increased local concentration of the disordered protein with bound RNA and to the appearance of RNP droplets as evidenced by speckle formation. By varying expression levels and applied BL dose, the number and average size of the droplets could be varied. Cry2olig greatly enhanced clustering and droplet formation. An alternative to Cry2olig might be provided by the recent observation<sup>244</sup> that either ligation of *AiCRY2* to oligomeric fluorescent proteins or C-terminal appendage of a short peptide to *AiCRY2* enhanced BL-induced clustering propensity. Arguably, these later strategies may be combined with the E490G mutation that gave rise to Cry2olig.

**4.3.4. Light-induced Interactions Among Organelles and Cells**—Optogenetic approaches based on BL receptors have also enabled the control of interactions among organelles and entire cells. In one study,<sup>245</sup> the iLID system<sup>203</sup> for BL-activated heterodimerization was deployed to trigger the formation of contact sites between the endoplasmic reticulum and mitochondria. To this end, the two components of iLID were directed to the ER membrane and the mitochondrial outer membrane, respectively. The tethering sites that were formed between ER and mitochondrion upon BL exposure may resemble the naturally occurring contact structures that are implicated in cellular signaling and apoptosis, among other processes.<sup>246</sup> The strategy employed in this work readily extends to other organelles and may be used to induce spatial contacts among them. Recently, the surface attachment, cell-cell contacts and biofilm formation of *E. coli* bacteria were regulated in BL-dependent manner by LOV-mediated expression of a specific membrane protein.<sup>247</sup> A different system relies on LOV receptors for BL-induced heterodimerization to also control by light bacterial adhesion to a substrate.<sup>248</sup> In this approach, the Magnet photoreceptors were deposited on a solid support and expressed on the surface of *E. coli* cells, respectively. BL promoted interaction of the Magnet components and resulted in bacterial attachment. As demonstrated in this study, LOV BL receptors can apparently retain flavin chromophore binding and light sensitivity upon cell-surface expression. Prospectively, this approach may be adapted to eukaryotic cells to control interactions among them and their spatial arrangement on substrates, with potential applications in tissue engineering.

#### 4.4. Cytoskeleton Dynamics

The optogenetic toolkit for manipulating cytoskeleton structure and dynamics by BL is similarly rich as that for regulating gene expression, cf. sec. 4.1. The large number of

pertinent light-regulated actuators equally reflects the biological significance of the cytoskeleton and the relative ease with which it can be optogenetically controlled. Inside the cell, the structure and dynamics of the cytoskeleton are governed by an intricate network of factors that mutually interact in spatially and temporally defined manner. Approaches for regulating by light PPIs and subcellular localization are hence particularly applicable for optogenetic control of the cytoskeleton and associated processes. Indeed, optogenetics provides an unprecedented means of precisely interrogating individual nodes and connectivity of the signaling networks underlying cytoskeleton dynamics.

#### 4.4.1. Actin & Myosin

**4.4.1.1. Cytoskeleton Remodeling:** Actin (or, intermediate) filaments impart mechanical strength to eukaryotic cells and facilitate their motility.<sup>249</sup> The flexible actin filaments are formed by polymerization of globular monomeric actin and are organized in bundles, fibers and mesh-like networks. These higher-order assemblies and the constituent actin filaments are highly dynamic entities, constantly undergoing assembly and disassembly. These reactions are orchestrated in time and space by complex signaling networks which feature small GTPases of the Rho family as key nodes.<sup>250,251</sup> Specifically, the Rho GTPases Rac1, RhoA and Cdc42 are anchored to the plasma membrane and integrate inputs from upstream factors. These GTPases display low(er) activity in their GDP-bound forms, but when binding GTP, they activate a set of downstream effectors that modulate actin filament structure and dynamics. To optogenetically control the activity of Rac1, its membrane anchor was removed and it was coupled to *A*FKF1.<sup>114</sup> BL exposure prompted association of *A*FKF1 with membrane-anchored *A*GI and resulted in the recruitment of Rac1 to the plasma membrane which sufficed for triggering actin polymerization. Spatially confined BL illumination led to the formation of lamellipodia in mammalian cells. In a similar vein, Rac1 activity was controlled via the LARIAT method<sup>242</sup> by sequestration of the GTPase into *A*CRY2:*A*CIB1-based clusters and concomitant attenuation upon BL exposure. *Vice versa*, in a different study<sup>65</sup> *A*CRY2-mediated, BL-induced clustering of Rac1 resulted in its translocation to the plasma membrane and concomitant activation. A different strategy towards controlling Rac1 activity by BL was employed by Hahn and colleagues (Fig. 15).<sup>103</sup> In the engineered PA-Rac1 photoreceptor (cf. sec. 3.1.3.), Rac1 was linked to the C-terminal  $J\alpha$  helix of *A*sLOV2 and its interaction with downstream effectors, e.g., PAK1, was thus sterically impeded. BL absorption triggered  $J\alpha$  unfolding, prompted dissociation of *A*sLOV2 from Rac1 and thereby restored activity. Local illumination of mammalian cells elicited spatially defined actin remodeling, membrane ruffling and formation of lamellipodia. Fibroblasts could thus be induced to migrate in the direction of a focused BL laser spot. Introduction of a dominant-negative mutation into Rac1 sufficed to prompt fibroblasts to migrate away from a BL spot, instead of towards it. As two of many applications of PA-Rac1, migrating neutrophil cells within developing zebrafish embryos could be steered by BL,<sup>252</sup> and dendritic spines could be both selectively labeled and shrunk in mice.<sup>253</sup> Using the design strategy underpinning PA-Rac1, a photoactivatable variant of Cdc42, denoted PA-Cdc42, was obtained that mediated membrane ruffling and formation of filopodia in mammalian cells under BL.<sup>103</sup>

Rather than by optogenetically targeting Rac1 directly, actin cytoskeleton dynamics have also been controlled by regulating by BL factors upstream of Rac1. As for other small GTPases, the activity of Rho GTPases is regulated by guanine nucleotide exchange factors (GEF) that promote the exchange of bound GDP for GTP, and by GTPase-activating proteins (GAP) that stimulate GTP hydrolysis to GDP.<sup>250</sup> Accordingly, optogenetic control over cytoskeleton dynamics could be exerted by controlling the subcellular localization and activity of GEFs as a function of BL. The LARIAT approach for optogenetic trapping<sup>242</sup> was used to sequester the Rac1 GEFs Tiam1 and Vav2 upon BL illumination, resulting in a decrease of GTPase activity and membrane retraction in mammalian cells. In the CAD method,<sup>254</sup> based on the Magnets LOV photoreceptors for BL-induced heterodimerization,<sup>165</sup> Tiam1 was recruited to the plasma membrane upon BL exposure and elicited actin reorganization, membrane ruffling and formation of lamellipodia. CAD improved the efficiency of these BL-induced responses by conjugating Tiam1 with several copies of the Magnet LOV receptors. A versatile sequestration-based technique for optogenetically controlling the cytoskeleton was realized in the LOVTRAP method (Fig. 15).<sup>238</sup> Via phage display, affibodies,<sup>255</sup> named Zdark, were developed that strongly bind the dark-adapted state of the *AsLOV2* photosensor with its  $\text{J}\alpha$  helix folded and docked onto the core domain. BL exposure prompted  $\text{J}\alpha$  undocking and resulted in an about 150-fold decrease in the affinity of the best Zdark affibody variant for *AsLOV2*. By anchoring *AsLOV2* to the outer mitochondrial membrane, target proteins conjugated to Zdark were sequestered away from the plasma membrane in the absence of light. BL exposure triggered dissociation of the *AsLOV2*:Zdark complex and enabled the target proteins to reach the plasma membrane. In this way, the intracellular localization and activity of the GTPases Rac1 and RhoA, and of the GEF Vav2 could be controlled by BL with downstream effects similar to those described for the above optogenetic actuators. In a landmark approach,<sup>109</sup> several players engaged in regulating cytoskeleton dynamics were allosterically regulated by BL (Fig. 15). Informed by molecular dynamics simulations, the *AsLOV2* photosensor was inserted into target proteins at surface loops that are mechanically connected to their active sites (cf. sec. 3.1.2.). BL-induced unfolding of the *AsLOV2*  $\text{J}\alpha$  helix was thus coupled to a decrease in activity of the target protein. Using this generalizable strategy, photoinhibited (PI) variants of the soluble tyrosine kinase Src, of the GTPases Rac1, RhoA and Cdc42, and of the GEFs Vav2, GEF-H1 and Intersectin were generated. These and related optogenetic tools in hand, the complex processes determining actin cytoskeleton structure and reorganization can now be deciphered in ever more precise and detailed manner.

The GTPase RhoA was also subjected to BL control by fusing it with *AiCRY2* such that upon BL exposure clusters formed that translocated to the plasma membrane of mammalian cells.<sup>65</sup> RhoA then induced actin rearrangements that resulted in membrane spreading. BL-triggered inhibition of the related GTPases RhoG and Cdc42 was achieved with the LARIAT method via sequestration into *AiCRY2*:*AiCIB1*-based clusters.<sup>242</sup> In two related studies,<sup>256,257</sup> Cdc42 was optogenetically regulated by controlling via BL application the subcellular localization of the Cdc42-targeting GEF Intersectin. Using the iLID system for BL-activated heterodimerization,<sup>203</sup> Intersectin was recruited to the plasma membrane under BL and promoted local Cdc42 activation. In budding yeast, Cdc42 is involved in governing cell polarization and division by budding. Based on the TULIP setup for light-induced



heterodimerization,<sup>258</sup> either the Cdc42-specific GEF Cdc24 or the scaffold protein Bem1 that mediates the interaction between Cdc24 and Cdc42 were recruited to the plasma membrane upon BL exposure.<sup>259</sup> In either manner, cell polarity and the situation of the budding site could be optogenetically controlled via BL and mechanistically studied.

Optogenetic control over cytoskeleton reorganization was also exerted at levels other than the Rho GTPases and their GEFs. On the one hand, several transmembrane signal receptors impinge upon the actin cytoskeleton. BL-regulated versions of several such receptors, discussed in section 4.7., can hence be used to regulate actin dynamics. On the other hand, actin polymerization was directly triggered via *AiCRY2*-mediated BL-induced clustering of the SH3 domains of the Nck protein.<sup>52</sup> Local BL stimulation and resultant actin reorganization prompted the retraction of membrane protrusions in mammalian cells.

**4.4.1.2. Actin/Myosin-Based Transport:** Myosin motor proteins move along actin filaments and thereby mediate diverse motility processes, including muscle contraction and intracellular transport.<sup>249</sup> In the LOVDab design,<sup>260</sup> a short peptide derived from Dab2, a cargo protein for myosin VI-mediated transport, was appended to the J $\alpha$  helix of *AsLOV2* such that its exposure was governed by BL. Light-induced J $\alpha$  unfolding allowed the Dab peptide epitope to bind to myosin VI which translocates to the minus end of actin filaments. By anchoring LOVDab to the membrane of peroxisomes, the intracellular transport of these organelles could be stalled in BL-activated manner. In a related strategy,<sup>261</sup> the TULIP system<sup>258</sup> was harnessed to control by BL the interaction between a peroxisome-located protein and myosin Vb, also resulting in interference with intracellular organelle transport.

**4.4.2. Microtubules—**Microtubules (MT) are composed of  $\alpha$ - and  $\beta$ -tubulin that polymerize to form hollow cylinders.<sup>249</sup> As is the case for actin filaments (cf. sec. 4.4.1.), MTs are highly dynamic and constantly undergo assembly and disassembly reactions. At the so-called minus end, disassembly outweighs assembly, and a net shrinkage of the MT results; *vice versa*, at the plus end, assembly dominates, and the MTs display net growth. MT dynamics are subject to the regulation by various factors which offer footholds for optogenetics. As a case in point, end-binding proteins (EB) mediate the interaction between the plus end of MTs and a diverse set of tip-interacting proteins (TIP). To control these interactions by BL,<sup>262</sup> the N-terminal half of a split EB1 that binds to the MT plus end was fused with the *AsLOV2* photosensor and the C-terminal half of EB1 that mediates interactions with TIPs was fused to the interacting affibody Zdark (Fig. 16).<sup>238</sup> In darkness, *AsLOV2* and Zdark associated and an active EB1 thus resulted; BL exposure triggered dissociation and rendered EB1 unable to recruit TIPs. BL illumination hence resulted in local attenuation of MT growth at their plus ends which could culminate in MT depolymerization.

Transport along MTs is mediated by kinesin and dynein motor proteins which (mostly) walk towards the plus and minus ends, respectively.<sup>249</sup> Employing the TULIP system,<sup>258</sup> the interaction between a peroxisome-anchored protein and a kinesin motor could be turned on by BL, resulting in translocation of the organelles towards the MT plus ends and accumulation in the periphery of mammalian cells (Fig. 16).<sup>261</sup> Owing to its modularity, the method could be extended to myosin (cf. sec. 4.4.1.2.) and dynein motor proteins. When

dynein was thus recruited in BL-activated manner, the peroxisomes instead translocated to the minus ends of MTs, i.e. to the cell center. Likewise, the intracellular localization of mitochondria was regulated by BL using this technique. A conceptually similar strategy<sup>263</sup> employed the photoassociating *AiCRY2:AiCIB1* pair rather than the TULIP system. Via BL-induced recruitment of kinesin and dynein motors to peroxisomes, lysosomes and mitochondria, these organelles could be moved to the cell center or periphery, respectively.

**4.4.3. Endocytosis & Exocytosis**—Vesicular transport in mammalian cells was also targeted by optogenetics. The dominant endocytic pathway in eukaryotes is mediated by clathrin which polymerizes at the plasma membrane as a cage-like structure and thereby allows membrane vesicles to pinch off.<sup>249</sup> To optogenetically control endocytosis, the light chain of clathrin was connected to *AiCRY2* such that under BL clusters formed.<sup>52</sup> Said clusters impaired clathrin assembly and slowed down endocytosis. By contrast, in a recent study,<sup>264</sup> clathrin-mediated endocytosis could be stimulated by BL. To this end, the TULIP system<sup>258</sup> for BL-activated heterodimerization was employed to recruit a clathrin-binding protein to the plasma membrane which in turn triggered endocytosis. *AiCRY2* also underpins the IM-LARIAT strategy for controlling by BL vesicular transport (Fig. 17).<sup>265</sup> Small GTPases of the Rab family are integral to coordinating vesicular trafficking between membrane-surrounded organelles and the cell membrane. Individual Rab proteins were fused with *AiCIB1* and coexpressed in mammalian cells with *AiCRY2*.<sup>265</sup> BL induced *AiCRY2* clustering and binding of the Rab-*AiCIB1* conjugates; vesicles were thus gummed up and transport impaired. By targeting different Rab GTPases, various branches of the trafficking pathway could be subjected to BL control, including different stages of endocytosis (early and late endosomes) and exocytosis (vesicles trafficking between endoplasmic reticulum and Golgi apparatus, or between Golgi and plasma membrane, as well as secretory vesicles). The trafficking from the endoplasmic reticulum to the Golgi could also be optogenetically regulated by linking target cargo proteins to one or several copies of *AiUVR8*<sup>266</sup> that in darkness, forms a homodimer but that dissociates following UV-light exposure. Conjugation of target cargo to *AiUVR8* promoted formation of aggregates in the endoplasmic reticulum and effectively suspended vesicular trafficking of the cargo to the Golgi. Under UV light, *AiUVR8* dissociated, the aggregates dissolved and vesicular transport of the cargo protein to the Golgi and onward proceeded. Lastly, the secretion of vesicles in pancreatic cells could be optogenetically perturbed via BL control of phosphatidylinositol signaling, cf. sec. 4.7.2.<sup>267</sup>

#### 4.5. Intracellular Protein Half-Life & Proteolytic Cleavage

In many optogenetic applications, the target effector output and downstream cellular responses are up-regulated by light absorption. Provided a given application scenario only requires slow time resolution, light-regulated expression provides an easily implementable and highly versatile means of optogenetic activation of desired cellular responses. At the same time, there are use cases where shutting-off or down-regulation of cellular activities in response to light stimuli are demanded. The LARIAT system,<sup>242</sup> described in section 4.3.3., offers a general path towards BL-induced reversible down-regulation of cellular activities via sequestration of the proteins into microcompartments. Alternatively, the cellular activity levels of a target effector may be irreversibly reduced by prompting its active degradation

via the proteasome system.<sup>268</sup> Inside eukaryotic cells, proteins can be tagged for destruction by ubiquitination, followed by proteolytic cleavage at the proteasome. Proteins to be destroyed are recognized by the cellular ubiquitination machinery via specific degradation signals, denoted degrons, that often amount to short peptide epitopes. Two systems<sup>269,270</sup> for triggering intracellular protein degradation via the ubiquitin:proteasome machinery were implemented based on the widely used *AsLOV2* photosensor or its homolog *A $\Delta$ LOV2* from *Arabidopsis thaliana* phototropin 1 (Fig. 18). To this end, degron sequences were interleaved with or appended to the *AsLOV2/A $\Delta$ LOV2* J $\alpha$  helix such that they were largely sequestered in the darkness when J $\alpha$  is mostly folded. BL-promoted J $\alpha$  unfolding exposed the degron epitopes, thereby prompting the proteasomal degradation of *AsLOV2/A $\Delta$ LOV2* and covalently linked target proteins. These co-called photosensitive degrons (psd) allowed the intracellular half-life in yeast of suitably tagged effector proteins to be decreased by BL by around sixfold.<sup>271</sup> Notably, assuming single-exponential kinetics for the degradation process, a sixfold difference in half-life can translate into much higher differences in actual target protein concentrations between dark and BL conditions. Using the psd strategy, the steady-state levels of metabolic enzymes and progression through the yeast cell cycle were controlled by BL. Subsequently,<sup>271</sup> a suite of psd systems were generated that included variants with up to tenfold decrease of protein half-life by BL. A related approach, called B-LID,<sup>270</sup> was implemented in mammalian cells where the steady-state levels of a fluorescent reporter protein could be lowered following BL exposure by around five- to tenfold. Similarly, B-LID was applied in zebrafish to induce by BL the degradation of a reporter protein. In a later study,<sup>272</sup> B-LID was covalently linked to a protein fragment, denoted Med25VBD, of the eukaryotic mediator complex to bestow light sensitivity on the widely used Tet-ON/Tet-OFF gene-regulatory systems. In these systems, the Tet repressor is linked to a *trans*-activating domain that recruits components of the eukaryotic transcriptional machinery and thereby induces gene expression. As Med25VBD competes for binding to the *tAD*, it effectively represses expression from the Tet-ON promoter. When linked to B-LID, Med25VBD can be degraded in BL-stimulated manner, resulting in relief of transcriptional repression. Notably, the Med25VBD-B-LID complex does not perturb DNA binding of the Tet repressor nor its regulation by tetracycline analogs, and it can therefore be employed as an optogenetic upgrade to existing Tet-ON systems. Recently, the LovD approach for BL-induced protein degradation closely recapitulated the psd setup<sup>273</sup> except for employing the *AsLOV2* rather than the *A $\Delta$ LOV2* photosensor. Using LovD, the abundance and intracellular half-life of reporter proteins in mammalian cells could be controlled by BL.

Whereas in the psd, B-LID and LovD systems the *AsLOV2/A $\Delta$ LOV2* module is used to regulate by BL the accessibility of degron epitopes interwoven with the J $\alpha$  helix, in two similar approaches, denoted Cal-Light<sup>274</sup> and FLARE,<sup>275</sup> the cleavage sequence of the TEV protease was embedded in this helix. BL prompted exposure of this sequence and allowed cleavage by the TEV protease to occur. To enhance regulatory efficiency, the Cal-Light method was further combined with a split-TEV protease activated by BL.<sup>276</sup> To this end, TEV protease fragments were linked with *ACRY2* and *ACIB1*, respectively; BL hence induced association of the split parts and increase in protease activity. As another class of proteases, caspases that mediate the programmed cell death have been put under BL control, see section 4.8.<sup>199,277</sup>

## 4.6. Second Messengers

Widely distributed in nature as components of signal transduction cascades, second messengers serve to amplify and relay signals inside cells.<sup>278</sup> Upon perception of a suitable stimulus, second messengers are released from storage compartments or produced enzymatically; *vice versa*, signaling is eventually suspended by sequestration or enzymatic degradation of the second messengers. As the production/release and degradation/removal processes are often regulated in spatiotemporally precise manner, intracellular microdomains of elevated second messenger concentration result in time and space. Given inherent amplification, spatiotemporal dynamics and a wide range of physiological responses regulated, second-messenger signaling has been a prime subject for optogenetic intervention.

### 4.6.1. Cyclic Nucleotides

**4.6.1.1. Cyclic Mononucleotides:** 3',5'-cyclic nucleotide monophosphates (cNMPs) are versatile second messengers engaged in the regulation of multiple physiological responses in both prokaryotes and eukaryotes.<sup>278</sup> Nucleotide cyclases catalyze the formation of cNMPs from the corresponding nucleotide triphosphates, and phosphodiesterases catalyze the hydrolytic breakdown to the (non-cyclic) nucleotide monophosphates (Fig. 19). In eukaryotic cells, the two most widespread cNMPs, 3',5'-cyclic adenosine monophosphate (cAMP) and 3',5'-cyclic guanosine monophosphate (cGMP), bind to and thereby regulate the activity of cyclic-nucleotide-gated (CNG) ion channels, protein kinases A or G (PKA or PKG), Epac (exchange protein directly activated by cAMP) and popeye-domain-containing proteins (PODCP). Inside eukaryotic cells, the activity of adenylate cyclases that produce cAMP is primarily controlled by intracellular calcium concentrations and by G-protein coupled receptors (GPCRs).

Sensory photoreceptors acting at the molecular level as photoactivated nucleotide cyclases have been identified in several organisms (Fig. 19A). Chronologically first, a BLUF photoreceptor, denoted as a photoactivated adenylate cyclase (PAC), was discovered in *Euglena gracilis* where it mediates a photophobic reaction in response to strong BL exposure.<sup>11</sup> Enzymatic analysis of the purified *E. gracilis* PAC (*EuPAC*) revealed its adenylate cyclase activity to be upregulated by around 80-fold under BL compared to darkness. *EuPAC* assumes heterotetrameric state with two copies each of the chains *EuPAC* $\alpha$  and *EuPAC* $\beta$ . Each  $\alpha$  and  $\beta$  chain comprises two BLUF photosensor and two class III adenylate cyclase effector modules. Remarkably, the initial discovery of *EuPAC* occurred around the same time as that of the channelrhodopsins (ChR),<sup>75,76</sup> thus predating the advent of optogenetics.<sup>4</sup> Notwithstanding its early discovery, *EuPAC* was not immediately deployed in optogenetics, arguably owing to its considerable molecular size and heterotetrameric architecture. The path towards optogenetic application was paved when it was realized that both *EuPAC* $\alpha$  and *EuPAC* $\beta$  mediate BL-stimulated adenylate cyclase activity on their own in the absence of the respective other PAC chain.<sup>279</sup> Notably, *EuPAC* $\alpha$  was around hundredfold more active than *EuPAC* $\beta$  but also showed higher basal activity in the dark. Heterologous expression of either *EuPAC* $\alpha$  or *EuPAC* $\beta$  enabled BL-stimulated cAMP production as demonstrated for frog oocytes, mammalian cells and *Drosophila melanogaster* flies.<sup>279</sup> Transgenic flies expressing *EuPAC* $\alpha$  in their brains showed BL-dependent behavioral responses, e.g., hyperactivity or freezing. Despite later efforts at optimization, the

application of *EuPAC* has remained limited, presumably due to the significant dark activity. A related bacterial PAC (denoted bPAC<sup>93</sup> or BlaC<sup>94</sup>), discovered in the bacterium *Beggiatoa* *sp.* by sequence homology, has largely superseded *EuPAC*. Compared to *EuPAC*, bPAC is smaller in size, consisting of single BLUF and type-III cyclase domains only, features a longer lifetime of the signaling state and displays a higher degree of regulation by BL (up to 300-fold).<sup>93</sup> Consequently, bPAC proved more efficient at activating CNG ion channels in frog oocytes than *EuPAC*.<sup>93</sup> Whereas bPAC/BlaC is specific for the BL-induced formation of cAMP, site-directed mutagenesis yielded the variant BlaG that produced cGMP around five times more efficiently than cAMP.<sup>94</sup> bPAC and BlaG have been used in a number of optogenetics studies, e.g., to control by BL flagellar beating of murine sperm.<sup>91</sup> In another example,<sup>286</sup> BlaG was derivatized by mutagenesis to alter the basal levels and BL-induced increases of cAMP/cGMP production in mammalian cells. An optimized variant, denoted EROS, was transfected into male rats where it supported BL-induced cGMP production, ensued by smooth muscle relaxation and penile erection. The recently elucidated three-dimensional structures of bPAC<sup>287</sup> and of a related PAC from the cyanobacterium *Oscillatoria acuminata* (oPAC)<sup>288</sup> revealed a homodimeric arrangement with the BLUF photosensor and the cyclase domains forming two dimers that are connected by a two-helix bundle. Diffraction data on BL-exposed PAC crystals hinted at the structural mechanism underpinning regulation of cyclase activity and stand to inform the engineering of improved bPAC/oPAC variants.<sup>287,289</sup> Another PAC, termed mPAC, was discovered in the cyanobacterium *Microcoleus chthonoplastes* PCC 7420 and uses a LOV rather than a BLUF photosensor.<sup>280</sup> Compared to bPAC, mPAC is somewhat larger in size and has a similar lifetime of the signaling state but a less pronounced BL-induced enhancement of catalytic activity. mPAC was deployed in a cyclase-deficient *Dictyostelium discoideum* strain where it partially restored fruiting-body formation that could be enhanced by BL.<sup>290</sup>

Distinct from the BL-regulated PACs, the photoreceptor *BeGC1* from the fungus *Blastocladiella emersonii* employs a rhodopsin photosensor and produces cGMP in response to green light.<sup>291</sup> As dark activity is exceedingly low and specificity for cGMP over cAMP is high, *BeGC1* has already found optogenetic application.<sup>134,135</sup> Furthermore, based on bacterial phytochromes, red-light-activated PACs<sup>292,293</sup> and a red-light-activated cAMP/cGMP-specific PDE, denoted LAPD,<sup>281</sup> were engineered. In a similar vein, a recent study reported a naturally occurring, light-regulated adenylate cyclase that is based on a CBCR photosensor unit.<sup>294</sup> Lastly, a recently reported photoreceptor from *Salpingoeca rosetta* comprises rhodopsin and PDE modules but showed only minute light-induced enhancement of catalytic activity.<sup>295</sup> In combination with genetically encoded sensors for the intracellular detection of cNMP levels, e.g., reference,<sup>296</sup> PACs and light-regulated PDEs enable the precise and online optogenetic control of these second messengers.

Optogenetic control of cNMP-dependent cellular responses was also accomplished via a BL-regulated version of PKA. An impaired kinase variant with attenuated catalytic activity was tethered to *AtCRY2* and could be recruited via BL to the *AtCIB1* protein immobilized at the outer mitochondrial membrane.<sup>297</sup> The resultant increase in local kinase concentration promoted the phosphorylation of target proteins associated with this organelle.

**4.6.1.2. Cyclic Dinucleotides:** Prokaryotes use as second messengers not only cAMP and (to much lesser extent) cGMP but also the cyclic dinucleotides c-di-GMP (cyclic diguanylate) and c-di-AMP (cyclic diadenylate).<sup>298</sup> In particular, c-di-GMP is engaged in the regulation of numerous processes in bacteria, including biofilm formation, motility and virulence.<sup>299</sup> Cyclic diguanylate is produced from two molecules of GTP by GGDEF diguanylate cyclases and is hydrolyzed to 5'-phosphoguananylyl-(3'-5')-guanosine by EAL phosphodiesterases. Given the wide range of processes regulated by c-di-GMP, it comes as no surprise that light-regulated variants of GGDEF and EAL enzymes exist in nature (Fig. 19B). Whereas GGDEF effectors are frequently regulated by bacteriophytochromes, EAL effectors are often found in conjunction with BLUF photosensors. As a case in point, the BlrP1 receptor from *Klebsiella pneumoniae* consists of a BLUF photosensor connected to an EAL effector.<sup>31</sup> Hydrolysis of c-di-GMP catalyzed by BlrP1 was modestly upregulated by BL but more strongly by pH changes. In a recent study, a fragment, termed EB1, of the *Magnetococcus marinus* BldP protein comprising BLUF and EAL domains was generated.<sup>285</sup> C-di-GMP hydrolysis activity of EB1 was upregulated by more than 30-fold under BL. Certain EAL effectors are connected to LOV rather than BLUF photosensors, e.g., in a photoreceptor from *Synechococcus elongatus* denoted SL2.<sup>284</sup> However, BL exposure only triggered a modest increase in EAL activity of SL2. Rather than by subjecting EAL activity under direct BL control, optogenetic perturbation of c-di-GMP-mediated processes, e.g., biofilm formation, was recently achieved by expression of a constitutively active EAL protein in light-dependent manner.<sup>300</sup> In combination with red-light-regulated GGDEF enzymes, BlrP1, EB1, SL2 and related BL-regulated EAL enzymes unlock optogenetic perturbation of diverse physiological processes in bacteria that are mediated by c-di-GMP.<sup>299</sup> Beyond targeting these processes, c-di-GMP-dependent genetic circuits were built that allow regulation of gene expression as a function of red light.<sup>282,283</sup> Moreover, c-di-GMP and c-di-AMP trigger the STING response which forms part of the vertebrate innate immune system.<sup>301</sup> Briefly, the presence of double-stranded DNA in the cytosol indicates the presence of a pathogen and leads to activation of the eukaryotic cGAMP synthase which produces the mixed cyclic dinucleotide cyclic GMP-AMP (cGAMP).<sup>302</sup> cGAMP, c-di-GMP and c-di-AMP bind to STING and thereby activate a number of downstream immune responses including induction of interferon  $\beta$ . Light-regulated enzymes of prokaryotic provenance that make or break cyclic dinucleotides thus hold immediate optogenetic potential for interrogating the vertebrate innate immune system.

**4.6.2. Calcium Ions**—Calcium is one of the most widely used second messengers that impacts on multiple physiological processes, among them gene expression, allosteric regulation of enzyme activity, nerve excitability, muscle contraction and apoptosis.<sup>303</sup> Although calcium is present in the extracellular space in millimolar concentrations, in the cytosol of eukaryotic cells the concentration is kept at sub-micromolar levels via the action of  $\text{Ca}^{2+}$ -ATPases and  $\text{Ca}^{2+}$  antiporters that actively transport calcium ions to the outside of the cell or into intracellular storage compartments, in particular the endoplasmic (or, sarcoplasmic) reticulum (ER). During signal transduction,  $\text{Ca}^{2+}$ -specific ion channels in the plasma or ER membrane are opened to allow passive influx of calcium ions along the electrochemical gradient. Calcium-dependent signaling generally involves spatial and temporal microdomains of elevated  $\text{Ca}^{2+}$  concentration.<sup>303</sup> Given the preeminent role of



in the above STIM:Orai1-based approaches larger BL-induced increases in intracellular calcium levels can be effected. Conceptually similar to PACR, a photoreceptor was engineered that specifically releases  $Zn^{2+}$  ions under BL.<sup>310</sup> A chimeric protein was constructed in which two copies of the *NcVivid* LOV photosensor bracket a tandem fusion of the Atox1 and WD4 proteins which bind at their interface a  $Zn^{2+}$  ion with picomolar affinity. BL induced homodimerization of *NcVivid* that in turn resulted in splaying apart of the Atox1:WD4 interface and concomitant release of the bound zinc ion. A palette of protein variants offered different zinc dissociation constants and BL-induced decreases of ion affinity by up to around 50-fold.

## 4.7. Receptor Signaling Cascades

In mammalian cells, an interconnected network of receptor signaling pathways couples extracellular stimuli to intracellular responses.<sup>278</sup> Ligand binding to the extracellular portion of a transmembrane receptor alters the activity of its intracellular portion and leads to the triggering of signal cascades. Several of the major signaling pathways in mammalian cells have now been unlocked for optogenetics. While GPCRs were rendered light-responsive mostly by employing rhodopsin photoreceptors (reviewed in this issue by Bamberg), other receptors and pathways have been put under BL control by using LOV and cryptochrome photoreceptors.

### 4.7.1. Mitogen-Activated Protein Kinase Pathways

**4.7.1.1. MAPK/ERK Pathway:** The mitogen-activated protein kinase (MAPK) pathway is usually triggered by binding of extracellular ligands, e.g., epidermal growth factor (EGF), to a cognate transmembrane receptor tyrosine kinase (RTK).<sup>278</sup> In response, the RTK autophosphorylates and thus turns on adapter proteins that act as a nucleotide exchange factor for the Ras GTPase. GTP-bound Ras then activates a MAP3K (MAPK kinase kinase), e.g., c-Raf, which in turn phosphorylates and thereby activates a MAP2K (MAPK kinase), e.g., MEK. Phosphorylated MAP2K acts as a kinase on the MAPK, e.g., ERK, which then activates by phosphorylation downstream effectors that usually exert gene-regulatory function, e.g., the transcription factor Fos.

Several research groups realized that ligand binding to RTKs often entails receptor dimerization as part of the activation mechanism which provides a leverage point for optogenetics (Fig. 21).<sup>190,311,312</sup> Grusch *et al.*<sup>190</sup> substituted the extracellular ligand-binding domain of the fibroblast growth factor (FGF) receptor tyrosine kinase for an intracellularly placed photoassociating LOV photosensor from the *V. frigida* or *P. tricornutum* aureochromes. BL could trigger dimerization of the modified RTK, termed opto-mFGFR1, and activation of the downstream MAPK/ERK pathway in mammalian cells, leading for example to gene-regulatory and cell-morphological responses. In at least one cell type, the PI3K/Akt pathway, cf. section 4.7.2., was activated in addition. Interestingly, no light regulation of RTK activity was obtained when employing photoassociating LOV domains other than the ones from the aureochromes. This finding could reflect that in the natural aureochrome receptors the LOV photosensor is situated C-terminally of the effector, thus resembling the arrangement in opto-mFGFR1, whereas the other LOV photosensors are invariably N-terminally situated in their parental receptors. The underlying modular design



strategy giving rise to opto-mFGFR1 proved portable and could endow the EGF and hRET RTKs with BL sensitivity, too. BL-regulated RTKs may empower drug development as they enable all-optical screening of candidate compounds affecting receptor signaling pathways, as recently demonstrated.<sup>313,314</sup> Following a rationale similar to that of Grusch *et al.*, a BL-controlled variant of the FGF receptor, denoted optoFGFR1, was obtained by fusing the intracellular C terminus of the FGF RTK to ACRY2.<sup>312</sup> BL promoted ACRY2 association and activation of the downstream MAPK/ERK, PI3K/Akt and phospholipase C $\gamma$  pathways. Using optoFGFR1, cytoskeleton dynamics, polarity and formation of lamellipodia in mammalian cells were controlled by BL, cf. section 4.4. Repetitive localized illumination induced cells to undergo phototaxis. A third approach<sup>311</sup> also subjected RTK signaling to BL control via intracellular fusion with ACRY2. Corresponding light-regulated variants of the tropomyosin-related kinases (Trk) A, B and C, denoted optoTrkA-C, triggered the MAPK/ERK and PI3K/Akt pathways in BL-activated manner. OptoTrkB allowed to control by BL the morphology of neuronal cells. Because in the optoFGFR1<sup>312</sup> and optoTrk<sup>311</sup> approaches the extracellular portions of the RTKs were left intact, the resultant optogenetic actuators retained sensitivity to the original extracellular ligands. All three approaches<sup>190,311,312</sup> have in common that a suitably modified BL-sensitive RTK needs to be transfected into target cells, potentially leading to non-physiological expression levels and background stemming from the endogenous RTK repertoire. To overcome this deficiency, the CLICR approach allows the optogenetic control of endogenous receptors and RTKs (Fig. 21).<sup>315</sup> In this strategy, ACRY2 was fused to a SH2 domain that specifically binds to the intracellular part of several RTKs. BL-induced ACRY2 clustering thus promoted association of RTKs, autophosphorylation and activation of the MAPK/ERK and PI3K/Akt pathways. Similar to the above studies, CLICR mediated BL-promoted formation of lamellipodia and phototaxis of mammalian cells. By exchanging the SH2 domain for other interacting domains, different subsets of RTKs and other receptors were targeted.

Optogenetic control of MAPK pathways was also realized at downstream nodes, thus effectively bypassing the RTKs and facilitating dissection and more precise interrogation of signaling cascades. In two similar approaches,<sup>316,317</sup> ACIB1 was directed to the plasma membrane via a lipid anchor, and c-Raf was fused with ACRY2. BL hence promoted translocation of c-Raf to the membrane which triggered its activation and that of the downstream MAPK/ERK pathway. Similar responses were elicited by BL as for the above light-regulated RTKs, including cell differentiation and proliferation. In a later report,<sup>318</sup> a similar system was applied in *Xenopus* embryos where it allowed to control by BL the MAPK/ERK pathway and developmental processes. The activation of c-Raf can also be accomplished remote from the plasma membrane via homodimerization or heterodimerization with the isoform B-Raf (Fig. 21).<sup>319</sup> To this end, ACRY2 was fused with c-Raf to allow BL-driven clustering and kinase activation. As an alternative to the homooligomerization of ACRY2, its BL-induced interaction with ACIB1 was exploited to assemble c-Raf:c-Raf homodimers or c-Raf:B-Raf heterodimers. By all approaches, BL activation of the MAPK/ERK pathway was achieved, thus for example providing a platform for the characterization of inhibitors of different Raf isoforms.<sup>320</sup>

**4.7.1.2. Other MAPK Pathways:** Two other mammalian RTK/MAPK pathways lead to the activation of the MAPKs JNK and p38 which are involved in cell differentiation, stress adaptation and apoptosis.<sup>278</sup> As JNK and p38 are regulated by several joint MAP3K and MAP2K enzymes, independent activation and detailed study of the interlocked pathways is challenging. As a possible remedy, light-activated specific inhibitors of JNK and p38 were established as optogenetic actuators.<sup>321</sup> By appending different peptide epitopes to the Ja helix of the *AsLOV2* photosensor, their solvent exposure and inhibitory effect on JNK and p38, respectively, could be regulated by BL.

To control by BL the MAPK mating pathway in yeast, the TULIP system for light-induced PPIs was engineered based on *AsLOV2*.<sup>258</sup> Using TULIP, the scaffolding protein Ste5 that spatially arranges the individual pathway components was recruited to the plasma membrane in BL-activated manner and MAPK signaling thus turned on. Alternatively, activation of the MAPK mating pathway was accomplished by recruiting the MAP3K of this pathway, Ste11, to the membrane upon BL stimulation.

**4.7.2. PI3K/Akt Pathway—**As another signaling cascade that is activated by RTKs and GPCRs, the PI3K/Akt pathway mediates cell proliferation, survival and migration, among other responses.<sup>278</sup> Upon activation by membrane receptors, PI3K (phosphatidylinositol 3-kinase) catalyzes the phosphorylation of the phospholipid phosphatidylinositol (PI) at several positions to yield various phosphoinositides. Diverse physiological and metabolic processes,<sup>322</sup> e.g., endocytosis, exocytosis, cell motility, cell adhesion and regulation of ion channels, are regulated by phosphoinositides, often in concert with other signaling pathways. Successive phosphorylation of PI by PI3K generates PI(3,4,5)P<sub>3</sub> which binds to Akt (also known as protein kinase B), thus allowing its membrane association and activation through phosphorylation. In turn, activated Akt phosphorylates and thereby regulates a series of downstream effectors. PI3K is counteracted by phosphatases that remove phosphoryl groups from PI(3,4,5)P<sub>3</sub> and other phosphoinositides. Moreover, the hydrolysis of PI(4,5)P<sub>2</sub> by phospholipase C yields the second messengers IP<sub>3</sub> (inositol-1,4,5-trisphosphate) and DAG (diacyl glycerol).<sup>278</sup>

Optogenetic control over the PI3K/Akt cascade has been established at several levels (Fig. 22). Owing to the interconnectedness of signaling networks, several of the above approaches for regulation by BL of MAPK pathways could also elicit activation of the PI3K/Akt pathway, e.g., the CLICR method.<sup>315</sup> Alternatively, optogenetic intervention in PI signaling was achieved by regulating the activity of PIP<sub>x</sub> phosphatases and kinases in BL-dependent manner.<sup>323,324</sup> By tethering *AtCIB1* to the plasma membrane, fusions between *AtCRY2* and desired effector enzymes acting on PIP<sub>x</sub> could be recruited to the plasma membrane and hence activated.<sup>323</sup> Light-induced activation of a PIP<sub>x</sub> phosphatase locally depleted PIP<sub>3</sub> and PIP<sub>2</sub> with effects on clathrin-mediated endocytosis, cytoskeleton dynamics and ion-channel activity in mammalian cells. *Vice versa*, recruitment of PI3K locally increased PIP<sub>3</sub> and PIP<sub>2</sub> amounts and impacted on cytoskeleton dynamics (cf. sec. 4.4.). In a closely similar approach,<sup>267</sup> the iLID system served to recruit upon BL exposure a PIP<sub>x</sub> phosphatase to the plasma membrane of pancreatic cells. The resultant local depletion of PIP<sub>x</sub> caused membrane-docked secretory vesicles to detach, thereby interfering with insulin secretion from these vesicles. Employing a shared principal design strategy, three groups<sup>325–327</sup>

targeted Akt, downstream of PI3K. *AiCIB1* was tethered to the plasma membrane, and an Akt-*AiCRY2* chimera could be recruited under BL. Membrane localization of Akt prompted its phosphorylation, resulting in activation of the PI3K/Akt pathway,<sup>326</sup> e.g., to elicit vesicle transport in adipocytes.<sup>325</sup> Notably, one of the downstream targets of Akt is Bad that is engaged in eliciting apoptosis; optogenetic control over the PI3K/Akt pathway may hence provide the means of controlling cell survival, cf. sec. 4.8.

**4.7.3. Other Receptor Signaling Pathways**—The Wnt signaling pathway is triggered by binding of a Wnt-family glycoprotein to a complex formed by a GPCR of the Frizzled family and coreceptors, e.g., LRP6.<sup>278</sup> Activation of the so-called canonical Wnt/ $\beta$ -catenin branch of the pathway depends on signal-induced clustering of the Frizzled:LRP6 complex which promotes intracellular stabilization of  $\beta$ -catenin. In turn,  $\beta$ -catenin accumulates, translates to the nucleus, forms higher-order oligomers and activates gene expression. By linking *AiCRY2* to a C-terminal fragment of LRP6, clusters of this fragment could be formed under BL and downstream  $\beta$ -catenin-mediated responses be triggered in mammalian cells.<sup>65</sup> In another study, the activity of  $\beta$ -catenin was optogenetically controlled via fusion to *AiCRY2*<sup>328</sup> to achieve BL-induced protein clustering. Conceptually similar to the LARIAT strategy,<sup>242</sup> sequestration of  $\beta$ -catenin into the photodynamically-formed clusters reduced its activity and allowed modulation of *Drosophila* development.

As transmembrane receptors, integrins are engaged in the bidirectional signaling between the cell exterior, i.e. cell-matrix and cell-cell interactions, and the cell interior.<sup>278</sup> Upon activation, integrins interact with intracellular kindlin and talin adapter proteins to trigger a series of downstream responses including activation of the focal adhesion kinase (FAK). To control these signaling processes by light, the interaction between integrin and kindlin was first disrupted via C-terminal truncation of the integrin.<sup>329</sup> The integrin:kindlin interaction and downstream signaling could then be rescued in light-activated manner by employing the TULIP system for heterodimerization.<sup>258</sup> Using this strategy, cell adhesion and migration of endothelial cells could be promoted and controlled by BL, cf. sec. 4.4. A related study optogenetically targeted FAK downstream of the integrin receptor.<sup>330</sup> FAK was C-terminally connected to *AiCRY2* to allow for BL-induced clustering, resultant autophosphorylation and concomitant activation of this kinase. The BL-activated FAK variant is suited to study the lower branches of the signaling network without upstream input by the integrin receptors. Similar to integrins, ephrin RTKs are also involved in bidirectional signaling between adjacent cells. Employing the same rationale as for the OptoTrks,<sup>311</sup> light sensitivity was bestowed on the ephrin receptor via C-terminal fusion with the Cry2olig variant of *AiCRY2*.<sup>331</sup> BL accordingly prompted RTK clustering, autophosphorylation and activation. Using the light-regulated ephrin RTK variant, actin cytoskeleton rearrangements and formation of filopodia could be triggered, cf. sec. 4.4. A related rationale also underpins the engineering of a BL-regulated variant of the transforming-growth-factor (TGF)  $\beta$  receptor.<sup>332</sup> The heterooligomeric TGF receptors are naturally activated upon ligand-induced association and resultant phosphorylation.<sup>278</sup> To control heterooligomer formation and downstream pathway activation by BL, the transmembrane and intracellular segments of one TGF receptor subunit was fused with *AiCIB1*, and the cytosolic portion of the other subunit

was connected to *AtCRY2*. BL illumination triggered subunit association and activation of the TGF  $\beta$  pathway.

Lastly, pattern recognition receptors (PRR) are parts of the innate immune system and mediate the detection of pathogen-associated molecular patterns. As one PRR, DAI resides in the cytosol and homodimerizes upon binding double-stranded DNA (of pathogenic origin). Dimerization of DAI prompts expression of target genes and downstream immune responses, in particular programmed necrosis of the infected cell.<sup>333</sup> To subject DAI activity to BL control, two copies of DAI were fused with *AtCRY2* and *AtCIB1*, respectively.<sup>334</sup> In mammalian cells, BL triggered DAI dimerization and thereby induced expression of target genes. Owing to homooligomerization of *AtCRY2*, a BL effect could also be elicited with DAI-*AtCRY2* in the absence of DAI-*AtCIB1*.

#### 4.8. Apoptosis

Apoptosis denotes the programmed cell death in multicellular eukaryotic organisms<sup>335</sup> and involves the successive activation of caspase cysteine proteases, mostly via proteolytic cleavage of pro-caspase precursors. Several intrinsic and extrinsic pathways lead to activation of initiator caspases, in particular caspase-9, and thereby initiate apoptosis. Once turned on, initiator caspases activate downstream executioner caspases, e.g., caspase-3 and caspase-7, by proteolytic cleavage. In turn, the executioner caspases operate on a number of targets, eventually culminating in the controlled destruction of the entire cell. Optogenetic control over apoptosis has been implemented at several stages (Fig. 23). A possible avenue towards controlling apoptosis by BL is provided by the PI3K/Akt pathway, cf. sec. 4.7.2., because one of the targets of this pathway is the proapoptotic protein Bad which upon phosphorylation is inhibited in mediating apoptosis. Another strategy directly targeted the initiation of apoptosis by the proapoptotic protein Bax.<sup>336</sup> Once activated by upstream events, Bax translocates to the outer mitochondrial membrane where it oligomerizes and contributes to perforating the mitochondrion.<sup>335</sup> Resultant outflow of cytochrome c from the mitochondrial intermembrane compartment causes activation of the cytosolic initiator caspase-9. By fusing *AtCIB1* to a protein within the outer mitochondrial membrane, *AtCRY2*-linked Bax could be recruited there in BL-dependent fashion and downstream apoptotic events be initiated. Using this approach, a 3.5-fold increase in the concentrations of activated executioner caspase-3 could be elicited in mammalian cells by BL. Optogenetic control was also exerted at the level of the initiator and executioner caspases. By connecting the catalytic domain of caspase-9 to the *NcVivid* photosensor, this caspase could be dimerized and its activity increased under BL,<sup>215</sup> even in the absence of cytosolic cytochrome c. In a viability assay, apoptosis was observed for few cells in darkness but for around half of the cells under BL. Furthermore, the catalytic activity of the executioner caspase-3 was directly regulated via insertion of the *AsLOV2* domain into a linker connecting two caspase subunits.<sup>337</sup> In the resultant enzyme, BL promoted a 2- to 3-fold enhancement of caspase activity, and studies in *Drosophila* demonstrated that the caspase-3 variant elicited apoptosis in BL-stimulated manner. In another approach, executioner caspase activity was regulated in BL-dependent manner by fusing the *AsLOV2* photosensor domain to the catalytic domain of caspase-7.<sup>277</sup> In darkness, steric occlusion between the two domains led to impairment of enzymatic activity; light-induced J $\alpha$  unfolding presumably

promoted domain dissociation and increase of caspase activity. Although the engineered photoreceptor induced apoptosis even in darkness, the efficiency of doing so could be upregulated by BL.

As a possible alternative to the above methods for BL-induced apoptosis, one may resort to optogenetic actuators for cell ablation that are based on incapacitated LOV sensors that produce ROS upon BL illumination (cf. sec. 5.). However, cell ablation may lead to uncontrolled cell death (necrosis) as opposed to apoptosis.

#### 4.9. Enzyme Activity

The previous sections have encountered a palette of BL-regulated enzymes in the context of epigenetic chromatin modifications (sec. 4.2.), cyclic nucleotides (section 4.6.1.), signaling cascades (section 4.7.) and apoptosis (section 4.8.). This section now explores how BL can be harnessed to modulate the activity of other enzymes. Specifically, metabolic pathways could thus be regulated by BL, conceivably leading to innovative biotechnological applications. Depending on the spatial and temporal resolution a given application demands, several general albeit mostly slower-acting strategies may apply. Short of directly regulating by BL enzymatic activity, one could instead regulate the expression of the enzyme of interest as a function of BL by resorting to well-established and versatile optogenetic actuators (cf. sec. 4.1.).<sup>198</sup> *Vice versa*, BL-promoted protein degradation (cf. sec. 4.5.) provides an avenue for downregulating enzymatic activity as has been demonstrated for a biosynthetic pathway in yeast.<sup>271</sup> Rather than degrading target enzymes, their activity levels may also be reduced reversibly by BL-induced sequestration into organelles and protein-based compartments (cf. sec. 4.3.3.). For example, the LARIAT approach<sup>242</sup> is suited for sequestering proteins of interest into clusters which may well entail attenuation of enzymatic activity. Beyond these general strategies for optogenetic actuation, several directly BL-regulated enzymes have been engineered.

In one of the early examples of photoreceptor engineering,<sup>338</sup> the catalytic activity of the *E. coli* dihydrofolate reductase enzyme that regenerates the important metabolic cofactor tetrahydrofolate was modestly regulated by BL. To achieve light sensitivity, the AsLOV2 photosensor was inserted via its N-terminal A'  $\alpha$  and its C-terminal Ja helices into a surface loop of dihydrofolate reductase known to be sensitive to modifications. One variant showed up to 2-fold BL-induced enhancement of enzymatic turnover albeit at the cost of a  $10^3$ -fold decrease in overall catalytic activity and a strong reduction of substrate affinity. Also via insertion of AsLOV2 into a surface loop, the catalytic activity of a mammalian pyruvate kinase that catalyzes the final step in glycolysis was subjected to BL control.<sup>339</sup> In the resultant chimeric enzyme, BL exposure elicited a 40% enhancement of substrate affinity as measured by steady-state kinetics. When expressed in mammalian cells, a modest BL-induced increase of catalytic activity could be detected. Although to date the performance of BL-regulated metabolic enzymes evidently leaves wanting, recent progress in photoreceptor engineering, especially reference<sup>109</sup>, could greatly benefit future efforts in this area.

Although beyond the scope of the present review, we note that, rather than being regulated by BL, a small set of enzymes directly harvest the energy contained in BL to drive demanding chemical conversions. Put another way, photons are to be considered a substrate

in these enzymatic reactions. The best-known representatives are the DNA photolyases which are homologous to cryptochromes (cf. sec. 2.1.3.), absorb BL via FAD cofactors and revert certain types of UV-induced damage, e.g., thymine dimers.<sup>340</sup> Excitingly, a groundbreaking report recently identified a metabolic enzyme from *Chlorella variabilis* that bears a FAD chromophore and harnesses BL energy to catalyze the decarboxylation of fatty acids to long-chain alkanes and alkenes.<sup>3</sup> Even earlier, an artificial system was constructed in which the FAD cofactor of a monooxygenase enzyme could be regenerated in light-driven manner in the presence of sacrificial electron donors.<sup>341,342</sup>

#### 4.10. Ion Channels & Synaptic Communication

A vast body of optogenetic experiments in the neurosciences rely on channelrhodopsins that serve as light-gated channels for cations<sup>75,76</sup> and, more recently, for anions.<sup>343–345</sup> Despite the immense utility of ChRs, there is scope for diversifying and improving light-gated ion channels, in particular with regards to their ion selectivity and conductivity. First, ChRs show little ion specificity, with the conventional ChRs<sup>75,76</sup> largely indiscriminately conducting several different mono- and divalent cations and protons. Second, the unitary conductance of a single ChR channel is low compared to other ion channels, particularly those engaged in the nervous system. Against this backdrop, several efforts have been undertaken to bestow light sensitivity on ion channels that possess high conductance and ion selectivity but that are normally light-inert (Fig. 24). Because certain ion channels are gated by second messengers, optogenetic actuators that modify the intracellular concentration of these second messengers can be harnessed to control by light ion-channel activity. For this application, PACs<sup>93,94,279,280</sup> are combined with CNG channels to trigger by BL channel opening, as illustrated above (cf. sec. 4.6.1., Fig. 24). Similarly, certain ion channels that are modulated in their activity by phosphoinositides<sup>322</sup> hold potential for optogenetic perturbation.

As already discussed in section 4.6.2., BL photoreceptors have been used to control gating of the Ca<sup>2+</sup>-specific CRAC channels and of voltage-gated calcium channels (Figs. 20 and 24).<sup>124,304,305,307,308</sup> An optogenetic approach<sup>348</sup> was also used to modulate by BL the Ca<sup>2+</sup> conduction through the voltage-dependent Ca<sub>v</sub>1.2 channel which is expressed in smooth muscle. Cluster formation of Ca<sub>v</sub>1.2 channels allows mutual interactions that modulate the gating dynamics and ion conductivity. The linkage of two copies of Ca<sub>v</sub>1.2 to either *A1FKF1* or *A1GI* allowed the average Ca<sub>v</sub>1.2 cluster size to be increased via the BL-induced formation of the *A1FKF1:A1GI* heterodimer. In ventricular myocytes, the voltage dependence of channel gating was thus altered by BL, the coupling between adjacent channels strengthened and thereby the overall Ca<sup>2+</sup> currents increased. In addition to Ca<sup>2+</sup>-specific channels, light-gated variants of ion channels selective for K<sup>+</sup> are of key interest because they could facilitate optogenetic silencing of excitable cells (Fig. 24). To this end, the so-called lumitoxins were constructed which connect a peptide toxin to a membrane-anchored *AsLOV2* photosensor.<sup>346</sup> In darkness, the toxin can bind to voltage-dependent potassium channels (K<sub>v</sub>) and thereby block ion conductance. BL-promoted Jα unfolding increased the average distance between the toxin and the membrane anchor such that the toxin could dissociate from the K<sub>v</sub> channel and thereby relieve channel blocking. In mammalian cells, the lumitoxins mediated the BL-dependent unblocking of specific K<sub>v</sub>

channels. By exchanging the toxin domain for other variants, different subsets of  $K_v$  channels could be selectively targeted. A different strategy was pursued in the engineering of the BL-gated  $K^+$  channel BLINK (Fig. 24).<sup>347</sup> The *AsLOV2* photosensor was linked via its C-terminal  $J\alpha$  helix to the N terminus of a minimal  $K^+$  channel of viral origin. Different linker and mutant variants of the chimeric protein were selected in yeast for light-regulated channel activity. The best performing construct, denoted BLINK, showed around 3-fold BL-induced increases of  $K^+$  conductivity in both frog oocytes and mammalian cell culture. Transient expression of BLINK in zebrafish embryos allowed modulation of their touch-induced escape response by BL. Although both the lumitoxins and BLINK offer room for improvement, their successful construction clearly demonstrates that light-induced channel gating is not restricted to rhodopsin photoreceptors nor to unspecific ion channels. Improved versions stand to become important optogenetic tools for the neurosciences.

Finally, BL-responsive photoreceptors were also employed to perturb and investigate neurotransmission through chemical synapses.<sup>349</sup> To this end, *ArcRY2* was directed to the postsynaptic density (PSD) via fusion to PSD scaffold proteins. BL was then applied to induce recruitment of *ArcCIB1*-linked AMPA-type glutamate receptors to the PSD. Resultant BL-induced elevated concentrations of AMPA receptors at the PSD were found to enhance excitatory neurotransmission. In addition, previous work<sup>52</sup> had shown that *ArcRY2* directed to the PSD can induce protein clustering at this site which could also provide an avenue towards modulating synaptic transmission.

## 5. Off-Label Use of Photoreceptors

Optogenetics in general and its numerous specific manifestations covered in section 4. capitalize on the ability of sensory photoreceptors to autonomously bind and functionally reconstitute their chromophores *in situ*. Flavin compounds, utilized by the BL-sensitive photoreceptors discussed here, ubiquitously recur as essential metabolic cofactors across many cell types and organisms, therefore allowing the versatile deployment of genetically-encoded optogenetic tools without the exogenous addition of non-native chromophores. These favorable attributes also enable modified versions of the BL-sensitive photoreceptors to serve in ‘off-label’ applications as fluorescent proteins (cf. sec. 5.1.) and generators of reactive oxygen species (cf. sec. 5.2.) rather than as signal receptors (Fig. 25). In sec. 5.3., we discuss mounting evidence that flavin-based receptors can be sensitive to oxygen and redox potential under physiological conditions, with consequences both intended, e.g., when deliberately using them as sensors for these parameters, and unintended, e.g., when these parameters influence the outcomes of optogenetics experiments.

### 5.1. Photoreceptors as Fluorophores

The relatively high fluorescence quantum yield of LOV domains ( $\Phi_F$  ca. 0.1-0.5 in the dark-adapted state for wt proteins) allows cellular applications based on fluorescence.<sup>350,352,353,356-358</sup> Collectively called flavin-mono-nucleotide-binding Fluorescent Proteins (FbFPs), LOV domains have been first introduced as fluorescent reporters of choice for anaerobic or microaerobic environments.<sup>359</sup> The ability to functionally incorporate their flavin chromophores in the absence of oxygen and their smaller size represent substantial

advantages over GFP (Green Fluorescent Protein) and structurally related FPs, which are significantly larger and require O<sub>2</sub>-dependent chromophore maturation.<sup>351</sup> FbFPs also form the basis of the genetically-encoded photosensitizers for the generation of singlet oxygen, the development and optogenetic applications of which are discussed in section 5.2. The fluorescence in LOV domains is lost upon formation of the thioadduct-containing signaling state LOV<sub>390</sub>, and if this last process is prevented by removal of the reactive cysteine, a permanently fluorescent molecule is yielded with  $\Phi_F$  between 0.13 and 0.51, and a molar brightness between 1,850 and 6,380 M<sup>-1</sup> cm<sup>-1</sup>.<sup>360,361</sup> The main photophysical parameters of FbFPs are summarized in Table 1.

In the seminal work of Drepper *et al.*,<sup>359</sup> two bacterial proteins – YtvA from *B. subtilis* (Uniprot code O34627) and SB2 from *Pseudomonas putida* (Q88JB0) – served as starting points to engineer BsFbFP (261 aa) and PpFbFP (149 aa), respectively. In both cases, the reactive cysteine was changed into alanine; in addition, BsFbFP was truncated to solely encompass its LOV domain (aa 1-137) and codon-optimized for *E. coli* expression to yield the well-known EcFbFP. These novel FP were tested in the facultative aerobic *Rhodobacter capsulatus* and in mammalian cells, and were found to be fluorescent under both standard and O<sub>2</sub>-depleted conditions. Soon afterwards, iLOV was engineered based on the LOV2 domain from *A. thaliana* phototropin 2 and was used for studying the dynamics of viral infections in plants and animal cells.<sup>362,363</sup> iLOV bears six mutations (R386F, S394T, S409G, C426A, I452T, F470L) which cumulatively enhanced fluorescence to  $\Phi_F = 0.32$  and minimized irreversible photobleaching. Notably, tagging viruses with GFP-derivatives often resulted in decreased infectivity and loss of FP through recombination events because of the limited size of viral genomes and high recombination rate. The smaller size of iLOV (ca. 11 kDa, ca. 55% the size of GFP) apparently overcame this problem and allowed optimal packing within the viral genome.<sup>362</sup> Furthermore, distinct from GFP, the lack of an obligate post-translational maturation step permitted visualization of the infection dynamics on the minutes timescale. Generally, the small size of FbFPs permits applications where steric constraints might impair protein translocation, for example allowing them to be applied to studies of *E. coli* infections.<sup>364</sup> In other words, this first wave of FbFPs demonstrated that LOV domains can be engineered into oxygen-independent, small and minimally perturbative fluorescent reporters.<sup>121</sup> Several variants of iLOV were later developed that bear additional mutations, with the aim of increasing photostability. Among these, phiLOV2.1 revealed that the N390S and N401Y changes are crucial for attaining this goal, likely by indirectly anchoring and rigidifying the FMN chromophore.<sup>365</sup> Strictly related to iLOV are miniSOG and derived genetically-encoded photosensitizers for reactive oxygen discussed in section 5.2. Extensive characterization of iLOV, Pp2FbFP and EcFbFP demonstrated further useful qualities of LOV-based FPs: a broad functional pH range with fluorescence largely retained between pH 4 and 11; high thermal stability of up to 60°C for iLOV; persistence of fluorescence under strongly reducing conditions up to a reduction potential of –660 mV; retention of oligomeric state with iLOV being a monomer and the other two proteins stable dimers; reliable detection of protein expression kinetics thanks to fast and complete maturation, even in bioprocesses that have semi-aerobic or anaerobic stages.<sup>366</sup>

Since, researchers have tried to further improve FbFPs by addressing one of several shortcomings. The relatively low molar brightness, generally one order of magnitude below



GFP-related FPs, has been slightly improved by engineering novel proteins from the algae *C. reinhardtii* (C<sub>1</sub>LOV) and *V. frigida* (V<sub>1</sub>LOV). C<sub>1</sub>LOV has a large  $\Phi_F = 0.51$  and the largest relative brightness ( $6,375 \text{ M}^{-1} \text{ cm}^{-1}$ ) so far reported for any FbFP, but the relatively low absorption of flavins intrinsically limits this parameter.<sup>361</sup> Thermal and photostability were further improved with novel FbFPs from thermostable bacteria, among which the most promising specimens were derived from *Meiothermus ruber* (M<sub>r</sub>FbFP) and a metagenomic sequence from Yellowstone National Park (“Chocolate Pots”, YNP3FbFP). The group of newly characterized FbFPs from thermostable organisms showed an array of different fluorescence lifetimes, from 1.5 to 4.6 ns, thus making them promising candidates for multitarget labeling in a fluorescence lifetime imaging (FLIM) approach.<sup>361</sup>

The strongest limitations of FbFP are represented by their relatively low brightness, as mentioned above, and by the difficulties in tuning their absorption and fluorescence maxima towards the red flank of the visible spectrum, that is considered the most useful for animal applications.<sup>121</sup> Despite many attempts by mutagenesis approaches, the natural chromophores of LOV domains have not been successfully red-shifted, cf. section 3.2.2. Rational optimization of spectral properties is complicated by the difficulty of predicting fluorescence excitation and emission spectra. As a case in point, the Q489K mutation in iLOV was calculated to have 52 and 97 nm red-shifts in the fluorescence excitation and emission spectra, respectively,<sup>367</sup> but experimental characterization of iLOV-Q489K showed instead an 8 nm blue-shift.<sup>128</sup> Recently, it was proposed that PFbFBs could be spectrally tuned and enhanced in fluorescence by means of structurally-modified chromophores, such as lumichrome and 7-methyl-8-chloro-riboflavin.<sup>126</sup> The apoprotein W619\_1-LOV from *Pseudomonas putida* (strain W619) bound to lumichrome increased its  $\Phi_F$  to 0.4 and was ca. 30 nm blue-shifted relative to the riboflavin-bound form. This approach is extremely interesting for elucidating the structural and local chemical factors that affect the photophysical parameters of FbFPs. By contrast, optogenetic use appears limited given the requirement for non-natural chromophores.

Fluorescence applications based on FbFPs have become numerous, mostly related to anaerobic and micro-aerobic environments, metabolic stages and hypoxic niches.<sup>350–353</sup> An extensive survey of these applications goes beyond the scope of this review, but it is worth underscoring the utility of FbFPs as real-time reporters for cell processes and host-microbe interactions in anaerobic, facultative aerobic and microaerobic microorganisms of great medical or technological importance, e.g., *Listeria*,<sup>368</sup> *Porphyromonas gingivalis*,<sup>369</sup> *Saccharomyces cerevisiae* and *Candida albicans*,<sup>370</sup> *Synechocystis sp.*,<sup>371</sup> *Trichomonas vaginalis*,<sup>372</sup> *Clostridium difficile*,<sup>373</sup> and *Campylobacter jejuni*.<sup>374</sup> Another FbFP-based application is the in-cell sensing of heavy metals ions, such as mercury<sup>375</sup> and arsenic.<sup>376</sup> Exploiting their intrinsic photochromicity (cf. section 3.2.2.),<sup>157,377</sup> wt LOV domains with intact cysteine residues can also function as LOV-based FPs. The photochromicity of *BsYtvA* has been employed for localization-based super-resolution microscopy, where blue light completely switched off fluorescence and violet light recovered fluorescence at the single-molecule level, thus achieving ca. 35 nm resolution.<sup>378</sup> More recently, rsLOV1 and rsLOV2 have been developed from *BsYtvA*-LOV for RESOLFT (reversible saturable/switchable optical linear fluorescence transitions) and STED (stimulated emission depletion) nanoscopy respectively: the new variants, encompassing aa 1-137, bear several mutations;

rsLOV1 can be photoswitched with ten-fold better efficiency as wt *BsYtvA*, while rsLOV2 is more brightly fluorescent (Table 1) and has a high photostability.<sup>379</sup> Illumination with UV/violet light drove the LOV domains into a photoequilibrium by exciting both the adduct-containing LOV<sub>390</sub> and the adduct-free LOV<sub>447</sub> states, whereas BL fully converted LOV<sub>447</sub> into LOV<sub>390</sub>.<sup>159</sup> The *in vivo* relevance of such UV/violet-driven photoconversion is unknown for LOV proteins,<sup>380</sup> but this property could be useful for visualizing LOV proteins within their natural host without labeling. Doing so would combine the power of super-resolution fluorescence microscopy with optogenetics, taking advantage of the ability of LOV domains to photoactivate different biological functions (cf. sec. 4.). FbFPs can function as donors in Förster resonance energy transfer (FRET) pairs, an approach that has been used for visualizing intracellular changes in oxygen levels<sup>381</sup> and pH.<sup>382</sup> In the former case, a tandem construct, denoted FluBO, was built with *EcFpFB* as the donor and enhanced yellow fluorescent protein (EYFP) as the acceptor. Notably, EYFP only forms the chromophore and hence becomes fluorescent when O<sub>2</sub> is present. FluBO was calibrated in *E.coli* cells and changed its fluorescence properties depending on the oxygen concentration at the time that the fluorophore matures.<sup>381</sup> In a similar approach, *EcFbFP* was fused to a palette of EYFPs having different pK<sub>a</sub> values. Given that *EcFbFP* fluorescence is tolerant towards acidic conditions, it was fused as a donor domain to EYFPs with pK<sub>a</sub> values of 5.7, 6.1 and 7.5. This FRET toolbox, called FluBpH, was characterized and calibrated both in solution and *in vivo*.<sup>382</sup> Finally, a fused protein comprising the LOV domain of *BsYtvA*-C62S and a bilin-binding, photochromic (red/green absorbing form) CBCR GAF domain was recently characterized and found to constitute a good and minimal FRET pair, with three-color fluorescence.<sup>383</sup> Perspectively, these FRET pairs could take advantage of photoswitchable LOV domains retaining their native photoreactive cysteine, and could thus be used in super-resolution microscopy, cf. above.

As a whole, LOV-based FbFPs offer several advantages over GFP-related proteins owing to their smaller size, pH and thermal tolerance, utility under anaerobic conditions and ability to generate reactive oxygen species, detailed below. Nevertheless, to date FbFPs have intrinsic limitations especially in terms of relatively low molar brightness and limited spectral tunability.

## 5.2. Photoreceptors as Generators of Reactive Oxygen Species

For organisms that use flavins for photoreception, an aerobic environment represents a potential risk, because flavins are efficient photosensitizers (PS) towards molecular oxygen, leading to the formation of reactive oxygen species.<sup>384</sup> To effectively prevent harmful ROS generation inside of the cell, prokaryotes and eukaryotes accordingly implement homeostatic and protective mechanisms for preserving the integrity of the flavin cellular pool.<sup>385</sup> For example, in archaea and bacteria dodecins sequester free flavins that are liable to photo-induced degradation and ROS production; once the flavins are bound to dodecins, the excitation energy of absorbed light quanta can be rapidly dissipated via ultrafast proton and electron transfer mechanisms.<sup>386</sup> Similar mechanisms might be operating in BL photoreceptors as well. Essentially, the generation of reactive oxygen species by photosensitizers proceeds via one of two general mechanisms: in type I, a PS donates an electron to O<sub>2</sub> thereby forming the superoxide anion radical (O<sub>2</sub><sup>-</sup>); in type II

photosensitization, the triplet state of a PS performs energy transfer (ET) to O<sub>2</sub> via the Dexter mechanism, leading to transition from the triplet ground state O<sub>2</sub> to the strong oxidant, excited singlet state <sup>1</sup>O<sub>2</sub> (short <sup>1</sup>O).<sup>387</sup> Both mechanisms are diffusion-limited and require bimolecular collision between a PS excited state and oxygen; therefore, long-lived excited states of a chromophore are particularly relevant. The triplet states of both free and LOV-bound FMN (<sup>3</sup>FMN) have an energy level of ca. 200 kJ mol<sup>-1</sup>,<sup>168,388</sup> a perfect situation to perform efficient ET to oxygen and generate <sup>1</sup>O, that lies 94 kJ mol<sup>-1</sup> above the ground state O<sub>2</sub> triplet.<sup>389</sup> ET between triplet states is allowed, and for free FMN in solution it results in quite a high quantum yield for singlet-oxygen formation  $\Phi = 0.51 - 0.65$ .<sup>384,390</sup> In wt LOV domains, formation of the thioadduct with the substrate cysteine is relatively fast (2-4  $\mu$ s) and <sup>1</sup>O formation is negligible. However, recently researchers became interested in deliberately modifying LOV domains such that the triplet lifetime is extended, competitive triplet quenching reactions are minimized and the yield for <sup>1</sup>O formation is enhanced. In this manner, LOV domains became genetically encoded photosensitizers for a variety of applications, with the added values of fluorescence and of small size. The first implementation arrived with the so-called miniSOG (mini Singlet Oxygen Generator)<sup>391</sup> and derived/related proteins. This seminal work also demonstrated that a simple substitution of the reactive cysteine (e.g., with serine or alanine) is not sufficient to generate <sup>1</sup>O, even if the triplet lifetime considerably increases and becomes oxygen dependent,<sup>392</sup> meaning that FbFPs are poor <sup>1</sup>O sensitizers if they are not further engineered (cf. below). The topic of LOV-based photosensitizers has been excellently reviewed recently,<sup>354,355</sup> and we will hence summarize applications more closely related to optogenetics as well as most recent updates.

MiniSOG was first designed based on the LOV2 domain from *A. thaliana* phototropin 2 (*Atp*hot2-LOV2, UniProt P93025, residues 387492)<sup>391</sup> to be employed for CLEM (Correlative Light Electron Microscopy) (cf. sec. 5.1.).<sup>393,394</sup> In this application, miniSOG sensitized sufficient <sup>1</sup>O to locally precipitate diaminobenzidine and to allow staining with osmium contrast agents, thus combining fluorescence imaging with the high resolution of electron microscopy (EM). Six mutations were introduced into *Atp*hot2-LOV2 (numbering refers to the 106 aa sequence of miniSOG; to recover original numbering in *Atp*hot2 one must add 386): C40G, that abolishes light-induced thioether formation, to provide constitutive fluorescence and to give more space for O<sub>2</sub> diffusion to the FMN cavity; I1M, N4S, S8T, S23G and F84L to increase brightness. By using miniSOG, Shu *et al.* succeeded in discriminating the localization of two closely situated synaptic cell-adhesion molecules in cultured neurons and in intact mouse brain, thus overcoming problems arising with conventional antibody staining. CLEM applications of miniSOG have become countless and excel in terms of target discrimination and spatial resolution compared to immunolabeling and chemical staining.<sup>354,395-399</sup> In particular, miniSOG is substantially smaller than GFP-based fluorescent proteins, has low toxicity, and produces strong EM contrast.<sup>394</sup> A key question is the value of  $\Phi$  for miniSOG, initially reported as 0.47<sup>391</sup> and later corrected to 0.03 as directly detected by <sup>1</sup>O phosphorescence.<sup>400</sup> The original overestimation of  $\Phi$  was probably due the use of anthracene-9,10-dipropionic acid as the <sup>1</sup>O<sub>δ</sub> sensor, a molecule that can be also oxidized by other ROS; furthermore, prolonged illumination of miniSOG likely resulted in degradation of FMN and/or protein, with a further apparent increase in  $\Phi_{\delta}$ .<sup>401,402</sup>

A second LOV-based photosensitizer with  $\Phi = 0.09$  was later designed from *Pp2FbFP* by introducing the L30M mutation.<sup>403</sup>

Notwithstanding the relatively low value for  $\Phi$ , miniSOG served as a novel generator for intracellular  $^1\text{O}$  in *E. coli*, thus confirming the *in vivo* efficiency of this photosensitizing, LOV-derived protein.<sup>404</sup> A substantial improvement of  $\Phi$  from 0.03 to 0.25 was achieved with the Q103L mutation, a substitution that removes hydrogen bonds between residue 103 and position C=O(4) of FMN.<sup>402</sup> The new derivative was called SOPP (singlet oxygen protein photosensitizer), and proved more efficient than miniSOG for both *in vitro* and *in vivo* studies.<sup>399,405</sup> The Q103V variant of SOPP had an even larger  $\Phi = 0.39$ .<sup>399</sup> Partial disruption of the hydrogen-bond network around FMN in SOPP resulted in a protein matrix that facilitates  $\text{O}_2$  diffusion, in a less efficient  $^3\text{FMN}$  quenching by electron transfer from the protein (due to larger electron density on the chromophore) and in a reduced rate of  $^3\text{FMN}$  deactivation by electronic-to-vibrational energy transfer.<sup>390,402</sup> Nevertheless, even if  $\Phi$  for SOPP increased with temperature between 10 and 43°C (up to 0.27), it did not reach the value of ca. 0.6 for free FMN: encapsulation of the protein within a protein matrix obviously hinders bimolecular collision with  $\text{O}_2$ .<sup>390</sup> Among the latest developed is miniSOG2, involving seven novel mutations: G22S, G40P, Q44R, R57H, L84F, H85R, M89I, some of which affect residues in close proximity to the chromophore (residues 40, 44, 57, 84) and are likely responsible for the 20 nm blue-shift in absorption and fluorescence spectra.<sup>406</sup> The value of  $\Phi$  for miniSOG2 remains to be determined. Very recently, Westberg and collaborators managed to rationally engineer very efficient variants of SOPP, named SOPP2 (W81L/L103V) and SOPP3 (W81L/H85N/M89I/Y98A/L103V).<sup>407</sup> Notably, residue W81 was identified as the most efficient electron donor for quenching of  $^3\text{FMN}$  in SOPP. The new variants have  $\Phi = 0.57$  and 0.6 respectively, reaching the value for free FMN in air (21 %  $\text{O}_2$ ). Most importantly, at 5 %  $\text{O}_2$ , that is closer to cellular conditions, they keep high  $\Phi$  values of 0.27 (SOPP2) and 0.50 (SOPP3). SOPP3 is presently the best photosensitizing protein at hand, and also brightly fluorescent with  $\Phi_F = 0.41$ .<sup>407</sup> A very recent development combines miniSOG or its Q103V variant, with phiLOV2.1 to produce phiSOG heterodimers that combine efficient DAB photo-oxidation (miniSOG-Q103V) and photostability (phiLOV2.1) (see Table 1).<sup>408</sup>

Beyond CLEM, optogenetic applications of LOV-derived PS for ROS production include chromophore-assisted light inactivation (CALI) of biological macromolecules, photo-induced cell ablation and immunophotosensitization.<sup>354</sup> In CALI, a biological macromolecule of interest is tagged with a PS and illuminated by light.<sup>409</sup> Genetically encoded PS are advantageous over free chromophores (e.g., malachite green or fluorescein) because they do not suffer from background labeling and do not require exogenous chemicals. Nevertheless, applications are still limited, mainly due to low  $\Phi_S$ , such as in the GFP-derived Killer Red protein,<sup>410</sup> and secondary photodamage. LOV-derived PS are promising tools for CALI, but require blue light that penetrates poorly in tissues and has potential harmful effects on cells and their components, possibly rendering the interpretation of experimental results challenging. MiniSOG-based CALI was first employed in *C. elegans* in an approach called InSynC.<sup>411</sup> By fusing miniSOG to SNARE proteins in cultured neurons, hippocampal slices and entire organisms, it was possible to inhibit synaptic release and influence *C. elegans* movement with light. Further work with the same nematode and

using heterologous SNARE proteins fused to miniSOG confirmed that the technique works, with the limitation that both fused and nontarget synaptic proteins were damaged by ROS, causing complex and multifaceted phenotypes.<sup>412</sup> Nevertheless, the InSynC technology is uniquely able to efficiently inhibit a specific axonal projection, as demonstrated by fusing miniSOG to presynaptic active zone proteins of the UNC-13 family.<sup>413</sup> To target DNA, miniSOG was fused to a histone where it could stimulate mutagenesis induced by ROS after blue-light illumination.<sup>414</sup> Another application of CALI is light-mediated inactivation of the mitochondrial electron transport chain of *C. elegans* by fusing miniSOG to a subunit of complex II.<sup>415</sup> The obtained phenotypes demonstrated crucial features of complex II and its selective importance for different cell types.

Cell ablation is a powerful tool in the study of eukaryotic developmental biology and in selectively killing cells for therapeutic purposes. It can be achieved by several methods,<sup>416–418</sup> recently also taking advantage of optogenetic approaches with KillerRed and LOV-derived proteins.<sup>419–422</sup> In such approaches, miniSOG can be fused to different cell compartments, e.g., mitochondria, cell membranes, but in each case cell death is induced by light-generated ROS that trigger apoptosis, necrosis and phagocytic pathways.<sup>354</sup> Phototoxic effects can be modulated with light intensity and exposure times. CALI worked with a few minutes of BL irradiation in the 0.5–3 W cm<sup>-2</sup> range,<sup>411,413</sup> whereas cell ablation required light intensities of 50 mW cm<sup>-2</sup> and a prolonged time of irradiation (above 30 min), or, even more efficiently, pulsed light.<sup>419,421</sup> MiniSOG was successfully employed for cell ablation in *C. elegans*,<sup>405,419–421</sup> where a distinct trait of this approach emerged. The phototoxic effects depended on intracellular targeting, with low level of toxicity in the cytoplasm, but high photodamage when miniSOG is targeted to mitochondria, resulting in complete destruction of the cells. Most importantly, photodamage was not induced in neighboring cells, thus making miniSOG-based cell ablation a promising tool. Owing to its precision, efficiency and selectivity, the above-mentioned miniSOG2 recently allowed to inactivate single neurons in larvae of *D. melanogaster*.<sup>406</sup> Very recently, photoablation of selected neurons in *C. elegans* with miniSOG showed that excitatory class A motor neurons have intrinsic and oscillatory activity.<sup>423</sup>

A major interest of cell ablation is the precise killing of tumor cells, a process that works very well with miniSOG in cultured cells, but much less so *in vivo*,<sup>424</sup> arguably due to poor transparency of skin to blue light and low oxygen concentration in the analyzed tumors.<sup>354</sup> Another factor could be related to the photosensitizing activity of miniSOG that, as discussed above, can also act via a type I mechanism, generating ROS that are deactivated by enzymes such as superoxide dismutase.<sup>425,426</sup> The use of LOV-derived proteins for killing tumor cells is still in its infancy, but advantages of these genetically encoded PS over protein-free chromophores employed in conventional photodynamic therapy, such as porphyrins, are emerging: higher solubility in non-membrane compartments ensures low toxicity in the long term, while precise targeting by fusion to selected proteins and compartments should improve efficiency. This latter aspect is also related to the development of fully genetically encoded immunophotosensitizers, where a targeting antibody is fused to a protein PS.<sup>354</sup> To produce so-called phototoxins, miniSOG was fused to antibodies and DARPins (designed ankyrin repeat proteins), specifically directed against HER2 tumor cell lines and were shown to have efficient phototoxicity, which was further

enhanced by coupling the treatment with antimetabolic drugs.<sup>427,428</sup> Intriguingly, recent reports demonstrated the BL-induced production of ROS by *A. thaliana* CRY2 under physiological conditions.<sup>429–431</sup> The resultant accumulation of ROS and hydrogen peroxide in the nucleus triggered the transcription of genes engaged in plant responses to abiotic and biotic stresses. Taken together, these observations imply that even unmodified photoreceptors (here, cryptochromes) can produce significant quantities of ROS at physiological conditions. Apparently, nature has harnessed this process as a parallel mechanism for transducing light signals.

### 5.3. Photoreceptors as Sensors of Oxygen and Redox Potential

The redox properties of flavins in solutions are well known.<sup>432</sup> The quinone form is fully oxidized (*ox*), one-electron reduction leads to the semiquinone form (*sq*), while the doubly reduced form is called hydroquinone (*hq*). The reduction of *ox* to *hq* follows the “*ece*” sequence: electrochemical step (electron transfer, *eT*), chemical step ( $H^+$  transfer), *eT* step to give *hq* as the only observed final product.<sup>433</sup> Redox titration of free FMN revealed the overlapping of the two *eT* steps, giving an overall value for the midpoint potential reported as  $E_{ox/hq} = -205$  mV<sup>434</sup>,  $-207$  mV,<sup>433</sup>  $-219$  mV<sup>435</sup> or  $-224$  mV.<sup>436</sup> Dissecting the single redox steps with different methodologies yielded more contrasting values of  $E_{ox/sq} = -238$  mV,<sup>437</sup>  $-246/-314/-313$  mV,<sup>433</sup> and  $E_{sq/hq} = -172$  mV,<sup>437</sup>  $-166/-124/-101$  mV.<sup>433</sup> Protonation equilibria of the *sq* state, further complicate the scenario.<sup>433</sup>

Upon photoexcitation of flavins,  $E_{ox/hq}$  strongly changes: given the singlet and triplet excited states energy level of 2.5 and 2.1 eV, respectively,<sup>168</sup> we can estimate  ${}^1E_{ox/hq} = +2.3$  V and  ${}^3E_{ox/hq} = +1.9$  V.<sup>168</sup> This dramatic shift in redox potentials promotes all flavin-based photochemical reactions described in section 2., which are initiated from the *ox* state in LOV, BLUF<sup>438</sup> and most CRY proteins.<sup>132,439,440</sup> This suggests that flavin-based photoreceptors might become light-insensitive at cellular redox potentials close to their own value of  $E_{ox/hq}$ . The intracellular redox potential of gram-negative bacteria was estimated as  $-270$  mV, but may become more negative under oxygen-depletion conditions,<sup>441</sup> and similar values were reported for eukaryotic cells.<sup>442</sup> The relevant question for optogenetics is whether LOV, BLUF and CRY proteins are robust against reducing conditions and keep their photochemically competent state against intracellular redox variations. The other biologically relevant aspect is the possibility that photoreceptors can also function as redox sensors.

As mentioned in section 5.1., *in vitro* FbFPs partially retain their fluorescence even under strongly reducing conditions, up to a redox potential of ca.  $-660$  mV.<sup>366</sup> This reflects the quite negative values of  $E_{ox/hq}$  measured for LOV proteins at the ground state of  $-290$  mV for *CtLOV*-wt and  $-280$  mV for *CtLOV*-C57S;<sup>436</sup>  $-303$  mV for *BsYtvA*;  $-308$  mV for *Asphot1*-LOV2;<sup>443</sup> and  $-258$  mV for the LOV histidine kinase protein of *Caulobacter crescentus*.<sup>11</sup> In agreement with observations on FbFPs,<sup>366</sup> only 20% of *CtLOV*-C57S is reduced at a redox potential as low as  $-428$  mV.<sup>436</sup> Chemical reduction of LOV proteins resulted in production of the *hq* form only (i.e. a two-electron reduction), while photochemical reduction of *CtLOV*-C57S (where the FMN-Cys adduct cannot be formed) using EDTA as sacrificial electron donor, produced a neutral *sq* stable under deoxygenated

conditions, that slowly recovered to *ox* after O<sub>2</sub> admission.<sup>436</sup> BLUF proteins showed a value of  $E_{ox/hq}$  intermediate between free chromophores and LOV domains, localized at  $-260$  mV for *R. sphaeroides* AppA, i.e. 50 mV more negative than free FAD in solution.<sup>443</sup> The midpoint potential can be increased by the Q63H mutation and, more dramatically, by the double exchange Y21F/W104F, but surprisingly not by Y21F alone. As for LOV proteins, the *sq* was not detected for BLUF proteins during chemical reduction.<sup>443</sup> For cryptochromes the scenario is more complicated: for *A. thaliana* CRY1 a value of  $E_{ox/hq} = -161$  mV was reported, but for this protein also the *sq* species was detected with similar  $E_{sq/hq} = -153$  mV,<sup>444</sup> quite close to a previously determined value  $E_{sq/hq} = -181$  mV and  $E_{ox/sq} = -143$  mV.<sup>445</sup> In the photolyases (PLs), a class of photoenzymes that are closely related to cryptochromes (cf. sec. 2.1.3.), the midpoint potential is less negative with  $E_{sq/hq} = -39/-48$  mV<sup>444</sup> or even  $+16$  mV<sup>446</sup> for the enzyme alone (no detection of the *ox* state during oxidative titration of the PL active form), and increasing to  $+28^{444}/+81^{446}$  mV when the enzyme is bound to damaged DNA. This ensures that bound PL remains in its competent form for DNA photorepair, while the more delicate redox equilibria of cryptochromes account for their quite complex photochemical properties,<sup>132,440</sup> and possibly renders these photoreceptors more susceptible to intracellular redox conditions.

Following the consideration of midpoint potentials of flavin-based photoreceptors, we turn to their possible, flavin-centered, double role as light and redox sensors. This was discussed, yet not demonstrated for *ChLuvK*<sup>71</sup> but some intriguing findings emerged during the last years. For example, the *Trichoderma reesei* *TtENV1* protein integrated both light and oxidative stress sensing by the LOV domain. Functional dimerization of *TtENV1* required both BL and oxidative conditions, where redox sensing relied on an additional cysteine residue that enabled cross-linking within the dimer.<sup>447</sup> This cysteine is localized in a hinge region between the N-terminal cap and the first  $\beta$  strand of the LOV core, a region that undergoes light-driven conformational changes.

In LOV receptors, photoadduct formation is the key event initiating signaling, but is the FMN-Cys covalent bond necessary to trigger signal propagation, or is protonation of N5 (promoting flipping of a conserved glutamine) possibly sufficient? Yee and co-authors elegantly demonstrated that even in the absence of the reactive cysteine light- and chemically-driven conformational changes of LOV proteins do indeed occur, via the formation of a flavin *sq*.<sup>27</sup> Experimentally, this was readily demonstrated by removing the conserved functional cysteine in well-characterized LOV proteins. However, a LOV-like domain that does not possess the substrate cysteine, BAT-LOV from the archaeon *Halorubrum hochstenium* (*HhBAT-LOV*), could not be photo-reduced without replacing several aromatic amino acids close to the chromophore, because the excited state of *HhBAT-LOV* was efficiently quenched by these amino acids. An attempt to convert *HhBAT-LOV* to a canonical LOV domain by introduction of an active-site cysteine residue failed to produce any photoadduct, although the photo-reduction rate was increased. The authors speculated that canonical, adduct-forming LOV domains arose from ancestral redox-active flavoproteins via the introduction of a cysteine residue that rendered these proteins less susceptible to changes in cellular redox potential, less prone to photodamage, but more effective in photosensing.<sup>27</sup> Recently, Magerl *et al.* succeeded in blocking the canonical photocycle of a cysteinebearing LOV domain, by introducing a tyrosine in the vicinity of the

FMN, thereby inducing proton-coupled electron transfer towards the flavin chromophore with no formation of the adduct.<sup>448</sup> Transient absorption spectroscopy indicated that a radical FMN<sup>-•</sup>:Tyr<sup>+•</sup> pair was formed which decayed on the microsecond time-scale, with concomitant protonation of N5. MD simulations also implied that this tyrosine is the likely proton donor for this reaction.

As a whole, the data available for LOV and BLUF proteins currently do not support a physiologically relevant role as dual light and redox sensors centered solely on the flavin chromophore. However, the redox properties of flavins can be modulated to elucidate some critical aspects of the photocycle, and to understand evolution and natural abundance of these photoreceptors. When light and redox or O<sub>2</sub> sensing are found in the same proteins, additional elements are present, as mentioned above. In the more nuanced scenario of cryptochromes, the redox state of the cell could have a role in their functionality and alternative photo-induced pathways of activation. The interplay of BL and O<sub>2</sub> is one of the most intriguing issues in the field of flavin-based photoreceptors.<sup>123</sup>

## 6. Conclusions

As the preceding sections conclusively illustrate, within a strikingly short time span UV-light-/BL-sensitive receptors have unlocked numerous cellular activities and parameters for reversible, non-invasive and spatiotemporally precise optogenetic intervention. UV-light- and BL-sensitive photoreceptors have thus greatly contributed to decisively expanding the application scope of optogenetics beyond the light-triggered perturbation of membrane potential and the neurosciences. In particular, the engineering of novel photoreceptors has been nothing but amazingly successful, and the set of available optogenetic actuators has greatly grown, with new additions standing to arrive in the near future. Notably, photoreceptor engineering is rooted in a detailed although often incomplete molecular characterization of the underlying natural photoreceptors. The modular architecture of many natural photoreceptors, prominently evidenced in the LOV, BLUF and phytochrome classes, already hints at inherent versatility of the underlying mechanisms of light-dependent allostery. This versatility has indeed been borne out and duly exploited in photoreceptor engineering, strikingly so for the near-ubiquitous *AsLOV2* photosensor; empowered by human ingenuity and creativity, even this single building block has sufficed for regulating by light numerous effectors and cellular pathways. Light-regulated order-disorder transitions as embodied by the C-terminal J $\alpha$  helix of *AsLOV2* represent one of the two most successful engineering concepts, with the other being light-dependent association/dissociation reactions. By resorting to these versatile (and, other) photoreceptor engineering strategies, additional effector activities will be subjected to light control in due course. In fact, photoreceptor engineering has become so successful that comprehensive optogenetic application often lags behind the actual design of a given light-regulated actuator. By fully capitalizing on the already existing and additionally upcoming photoreceptors, the inner workings of cellular systems can be interrogated and hopefully disentangled in unprecedented and ever more exact and efficient manner. While the current treatise has been deliberately restricted in scope to soluble UV-light- and BL-sensitive photoreceptors, we note in closing that many of the concepts and considerations also apply to other classes of soluble photoreceptors. In addition to phytochromes treated in this issue by Gärtner, the



more recently described vitamin-B<sub>12</sub>-based photoreceptors<sup>449</sup> and the orange-carotenoid protein<sup>450</sup> also appear as attractive building blocks for photoreceptor engineering.

## Acknowledgements

We thank our coworkers and colleagues for collaboration and many inspiring interactions. Funding by the FIL 2016 program of the University of Parma (A.L.), National Institutes of Health (R01 GM106239 to K.H.G.), the Alexander-von-Humboldt Foundation (A.M.) and the Deutsche Forschungsgemeinschaft (A.M.) is gratefully acknowledged.

## Biography

### Aba Losi

Aba Losi received her Ph.D. in biophysics in 1997 at the University of Parma (Italy). During her post-doctoral training with Silvia Braslavsky (Max Planck Institute for Radiation Chemistry, Germany), she explored the energy landscape of photoreceptors by means of pulsed photoacoustics. She is presently enrolled as associate professor at the University of Parma (Italy), lecturing physics, photobiophysics and photobiology. Her research is focused on functional aspects of blue-light photoreceptors in bacteria and their applications in biophysics, as well as their evolution and physiological role.

### Kevin Gardner

Kevin Gardner received his training in biochemistry and biophysics with undergraduate work at UC Davis (B.S., Biochemistry, 1989), graduate work at Yale (Ph.D., Molecular Biophysics & Biochemistry, 1995) and postdoctoral research at the University of Toronto. After establishing his independent research group at UT Southwestern Medical Center, he moved his lab in 2014 to the CUNY Advanced Science Research Center to establish and direct the new Structural Biology Initiative there. In parallel, he also started as the Einstein Professor of Chemistry & Biochemistry at the City College of New York. Using a combination of structural biology, biochemistry and cell-biology approaches, his research examines the atomic-level signaling mechanisms of proteins used by cells to sense and respond to the environment around them, with the goal of understanding the natural regulation of these systems and artificially controlling them.

### Andreas Möglich

Andreas Möglich studied biochemistry at the University of Regensburg (Germany) and obtained his diploma degree in 2001. Following his graduation in biophysics at the Biozentrum of the University of Basel (Switzerland) in 2005, he moved to the University of Chicago for postdoctoral studies under Dr. Keith Moffat's guidance. On the back of a Sofja-Kovalevskaya Award by the Alexander-von-Humboldt Foundation, he returned to Germany in 2010 to assume a professorship in Biophysical Chemistry at the Humboldt University Berlin. In spring 2015, he became a full professor for Biochemistry at the University of Bayreuth (Germany). His research group focuses on the structure, mechanism, function, engineering and optogenetic application of sensory photoreceptors, in particular of light-oxygen-voltage and phytochrome photoreceptors.

**ABBREVIATIONS**

<b>4-HCA</b>	4-hydroxycinnamic acid
<b><math>\Phi</math></b>	quantum yield
<b>aa</b>	amino acids
<b>BL</b>	blue light
<b>BLUF</b>	sensors of blue light using flavin adenine dinucleotide
<b>CALI</b>	chromophore-assisted light inactivation
<b>cAMP</b>	3',5'-cyclic adenosine monophosphate
<b>Cas</b>	CRISPR associated
<b>CBCR</b>	cyanobacteriochrome
<b>CCT</b>	cryptochrome C terminus
<b>c-di-AMP</b>	cyclic diadenylate
<b>c-di-GMP</b>	cyclic diguanylate
<b>cGMP</b>	3',5'-cyclic guanosine monophosphate
<b>ChR</b>	channelrhodopsin
<b>CIB</b>	cryptochrome-interacting basic-helix-loop-helix protein
<b>CLEM</b>	correlative light electron microscopy
<b>CNG</b>	cyclic-nucleotide-gated
<b>cNMP</b>	3',5'-cyclic nucleotide monophosphate
<b>CRAC</b>	Ca <sup>2+</sup> -release-activated Ca <sup>2+</sup> channels
<b>CRISPR</b>	clustered regularly interspaced short palindromic repeats
<b>Cry</b>	cryptochrome
<b>DARPin</b>	designed ankyrin repeat protein
<b>DBD</b>	DNA-binding domain
<b>dCas</b>	cleavage-deficient variant of Cas
<b>DSB</b>	double-strand break
<b>EB</b>	end-binding (protein)
<b>EGF</b>	epidermal growth factor
<b>EM</b>	electron microscopy

<b>Epac</b>	exchange protein directly activated by cAMP
<b>ER</b>	endoplasmic reticulum
<i>eT</i>	electron transfer
<b>ET</b>	energy transfer
<b>EYFP</b>	enhanced yellow fluorescent protein
<b>FAD</b>	flavin adenine dinucleotide
<b>FAK</b>	focal adhesion kinase
<b>FbFP</b>	flavin-mononucleotide-binding fluorescent protein
<b>FLIM</b>	fluorescence lifetime imaging
<b>FMN</b>	flavin mononucleotide
<b>FP</b>	fluorescent protein
<b>FRET</b>	Förster resonance energy transfer
<b>GAP</b>	GTPase-activating protein
<b>GEF</b>	guanine nucleotide exchange factor
<b>GFP</b>	green fluorescent protein
<b>GPCR</b>	G-protein coupled receptor
<i>hq</i>	fully reduced hydroquinone state of flavin
<b>HTH</b>	helix-turn-helix
<b>LAD</b>	light-activated dimerization
<b>LOV</b>	light-oxygen-voltage
<b>MAP2K</b>	mitogen-activated protein kinase kinase
<b>MAP3K</b>	mitogen-activated protein kinase kinase kinase
<b>MAPK</b>	mitogen-activated protein kinase
<b>miniSOG</b>	mini Singlet Oxygen Generator
<b>MT</b>	microtubules
<b>MW</b>	molecular weight
<b>NES</b>	nuclear export signal
<b>NLS</b>	nuclear localization signal
<i>ox</i>	oxidized quinone state of flavin

<b>PA</b>	photoactivated
<b>PAC</b>	photoactivated adenylate cyclase
<b>PDE</b>	phosphodiesterase
<b>PHR</b>	photolyase homology region
<b>PI</b>	photoinhibited
<b>PI</b>	phosphatidylinositol
<b>PIF</b>	phytochrome-interacting factor
<b>PKA</b>	protein kinase A
<b>PKG</b>	protein kinase G
<b>PODCP</b>	popeye-domain-containing protein
<b>POI</b>	protein of interest
<b>PPI</b>	protein-protein interaction
<b>PRR</b>	pattern recognition receptor
<b>PS</b>	photosensitizer
<b>PYP</b>	photoactive yellow protein
<b>REST</b>	repressor element 1-silencing transcription factor
<b>RNP</b>	ribonucleoprotein
<b>ROS</b>	reactive oxygen species
<b>RTK</b>	receptor tyrosine kinase
<b>sec.</b>	section
<b>sgRNA</b>	single guide RNA
<b>SHK</b>	sensor histidine kinase
<b>SOPP</b>	singlet oxygen protein photosensitizer
<i>sq</i>	partially reduced semiquinone radical state of flavin
<i>tAD</i>	<i>trans</i> -activation domain
<b>TALE</b>	transcription factor like effector
<b>TCS</b>	two-component system
<b>TF</b>	transcription factor
<b>TGF</b>	transforming growth factor

<b>TIP</b>	tip-interacting protein
<b>TrpR</b>	tryptophan repressor
<b>WC</b>	white collar
<b>wt</b>	wild type

## 8. References

- (1). Möglich A; Yang X; Ayers RA; Moffat K Structure and Function of Plant Photoreceptors. *Annu. Rev. Plant Biol* 2010, 61, 21–47. [PubMed: 20192744]
- (2). Hegemann P Algal Sensory Photoreceptors. *Annu. Rev. Plant Biol.* 2008, 59, 167–189. [PubMed: 18444900]
- (3). Sorigué D; Légeret B; Cuiné S; Blangy S; Moulin S; Billon E; Richaud P; Brugière S; Couté Y; Nurizzo D; et al. An Algal Photoenzyme Converts Fatty Acids to Hydrocarbons. *Science* 2017, 357, 903–907. [PubMed: 28860382]
- (4). Deisseroth K; Feng G; Majewska AK; Miesenböck G; Ting A; Schnitzer MJ Next-Generation Optical Technologies for Illuminating Genetically Targeted Brain Circuits. *J. Neurosci.* 2006, 26, 10380–10386. [PubMed: 17035522]
- (5). Li X; Gutierrez DV; Hanson MG; Han J; Mark MD; Chiel H; Hegemann P; Landmesser LT; Herlitze S Fast Noninvasive Activation and Inhibition of Neural and Network Activity by Vertebrate Rhodopsin and Green Algae Channelrhodopsin. *Proc. Natl. Acad. Sci. U. S. A.* 2005, 102, 17816–17821. [PubMed: 16306259]
- (6). Bi A; Cui J; Ma Y-P; Olshevskaya E; Pu M; Dizhoor AM; Pan Z-H Ectopic Expression of a Microbial-Type Rhodopsin Restores Visual Responses in Mice with Photoreceptor Degeneration. *Neuron* 2006, 50, 23–33. [PubMed: 16600853]
- (7). Nagel G; Brauner M; Liewald JF; Adeishvili N; Bamberg E; Gottschalk A Light Activation of Channelrhodopsin-2 in Excitable Cells of *Caenorhabditis Elegans* Triggers Rapid Behavioral Responses. *Curr. Biol.* 2005, 15, 2279–2284. [PubMed: 16360690]
- (8). Boyden ES; Zhang F; Bamberg E; Nagel G; Deisseroth K Millisecond-Timescale, Genetically Targeted Optical Control of Neural Activity. *Nat. Neurosci.* 2005, 8, 1263–1268. [PubMed: 16116447]
- (9). Huala E; Oeller PW; Liscum E; Han IS; Larsen E; Briggs WR Arabidopsis NPH1: A Protein Kinase with a Putative Redox-Sensing Domain. *Science* 1997, 278, 2120–2123. [PubMed: 9405347]
- (10). Christie JM; Reymond P; Powell GK; Bernasconi P; Raibekas AA; Liscum E; Briggs WR Arabidopsis NPH1: A Flavoprotein with the Properties of a Photoreceptor for Phototropism. *Science* 1998, 282, 1698–1701. [PubMed: 9831559]
- (11). Iseki M; Matsunaga S; Murakami A; Ohno K; Shiga K; Yoshida K; Sugai M; Takahashi T; Hori T; Watanabe M A Blue-Light-Activated Adenylyl Cyclase Mediates Photoavoidance in *Euglena Gracilis*. *Nature* 2002, 415, 1047–1051. [PubMed: 11875575]
- (12). Gomelsky M; Klug G BLUF: A Novel FAD-Binding Domain Involved in Sensory Transduction in Microorganisms. *Trends Biochem Sci* 2002, 27, 497–500. [PubMed: 12368079]
- (13). Ahmad M; Lin C; Cashmore AR Mutations throughout an Arabidopsis Blue-Light Photoreceptor Impair Blue-Light-Responsive Anthocyanin Accumulation and Inhibition of Hypocotyl Elongation. *Plant J* 1995, 8, 653–658. [PubMed: 8528277]
- (14). Meyer TE Isolation and Characterization of Soluble Cytochromes, Ferredoxins and Other Chromophoric Proteins from the Halophilic Phototrophic Bacterium *Ectothiorhodospira Halophila*. *Biochim. Biophys. Acta* 1985, 806, 175–183. [PubMed: 2981543]
- (15). Brown BA; Cloix C; Jiang GH; Kaiserli E; Herzyk P; Kliebenstein DJ; Jenkins GI A UV-B-Specific Signaling Component Orchestrates Plant UV Protection. *Proc. Natl. Acad. Sci. U. S. A.* 2005, 102, 18225–18230. [PubMed: 16330762]

- (16). Glantz ST; Carpenter EJ; Melkonian M; Gardner KH; Boyden ES; Wong GK-S; Chow BY Functional and Topological Diversity of LOV Domain Photoreceptors. *Proc. Natl. Acad. Sci. U. S. A.* 2016, 113, E1442–1451. [PubMed: 26929367]
- (17). Möglich A; Ayers RA; Moffat K Structure and Signaling Mechanism of Per-ARNT-Sim Domains. *Structure* 2009, 17, 1282–1294. [PubMed: 19836329]
- (18). Henry JT; Crosson S Ligand-Binding PAS Domains in a Genomic, Cellular, and Structural Context. *Annu. Rev. Microbiol.* 2011, 65, 261–286. [PubMed: 21663441]
- (19). Harper SM; Neil LC; Gardner KH Structural Basis of a Phototropin Light Switch. *Science* 2003, 301, 1541–1544. [PubMed: 12970567]
- (20). Halavaty AS; Moffat K N- and C-Terminal Flanking Regions Modulate Light-Induced Signal Transduction in the LOV2 Domain of the Blue Light Sensor Phototropin 1 from *Avena Sativa*. *Biochemistry* 2007, 46, 14001–14009. [PubMed: 18001137]
- (21). Nash AI; McNulty R; Shillito ME; Swartz TE; Bogomolni RA; Luecke H; Gardner KH Structural Basis of Photosensitivity in a Bacterial Light-Oxygen-Voltage/helix-Turn-Helix (LOV-HTH) DNA-Binding Protein. *Proc. Natl. Acad. Sci. U. S. A.* 2011, 108, 9449–9454. [PubMed: 21606338]
- (22). Zoltowski BD; Schwerdtfeger C; Widom J; Loros JJ; Bilwes AM; Dunlap JC; Crane BR Conformational Switching in the Fungal Light Sensor Vivid. *Science* 2007, 316, 1054–1057. [PubMed: 17510367]
- (23). Alexandre MT; Domratcheva T; Bonetti C; van Wilderen LJ; van Grondelle R; Groot ML; Hellingwerf KJ; Kennis JT Primary Reactions of the LOV2 Domain of Phototropin Studied with Ultrafast Mid-Infrared Spectroscopy and Quantum Chemistry. *Biophys J* 2009, 97, 227–237. [PubMed: 19580760]
- (24). Zayner JP; Antoniou C; Sosnick TR The Amino-Terminal Helix Modulates Light-Activated Conformational Changes in AsLOV2. *J. Mol. Biol.* 2012, 419, 61–74. [PubMed: 22406525]
- (25). Pfeifer A; Mathes T; Lu Y; Hegemann P; Kottke T Blue Light Induces Global and Localized Conformational Changes in the Kinase Domain of Full-Length Phototropin. *Biochemistry* 2010, 49, 1024–1032. [PubMed: 20052995]
- (26). Harper SM; Christie JM; Gardner KH Disruption of the LOV-Ja Helix Interaction Activates Phototropin Kinase Activity. *Biochemistry* 2004, 43, 16184–16192. [PubMed: 15610012]
- (27). Yee EF; Diensthuber RP; Vaidya AT; Borbat PP; Engelhard C; Freed JH; Bittl R; Möglich A; Crane BR Signal Transduction in Light–oxygen–voltage Receptors Lacking the Adduct-Forming Cysteine Residue. *Nat. Commun.* 2015, 6, 10079. [PubMed: 26648256]
- (28). Pudasaini A; El-Arab KK; Zoltowski BD LOV-Based Optogenetic Devices: Light-Driven Modules to Impart Photoregulated Control of Cellular Signaling. *Front. Mol. Biosci.* 2015, 2, 18. [PubMed: 25988185]
- (29). Finn RD; Mistry J; Schuster-Böckler B; Griffiths-Jones S; Hollich V; Lassmann T; Moxon S; Marshall M; Khanna A; Durbin R; et al. Pfam: Clans, Web Tools and Services. *Nucleic Acids Res* 2006, 34 (Database issue), D247–D251. [PubMed: 16381856]
- (30). Wu Q; Gardner KH Structure and Insight into Blue Light-Induced Changes in the BlrP1 BLUF Domain. *Biochemistry* 2009, 48, 2620–2629. [PubMed: 19191473]
- (31). Barends TR; Hartmann E; Griese JJ; Beitlich T; Kirienko NV; Ryjenkov DA; Reinstein J; Shoeman RL; Gomelsky M; Schlichting I Structure and Mechanism of a Bacterial Light-Regulated Cyclic Nucleotide Phosphodiesterase. *Nature* 2009, 459, 1015–1018. [PubMed: 19536266]
- (32). Jung A; Domratcheva T; Tarutina M; Wu Q; Ko W; Shoeman RL; Gomelsky M; Gardner KH; Schlichting I Structure of a Bacterial BLUF Photoreceptor: Insights into Blue Light-Mediated Signal Transduction. *Proc. Natl. Acad. Sci. U. S. A.* 2005, 102, 12350–12355. [PubMed: 16107542]
- (33). Yuan H; Bauer CE PixE Promotes Dark Oligomerization of the BLUF Photoreceptor PixD. *Proc. Natl. Acad. Sci.* 2008, 105, 11715–11719. [PubMed: 18695243]
- (34). Kraft BJ; Masuda S; Kikuchi J; Dragnea V; Tollin G; Zaleski JM; Bauer CE Spectroscopic and Mutational Analysis of the Blue-Light Photoreceptor AppA: A Novel Photocycle Involving

- Flavin Stacking with an Aromatic Amino Acid. *Biochemistry* 2003, 42, 6726–6734. [PubMed: 12779327]
- (35). Gauden M; Yeremenko S; Laan W; van Stokkum IHM; Ihalainen JA; van Grondelle R; Hellingwerf KJ; Kennis JTM Photocycle of the Flavin-Binding Photoreceptor AppA, a Bacterial Transcriptional Antirepressor of Photosynthesis Genes. *Biochemistry* 2005, 44, 3653–3662. [PubMed: 15751942]
- (36). Laan W; van der Horst MA; van Stokkum I; Hellingwerf KJ Initial Characterization of the Primary Photochemistry of AppA, A Blue-Light-Using Flavin Adenine Dinucleotide-Domain Containing Transcriptional Antirepressor Protein from *Rhodobacter Sphaeroides*: A Key Role for Reversible Intramolecular Proton Transfer from. *Photochem Photobiol* 2003, 78, 290–297. [PubMed: 14556317]
- (37). Stelling AL; Ronayne KL; Nappa J; Tonge PJ; Meech SR Ultrafast Structural Dynamics in BLUF Domains: Transient Infrared Spectroscopy of AppA and Its Mutants. *J. Am. Chem. Soc.* 2007, 129, 15556–15564. [PubMed: 18031038]
- (38). Domratcheva T; Grigorenko BL; Schlichting I; Nemukhin AV Molecular Models Predict Light-Induced Glutamine Tautomerization in BLUF Photoreceptors. *Biophys. J.* 2008, 94, 3872–3879. [PubMed: 18263659]
- (39). Domratcheva T; Hartmann E; Schlichting I; Kottke T Evidence for Tautomerisation of Glutamine in BLUF Blue Light Receptors by Vibrational Spectroscopy and Computational Chemistry. *Sci. Rep.* 2016, 6, 22669. [PubMed: 26947391]
- (40). Gauden M; Grinstead JS; Laan W; Van Stokkum IHM; Avila-Perez M; Toh KC; Boelens R; Kaptein R; Van Grondelle R; Hellingwerf KJ; et al. On the Role of Aromatic Side Chains in the Photoactivation of BLUF Domains. *Biochemistry* 2007, 46, 7405–7415. [PubMed: 17542622]
- (41). Yu X; Liu H; Klejnot J; Lin C The Cryptochrome Blue Light Receptors. *Arab. B.* 2010, 8, e0135.
- (42). Coesel S; Mangogna M; Ishikawa T; Heijde M; Rogato A; Finazzi G; Todo T; Bowler C; Falcatore A Diatom PtCPF1 Is a New Cryptochrome/photolyase Family Member with DNA Repair and Transcription Regulation Activity. *EMBO Rep.* 2009, 10, 655–661. [PubMed: 19424294]
- (43). Zoltowski BD; Gardner KH Tripping the Light Fantastic: Blue-Light Photoreceptors as Examples of Environmentally Modulated Protein–Protein Interactions. *Biochemistry* 2011, 50, 4–16. [PubMed: 21141905]
- (44). Brautigam CA; Smith BS; Ma Z; Palnitkar M; Tomchick DR; Machius M; Deisenhofer J Structure of the Photolyase-like Domain of Cryptochrome 1 from *Arabidopsis Thaliana*. *Proc. Natl. Acad. Sci.* 2004, 101, 12142–12147. [PubMed: 15299148]
- (45). Duan L; Hope J; Ong Q; Lou HY; Kim N; McCarthy C; Acero V; Lin MZ; Cui B Understanding CRY2 Interactions for Optical Control of Intracellular Signaling. *Nat. Commun.* 2017, 8, 547. [PubMed: 28916751]
- (46). Zeugner A; Byrdin M; Bouly JP; Bakrim N; Giovani B; Brettel H; Ahmad M Light-Induced Electron Transfer in *Arabidopsis* Cryptochrome-1 Correlates with in Vivo Function. *J. Biol. Chem.* 2005, 280, 19437–19440. [PubMed: 15774475]
- (47). Ahmad M Action Spectrum for Cryptochrome-Dependent Hypocotyl Growth Inhibition in *Arabidopsis*. *PLANT Physiol.* 2002, 129, 774–785. [PubMed: 12068118]
- (48). Banerjee R; Schleicher E; Meier S; Viana RM; Pokorny R; Ahmad M; Bittl R; Batschauer A The Signaling State of *Arabidopsis* Cryptochrome 2 Contains Flavin Semiquinone. *J. Biol. Chem.* 2007, 282, 14916–14922. [PubMed: 17355959]
- (49). VanVickle-Chavez SJ; Van Gelder RN Action Spectrum of *Drosophila* Cryptochrome. *J. Biol. Chem.* 2007, 282, 10561–10566. [PubMed: 17284451]
- (50). Liu H; Yu X; Li K; Klejnot J; Yang H; Lisiero D; Lin C Photoexcited CRY2 Interacts with CIB1 to Regulate Transcription and Floral Initiation in *Arabidopsis*. *Science* 2008, 322, 1535–1539. [PubMed: 18988809]
- (51). Kennedy MJ; Hughes RM; Peteya LA; Schwartz JW; Ehlers MD; Tucker CL Rapid Blue-Light-Mediated Induction of Protein Interactions in Living Cells. *Nat. Methods* 2010, 7, 973–975. [PubMed: 21037589]

- (52). Taslimi A; Vrana JD; Chen D; Borinskaya S; Mayer BJ; Kennedy MJ; Tucker CL An Optimized Optogenetic Clustering Tool for Probing Protein Interaction and Function. *Nat. Commun.* 2014, 5, 4925. [PubMed: 25233328]
- (53). Taslimi A; Zoltowski B; Miranda JG; Pathak GP; Hughes RM; Tucker CL Optimized Second-Generation CRY2-CIB Dimerizers and Photoactivatable Cre Recombinase. *Nat. Chem. Biol.* 2016, 12, 425–430. [PubMed: 27065233]
- (54). Ramachandran PL; Lovett JE; Carl PJ; Cammarata M; Lee JH; Jung YO; Ihee H; Timmel CR; van Thor JJ The Short-Lived Signaling State of the Photoactive Yellow Protein Photoreceptor Revealed by Combined Structural Probes. *J. Am. Chem. Soc.* 2011, 133, 9395–9404. [PubMed: 21627157]
- (55). Yang C; Kim SO; Kim Y; Yun SR; Choi J; Ihee H Photocycle of Photoactive Yellow Protein in Cell-Mimetic Environments: Molecular Volume Changes and Kinetics. *J. Phys. Chem. B* 2017, 121, 769–779. [PubMed: 28058827]
- (56). Genick UK; Borgstahl GE; Ng K; Ren Z; Pradervand C; Burke PM; Srajer V; Teng TY; Schildkamp W; McRee DE; et al. Structure of a Protein Photocycle Intermediate by Millisecond Time-Resolved Crystallography. *Science* 1997, 275, 1471–1475. [PubMed: 9045611]
- (57). Ihee H; Rajagopal S; Srajer V; Pahl R; Anderson S; Schmidt M; Schotte F; Anfinrud PA; Wulff M; Moffat K From The Cover: Visualizing Reaction Pathways in Photoactive Yellow Protein from Nanoseconds to Seconds. *Proc. Natl. Acad. Sci.* 2005, 102, 7145–7150. [PubMed: 15870207]
- (58). Imamoto Y; Kataoka M Structure and Photoreaction of Photoactive Yellow Protein, a Structural Prototype of the PAS Domain Superfamily. *Photochem. Photobiol.* 2007, 83, 40–49. [PubMed: 16939366]
- (59). Sprenger WW; Hoff WD; Armitage JP; Hellingwerf KJ The Eubacterium *Ectothiorhodospira Halophila* Is Negatively Phototactic, with a Wavelength Dependence That Fits the Absorption Spectrum of the Photoactive Yellow Protein. *J. Bacteriol.* 1993, 175, 3096–3104. [PubMed: 8491725]
- (60). Favory JJ; Stec A; Gruber H; Rizzini L; Oravec A; Funk M; Albert A; Cloix C; Jenkins GI; Oakeley EJ; et al. Interaction of COP1 and UVR8 Regulates UV-B-Induced Photomorphogenesis and Stress Acclimation in *Arabidopsis*. *EMBO J.* 2009, 28, 591–601. [PubMed: 19165148]
- (61). Rizzini L; Favory JJ; Cloix C; Faggionato D; O'Hara A; Kaiserli E; Baumeister R; Schafer E; Nagy F; Jenkins GI; et al. Perception of UV-B by the *Arabidopsis* UVR8 Protein. *Science* 2011, 332, 103–106. [PubMed: 21454788]
- (62). Di Wu; Hu Q; Yan Z; Chen W; Yan C; Huang X; Zhang J; Yang P; Deng H; Wang J; et al. Structural Basis of Ultraviolet-B Perception by UVR8. *Nature* 2012, 484, 214–219. [PubMed: 22388820]
- (63). Christie JM; Arvai AS; Baxter KJ; Heilmann M; Pratt AJ; O'Hara A; Kelly SM; Hothorn M; Smith BO; Hitomi K; et al. Plant UVR8 Photoreceptor Senses UV-B by Tryptophan-Mediated Disruption of Cross-Dimer Salt Bridges. *Science* 2012, 335, 1492–1496. [PubMed: 22323738]
- (64). Berntsson O; Diensthuber RP; Panman MR; Björling A; Gustavsson E; Hoerlke M; Hughes AJ; Henry L; Niebling S; Takala H; et al. Sequential Conformational Transitions and  $\alpha$ -Helical Supercoiling Regulate a Sensor Histidine Kinase. *Nat. Commun* 2017, 8, 284. [PubMed: 28819239]
- (65). Bugaj LJ; Choksi AT; Mesuda CK; Kane RS; Schaffer DV Optogenetic Protein Clustering and Signaling Activation in Mammalian Cells. *Nat. Methods* 2013, 10, 249–252. [PubMed: 23377377]
- (66). Shin Y; Berry J; Pannucci N; Haataja MP; Toettcher JE; Brangwynne CP Spatiotemporal Control of Intracellular Phase Transitions Using Light-Activated optoDroplets. *Cell* 2017, 168, 159–171. [PubMed: 28041848]
- (67). Ziegler T; Möglich A Photoreceptor Engineering. *Front. Mol. Biosci.* 2015, 2, 30. [PubMed: 26137467]
- (68). Ren S; Sato R; Hasegawa K; Ohta H; Masuda S A Predicted Structure for the PixD-PixE Complex Determined by Homology Modeling, Docking Simulations, and a Mutagenesis Study. *Biochemistry* 2013, 52, 1272–1279. [PubMed: 23346988]



- (69). Vaidya AT; Chen C-H; Dunlap JC; Loros JJ; Crane BR Structure of a Light-Activated LOV Protein Dimer That Regulates Transcription. *Sci. Signal.* 2011, 4, ra50. [PubMed: 21868352]
- (70). Takakado A; Nakasone Y; Terazima M Photoinduced Dimerization of a Photosensory DNA-Binding Protein EL222 and Its LOV Domain. *Phys. Chem. Chem. Phys.* 2017, 19, 24855–24865. [PubMed: 28868541]
- (71). Purcell EB; McDonald CA; Palfey BA; Crosson S An Analysis of the Solution Structure and Signaling Mechanism of LovK, a Sensor Histidine Kinase Integrating Light and Redox Signals. *Biochemistry* 2010, 49, 6761–6770. [PubMed: 20593779]
- (72). Strickland D; Yao X; Gawlak G; Rosen MK; Gardner KH; Sosnick TR Rationally Improving LOV Domain-Based Photoswitches. *Nat. Methods* 2010, 7, 623–626. [PubMed: 20562867]
- (73). Crick F The Impact of Molecular Biology on Neuroscience. *Philos. Trans. R. Soc. B Biol. Sci.* 1999, 354, 2021–2025.
- (74). Zemelman BV; Lee GA; Ng M; Miesenböck G Selective Photostimulation of Genetically ChARGed Neurons. *Neuron* 2002, 33, 15–22. [PubMed: 11779476]
- (75). Nagel G; Ollig D; Fuhrmann M; Kateriya S; Musti AM; Bamberg E; Hegemann P Channelrhodopsin-1: A Light-Gated Proton Channel in Green Algae. *Science* 2002, 296, 2395–2398. [PubMed: 12089443]
- (76). Nagel G; Szellas T; Huhn W; Kateriya S; Adeishvili N; Berthold P; Ollig D; Hegemann P; Bamberg E Channelrhodopsin-2, a Directly Light-Gated Cation-Selective Membrane Channel. *Proc. Natl. Acad. Sci. U. S. A.* 2003, 100, 13940–13945. [PubMed: 14615590]
- (77). Crosson S; Moffat K Structure of a Flavin-Binding Plant Photoreceptor Domain: Insights into Light-Mediated Signal Transduction. *Proc Natl Acad Sci U S A* 2001, 98, 2995–3000. [PubMed: 11248020]
- (78). Crosson S; Moffat K Photoexcited Structure of a Plant Photoreceptor Domain Reveals a Light-Driven Molecular Switch. *Plant Cell* 2002, 14, 1067–1075. [PubMed: 12034897]
- (79). Deisseroth K Optogenetics. *Nat Methods* 2011, 8, 26–29. [PubMed: 21191368]
- (80). Hegemann P; Möglich A Channelrhodopsin Engineering and Exploration of New Optogenetic Tools. *Nat. Methods* 2011, 8, 39–42. [PubMed: 21191371]
- (81). Repina NA; Rosenbloom A; Mukherjee A; Schaffer DV; Kane RS At Light Speed: Advances in Optogenetic Systems for Regulating Cell Signaling and Behavior. *Annu. Rev. Chem. Biomol. Eng.* 2017, 8, 13–39. [PubMed: 28592174]
- (82). Eleftheriou C; Cesca F; Maragliano L; Benfenati F; Maya-Vetencourt JF Optogenetic Modulation of Intracellular Signalling and Transcription: Focus on Neuronal Plasticity. *J. Exp. Neurosci* 2017, 11, 1179069517703354. [PubMed: 28579827]
- (83). Fan LZ; Lin MZ Optical Control of Biological Processes by Light-Switchable Proteins. *Wiley Interdiscip. Rev. Dev. Biol.* 2015, 4, 545–554. [PubMed: 25858669]
- (84). Kolar K; Weber W Synthetic Biological Approaches to Optogenetically Control Cell Signaling. *Curr. Opin. Biotechnol.* 2017, 47, 112–119. [PubMed: 28715701]
- (85). Endo M; Ozawa T Strategies for Development of Optogenetic Systems and Their Applications. *J. Photochem. Photobiol. C Photochem. Rev* 2017, 30, 10–23.
- (86). Liu Q; Tucker CL Engineering Genetically-Encoded Tools for Optogenetic Control of Protein Activity. *Curr. Opin. Chem. Biol.* 2017, 40, 17–23. [PubMed: 28527343]
- (87). Khamo JS; Krishnamurthy VV; Sharum SR; Mondal P; Zhang K Applications of Optobiology in Intact Cells and Multicellular Organisms. *J. Mol. Biol.* 2017, 429, 2999–3017. [PubMed: 28882542]
- (88). Tischer D; Weiner OD Illuminating Cell Signalling with Optogenetic Tools. *Nat. Rev. Mol. Cell Biol.* 2014, 15, 551–558. [PubMed: 25027655]
- (89). Ueda Y; Sato M Induction of Signal Transduction Using Non-Channelrhodopsin-Type Optogenetic Tools. *Chembiochem A Eur. J. Chem. Biol* 2018, *in press*, 10.1002/cbic.201700635.
- (90). Losi A; Mandalari C; Gärtner W From Plant Infectivity to Growth Patterns: The Role of Blue-Light Sensing in the Prokaryotic World. *Plants* 2014, 3, 70–94. [PubMed: 27135492]
- (91). Jansen V; Jikeli JF; Wachten D How to Control Cyclic Nucleotide Signaling by Light. *Curr. Opin. Biotechnol.* 2017, 48, 15–20. [PubMed: 28288335]

- (92). Motta-Mena LB; Reade A; Mallory MJ; Glantz S; Weiner OD; Lynch KW; Gardner KH An Optogenetic Gene Expression System with Rapid Activation and Deactivation Kinetics. *Nat. Chem. Biol.* 2014, 10, 196–202. [PubMed: 24413462]
- (93). Stierl M; Stumpf P; Udvari D; Gueta R; Hagedorn R; Losi A; Gärtner W; Petereit L; Efetova M; Schwarzel M; et al. Light-Modulation of Cellular cAMP by a Small Bacterial Photoactivated Adenylyl Cyclase, bPAC, of the Soil Bacterium *Beggiatoa*. *J. Biol. Chem.* 2011, 286, 1181–1188. [PubMed: 21030594]
- (94). Ryu M-H; Moskvina OV; Siltberg-Liberles J; Gomelsky M Natural and Engineered Photoactivated Nucleotidyl Cyclases for Optogenetic Applications. *J. Biol. Chem.* 2010, 285, 41501–41508. [PubMed: 21030591]
- (95). Park S-Y; Tame JRH Seeing the Light with BLUF Proteins. *Biophys. Rev.* 2017, 9, 169–176. [PubMed: 28510088]
- (96). Fankhauser C; Christie JM Plant Phototropic Growth. *Curr. Biol.* 2015, 25, R384–389. [PubMed: 25942556]
- (97). Pennacchietti F; Abbruzzetti S; Losi A; Mandalari C; Bedotti R; Viappiani C; Zancacchi FC; Diaspro A; Gärtner W The Dark Recovery Rate in the Photocycle of the Bacterial Photoreceptor YtvA Is Affected by the Cellular Environment and by Hydration. *PLoS One* 2014, 9, e107489. [PubMed: 25211155]
- (98). Jurk M; Dorn M; Kikhney A; Svergun D; Gärtner W; Schmieder P The Switch That Does Not Flip: The Blue-Light Receptor YtvA from *Bacillus Subtilis* Adopts an Elongated Dimer Conformation Independent of the Activation State as Revealed by a Combined AUC and SAXS Study. *J. Mol. Biol.* 2010, 403, 78–87. [PubMed: 20800068]
- (99). Engelhard C; Raffelberg S; Tang Y; Diensthuber RP; Möglich A; Losi A; Gärtner W; Bittl R A Structural Model for the Full-Length Blue Light-Sensing Protein YtvA from *Bacillus Subtilis*, Based on EPR Spectroscopy. *Photochem. Photobiol. Sci.* 2013, 12, 1855–1863. [PubMed: 23900620]
- (100). Halavaty AS; Moffat K Coiled-Coil Dimerization of the LOV2 Domain of the Blue-Light Photoreceptor Phototropin 1 from *Arabidopsis Thaliana*. *Acta Crystallogr. Sect. F Struct. Biol. Cryst. Commun.* 2013, 69, 1316–1321.
- (101). Yao X; Rosen MK; Gardner KH Estimation of the Available Free Energy in a LOV2-Ja Photoswitch. *Nat. Chem. Biol.* 2008, 4, 491–497. [PubMed: 18604202]
- (102). Jäckel C; Kast P; Hilvert D Protein Design by Directed Evolution. *Annu. Rev. Biophys.* 2008, 37, 153–173. [PubMed: 18573077]
- (103). Wu YI; Frey D; Lungu OI; Jaehrig A; Schlichting I; Kuhlman B; Hahn KM A Genetically Encoded Photoactivatable Rac Controls the Motility of Living Cells. *Nature* 2009, 461, 104–108. [PubMed: 19693014]
- (104). Strickland D; Moffat K; Sosnick TR Light-Activated DNA Binding in a Designed Allosteric Protein. *Proc. Natl. Acad. Sci. U. S. A.* 2008, 105, 10709–10714. [PubMed: 18667691]
- (105). Möglich A; Ayers RA; Moffat K Design and Signaling Mechanism of Light-Regulated Histidine Kinases. *J. Mol. Biol.* 2009, 385, 1433–1444. [PubMed: 19109976]
- (106). Ohlendorf R; Schumacher CH; Richter F; Möglich A Library-Aided Probing of Linker Determinants in Hybrid Photoreceptors. *ACS Synth. Biol.* 2016, 5, 1117–1126. [PubMed: 27002379]
- (107). Ohlendorf R; Vidavski RR; Eldar A; Möffat K; Möglich A From Dusk till Dawn: One-Plasmid Systems for Light-Regulated Gene Expression. *J. Mol. Biol.* 2012, 416, 534–542. [PubMed: 22245580]
- (108). Longwell CK; Labanieh L; Cochran JR High-Throughput Screening Technologies for Enzyme *Engineering*. *Curr. Opin. Biotechnol.* 2017, 48, 196–202. [PubMed: 28624724]
- (109). Dagliyan O; Tarnawski M; Chu P-H; Shirvanyants D; Schlichting I; Dokholyan NV; Hahn KM Engineering Extrinsic Disorder to Control Protein Activity in Living Cells. *Science* 2016, 354, 1441–1444. [PubMed: 27980211]
- (110). Kumar A; Burns DC; Al-Abdul-Wahid MS; Woolley GA A Circularly Permuted Photoactive Yellow Protein as a Scaffold for Photoswitch Design. *Biochemistry* 2013, 52, 3320–3331. [PubMed: 23570450]

- (111). Zhou H; Zoltowski BD; Tao P Revealing Hidden Conformational Space of LOV Protein VIVID Through Rigid Residue Scan Simulations. *Sci. Rep.* 2017, 7, 46626. [PubMed: 28425502]
- (112). Glantz ST; Carpenter EJ; Melkonian M; Gardner KH; Boyden ES; Wong GK-S; Chow BY Functional and Topological Diversity of LOV Domain Photoreceptors. *Proc. Natl. Acad. Sci. U. S. A.* 2016, 113, E1442–1451. [PubMed: 26929367]
- (113). Rockwell NC; Ohlendorf R; Möglich A Cyanobacteriochromes in Full Color and Three Dimensions. *Proc. Natl. Acad. Sci. U. S. A.* 2013, 110, 806–807. [PubMed: 23288903]
- (114). Yazawa M; Sadaghiani AM; Hsueh B; Dolmetsch RE Induction of Protein-Protein Interactions in Live Cells Using Light. *Nat. Biotechnol.* 2009, 27, 941–945. [PubMed: 19801976]
- (115). Diensthuber RP; Bommer M; Gleichmann T; Möglich A Full-Length Structure of a Sensor Histidine Kinase Pinpoints Coaxial Coiled Coils as Signal Transducers and Modulators. *Structure* 2013, 21, 1127–1136. [PubMed: 23746806]
- (116). Morgan S-A; Al-Abdul-Wahid S; Woolley GA Structure-Based Design of a Photocontrolled DNA Binding Protein. *J. Mol. Biol.* 2010, 399, 94–112. [PubMed: 20363227]
- (117). Fan HY; Morgan S-A; Brechun KE; Chen Y-Y; Jaikaran ASI; Woolley GA Improving a Designed Photocontrolled DNA-Binding Protein. *Biochemistry* 2011, 50, 1226–1237. [PubMed: 21214273]
- (118). Hühner J; Ingles-Prieto Á; Neusüß C; Lämmerhofer M; Janovjak H Quantification of Riboflavin, Flavin Mononucleotide, and Flavin Adenine Dinucleotide in Mammalian Model Cells by CE with LED-Induced Fluorescence Detection. *Electrophoresis* 2015, 36, 518–525. [PubMed: 25488801]
- (119). Mühlhäuser WWD; Fischer A; Weber W; Radziwill G Optogenetics - Bringing Light into the Darkness of Mammalian Signal Transduction. *Biochim. Biophys. Acta - Mol. Cell Res.* 2017, 1864, 280–292. [PubMed: 27845208]
- (120). van den Berg PA; Widengren J; Hink MA; Rigler R; Visser AJ Fluorescence Correlation Spectroscopy of Flavins and Flavoenzymes: Photochemical and Photophysical Aspects. *Spectrochim. Acta. A. Mol. Biomol. Spectrosc.* 2001, 57, 2135–2144. [PubMed: 11603835]
- (121). Shcherbakova DM; Shemetov AA; Kaberniuk AA; Verkhusha VV Natural Photoreceptors as a Source of Fluorescent Proteins, Biosensors, and Optogenetic Tools. *Annu. Rev. Biochem* 2015, 84, 519–550. [PubMed: 25706899]
- (122). Kobayashi H; Ogawa M; Alford R; Choyke PL; Urano Y New Strategies for Fluorescent Probe Design in Medical Diagnostic Imaging. *Chem. Rev.* 2010, 110, 2620–2640. [PubMed: 20000749]
- (123). Losi A; Gärtner W Solving Blue Light Riddles: New Lessons from Flavin-Binding LOV Photoreceptors. *Photochem. Photobiol.* 2017, 93, 141–158. [PubMed: 27861974]
- (124). He L; Zhang Y; Ma G; Tan P; Li Z; Zang S; Wu X; Jing J; Fang S; Zhou L; et al. Near-Infrared Photoactivatable Control of Ca(2+) Signaling and Optogenetic Immunomodulation. *Elife* 2015, 4, e10024. [PubMed: 26646180]
- (125). Di Ventura B; Kuhlman B Go in! Go out! Inducible Control of Nuclear Localization. *Curr. Opin. Chem. Biol.* 2016, 34, 62–71. [PubMed: 27372352]
- (126). Arinkin V; Granzin J; Röllen K; Krauss U; Jaeger K Structure of a LOV Protein in Apo-State and Implications for Construction of LOV-Based Optical Tools. *Sci. Rep.* 2017, 7, 42971. [PubMed: 28211532]
- (127). Raffelberg S; Gutt A; Gärtner W; Mandalari C; Abbruzzetti S; Viappiani C; Losi A The Amino Acids Surrounding the Flavin 7a-Methyl Group Determine the UVA Spectral Features of a LOV Protein. *Biol. Chem.* 2013, 394, 1517–1528. [PubMed: 23828427]
- (128). Davari MD; Kopka B; Wingen M; Bocola M; Drepper T; Jaeger K-E; Schwaneberg U; Krauss U Photophysics of the LOV-Based Fluorescent Protein Variant iLOV-Q489K Determined by Simulation and Experiment. *J. Phys. Chem. B* 2016, 120, 3344–3352. [PubMed: 26962999]
- (129). Khrenova MG; Meteleshko YI; Nemukhin AV Mutants of the Flavoprotein iLOV as Prospective Red-Shifted Fluorescent Markers. *J. Phys. Chem. B* 2017, 121, 10018–10025. [PubMed: 28992704]
- (130). Bury A; Hellingwerf KJ On the in Vivo Redox State of Flavin-Containing Photosensory Receptor Proteins. *Methods Mol. Biol.* 2014, 1146, 177–190. [PubMed: 24764093]

- (131). Beel B; Prager K; Spexard M; Sasso S; Weiss D; Muller N; Heinnickel M; Dewez D; Ikoma D; Grossman AR; et al. A Flavin Binding Cryptochrome Photoreceptor Responds to Both Blue and Red Light in *Chlamydomonas Reinhardtii*. *Plant Cell* 2012, 24, 2992–3008. [PubMed: 22773746]
- (132). Kottke T; Oldemeyer S; Wenzel S; Zou Y; Mittag M Cryptochrome Photoreceptors in Green Algae: Unexpected Versatility of Mechanisms and Functions. *J. Plant Physiol.* 2017, 217, 4–14. [PubMed: 28619534]
- (133). Spexard M; Thöing C; Beel B; Mittag M; Kottke T Response of the Sensory Animal-like Cryptochrome aCRY to Blue and Red Light As Revealed by Infrared Difference Spectroscopy. *Biochemistry* 2014, 53, 1041–1050. [PubMed: 24467183]
- (134). Scheib U; Stehfest K; Gee CE; Körschen HG; Fudim R; Oertner TG; Hegemann P The Rhodopsin–guanylyl Cyclase of the Aquatic Fungus *Blastocladiella Emersonii* Enables Fast Optical Control of cGMP Signaling. *Sci. Signal.* 2015, 8, rs8. [PubMed: 26268609]
- (135). Gao S; Nagpal J; Schneider MW; Kozjak-Pavlovic V; Nagel G; Gottschalk A Optogenetic Manipulation of cGMP in Cells and Animals by the Tightly Light-Regulated Guanylyl-Cyclase Opsin CycloP. *Nat. Commun.* 2015, 6, 8046. [PubMed: 26345128]
- (136). Monod J; Wyman J; Changeux JP On the Nature of Allosteric Transitions: A Plausible Model. *J Mol Biol* 1965, 12, 88–118. [PubMed: 14343300]
- (137). Möglich A; Ayers RA; Moffat K Addition at the Molecular Level: Signal Integration in Designed Per-ARNT-Sim Receptor Proteins. *J. Mol. Biol.* 2010, 400, 477–486. [PubMed: 20471402]
- (138). Konold PE; Mathes T; Weißenborn J; Groot ML; Hegemann P; Kennis JTM Unfolding of the C-Terminal Ja Helix in the LOV2 Photoreceptor Domain Observed by Time-Resolved Vibrational Spectroscopy. *J. Phys. Chem. Lett* 2016, 7, 3472–3476. [PubMed: 27537211]
- (139). Freddolino PL; Gardner KH; Schulten K Signaling Mechanisms of LOV Domains: New Insights from Molecular Dynamics Studies. *Photochem. Photobiol. Sci.* 2013, 12, 1158–1170. [PubMed: 23407663]
- (140). Takeda K; Nakasone Y; Zikihara K; Tokutomi S; Terazima M Dynamics of the Amino-Terminal and Carboxyl-Terminal Helices of *Arabidopsis* Phototropin 1 LOV2 Studied by the Transient Grating. *J. Phys. Chem. B* 2013, 117, 15606–15613. [PubMed: 23931584]
- (141). Choi S; Nakasone Y; Hellingwerf KJ; Terazima M Photochemical Reactions of the LOV and LOV-Linker Domains of the Blue Light Sensor Protein YtvA. *Biochemistry* 2016, 55, 3107–3115. [PubMed: 27203230]
- (142). Thöing C; Oldemeyer S; Kottke T Microsecond Deprotonation of Aspartic Acid and Response of the A/β Subdomain Precede C-Terminal Signaling in the Blue Light Sensor Plant Cryptochrome. *J. Am. Chem. Soc.* 2015, 137, 5990–5999. [PubMed: 25909499]
- (143). Sommer C; Dietz MS; Patschkowski T; Mathes T; Kottke T Light-Induced Conformational Changes in the Plant Cryptochrome Photolyase Homology Region Resolved by Selective Isotope Labeling and Infrared Spectroscopy. *Photochem. Photobiol.* 2017, 93, 881–887. [PubMed: 28500697]
- (144). Kondoh M; Shiraishi C; Müller P; Ahmad M; Hitomi K; Getzoff ED; Terazima M Light-Induced Conformational Changes in Full-Length *Arabidopsis Thaliana* Cryptochrome. *J. Mol. Biol.* 2011, 413, 128–137. [PubMed: 21875594]
- (145). Tanaka K; Nakasone Y; Okajima K; Ikeuchi M; Tokutomi S; Terazima M Oligomeric-State-Dependent Conformational Change of the BLUF Protein *TεPixD* (Tll0078). *J. Mol. Biol.* 2009, 386, 1290–1300. [PubMed: 19452599]
- (146). Kuroi K; Tanaka K; Okajima K; Ikeuchi M; Tokutomi S; Terazima M Anomalous Diffusion of *TεPixD* and Identification of the Photoreaction Product. *Photochem. Photobiol. Sci.* 2013, 12, 1180–1186. [PubMed: 23535998]
- (147). Tanaka K; Nakasone Y; Okajima K; Ikeuchi M; Tokutomi S; Terazima M Light-Induced Conformational Change and Transient Dissociation Reaction of the BLUF Photoreceptor *Synechocystis PixD* (Slr1694). *J. Mol. Biol.* 2011, 409, 773–785. [PubMed: 21530536]

- (148). Lamb JS; Zoltowski BD; Pabit SA; Crane BR; Pollack L Time-Resolved Dimerization of a PAS-LOV Protein Measured with Photocoupled Small Angle X-Ray Scattering. *J. Am. Chem. Soc.* 2008, 130, 12226–12227. [PubMed: 18715002]
- (149). Zoltowski BD; Vaccaro B; Crane BR Mechanism-Based Tuning of a LOV Domain Photoreceptor. *Nat. Chem. Biol.* 2009, 5, 827–834. [PubMed: 19718042]
- (150). El-Arab KK; Pudasaini A; Zoltowski BD Short LOV Proteins in *Methylocystis* Reveal Insight into LOV Domain Photocycle Mechanisms. *PLoS One* 2015, 10, e0124874. [PubMed: 25933162]
- (151). Lokhandwala J; Silverman Y de la Vega RI; Hopkins HC; Britton CW; Rodriguez-Iglesias A; Bogomolni R; Schmoll M; Zoltowski BD A Native Threonine Coordinates Ordered Water to Tune Light-Oxygen-Voltage (LOV) Domain Photocycle Kinetics and Osmotic Stress Signaling in *Trichoderma Reesei* *ENVOY*. *J. Biol. Chem.* 2016, 291, 14839–14850. [PubMed: 27226624]
- (152). Raffelberg S; Mansurova M; Gärtner W; Losi A Modulation of the Photocycle of a LOV Domain Photoreceptor by the Hydrogen-Bonding Network. *J. Am. Chem. Soc.* 2011, 133, 5346–5356. [PubMed: 21410163]
- (153). Zayner JP; Sosnick TR Factors That Control the Chemistry of the LOV Domain Photocycle. *PLoS One* 2014, 9, e87074. [PubMed: 24475227]
- (154). Diensthuber RP; Engelhard C; Lemke N; Gleichmann T; Ohlendorf R; Bittl R; Möglich A Biophysical, Mutational, and Functional Investigation of the Chromophore-Binding Pocket of Light-Oxygen-Voltage Photoreceptors. *ACS Synth. Biol.* 2014, 3, 811–819. [PubMed: 24926890]
- (155). Ganguly A; Thiel W; Crane BR Glutamine Amide Flip Elicits Long Distance Allosteric Responses in the LOV Protein Vivid. *J. Am. Chem. Soc.* 2017, 139, 2972–2980. [PubMed: 28145707]
- (156). Ganguly A; Manahan CC; Top D; Yee EF; Lin C; Young MW; Thiel W; Crane BR Changes in Active Site Histidine Hydrogen Bonding Trigger Cryptochrome Activation. *Proc. Natl. Acad. Sci. U. S. A.* 2016, 113, 10073–10078. [PubMed: 27551082]
- (157). Kennis JTM; van Stokkum IHM; Crosson S; Gauden M; Moffat K; van Grondelle R The LOV2 Domain of Phototropin: A Reversible Photochromic Switch. *J. Am. Chem. Soc.* 2004, 126, 4512–4513. [PubMed: 15070357]
- (158). Losi A; Gärtner W; Raffelberg S; Cella Zanacchi F; Bianchini P; Diaspro A; Mandalari C; Abbruzzetti S; Viappiani C A Photochromic Bacterial Photoreceptor with Potential for Super-Resolution Microscopy. *Photochem. Photobiol. Sci.* 2013, 12, 231–235. [PubMed: 23047813]
- (159). Song S-H; Madsen D; van der Steen JB; Pullman R; Freer LH; Hellingwerf KJ; Larsen DS Primary Photochemistry of the Dark- and Light-Adapted States of the YtvA Protein from *Bacillus Subtilis*. *Biochemistry* 2013, 52, 7951–7963. [PubMed: 24171435]
- (160). Bouly J-P; Schleicher E; Dionisio-Sese M; Vandebussche F; Van Der Straeten D; Bakrim N; Meier S; Batschauer A; Galland P; Bittl R; et al. Cryptochrome Blue Light Photoreceptors Are Activated through Interconversion of Flavin Redox States. *J. Biol. Chem.* 2007, 282, 9383–9391. [PubMed: 17237227]
- (161). Hennemann J; Iwasaki RI; Grund TN; Diensthuber RP; Richter F; Möglich A Optogenetic Control by Pulsed Illumination. *ChemBioChem* 2018, 10.1002/cbic.201800030.
- (162). Kolar K; Stork H; Knobloch C; Žnidari M; Weber W OptoBase. [www.optobase.org](http://www.optobase.org).
- (163). Rivera-Cancel G; Ko W; Tomchick DR; Correa F; Gardner KH Full-Length Structure of a Monomeric Histidine Kinase Reveals Basis for Sensory Regulation. *Proc. Natl. Acad. Sci. U. S. A.* 2014, 111, 17839–17844. [PubMed: 25468971]
- (164). Chen X; Liu R; Ma Z; Xu X; Zhang H; Xu J; Ouyang Q; Yang Y An Extraordinary Stringent and Sensitive Light-Switchable Gene Expression System for Bacterial Cells. *Cell Res.* 2016, 26, 854–857. [PubMed: 27311594]
- (165). Kawano F; Suzuki H; Furuya A; Sato M Engineered Pairs of Distinct Photoswitches for Optogenetic Control of Cellular Proteins. *Nat. Commun.* 2015, 6, 6256. [PubMed: 25708714]
- (166). Han T; Chen Q; Liu H Engineered Photoactivatable Genetic Switches Based on the Bacterium Phage T7 RNA Polymerase. *ACS Synth. Biol.* 2017, 6, 357–366. [PubMed: 27794600]

- (167). Baumschlager A; Aoki SK; Khammash M Dynamic Blue Light-Inducible T7 RNA Polymerases (Opto-T7RNAPs) for Precise Spatiotemporal Gene Expression Control. *ACS Synth. Biol.* 2017, 6, 2157–2167. [PubMed: 29045151]
- (168). Losi A; Polverini E; Quest B; Gärtner W First Evidence for Phototropin-Related Blue-Light Receptors in Prokaryotes. *Biophys J* 2002, 82, 2627–2634. [PubMed: 11964249]
- (169). Capra EJ; Laub MT Evolution of Two-Component Signal Transduction Systems. *Annu. Rev. Microbiol* 2012, 66, 325–347. [PubMed: 22746333]
- (170). Swartz TE; Tseng TS; Frederickson MA; Paris G; Comerci DJ; Rajashekara G; Kim JG; Mudgett MB; Splitter GA; Ugalde RA; et al. Blue-Light-Activated Histidine Kinases: Two-Component Sensors in Bacteria. *Science* 2007, 317, 1090–1093. [PubMed: 17717187]
- (171). Purcell EB; Siegal-Gaskins D; Rawling DC; Fiebig A; Crosson S A Photosensory Two-Component System Regulates Bacterial Cell Attachment. *Proc Natl Acad Sci U S A* 2007, 104, 18241–18246. [PubMed: 17986614]
- (172). Herrou J; Crosson S Function, Structure and Mechanism of Bacterial Photosensory LOV Proteins. *Nat. Rev. Microbiol.* 2011, 9, 713–723. [PubMed: 21822294]
- (173). Fernandez-Rodriguez J; Moser F; Song M; Voigt CA Engineering RGB Color Vision into *Escherichia Coli*. *Nat. Chem. Biol.* 2017, 13, 706–708. [PubMed: 28530708]
- (174). Magaraci MS; Veerakumar A; Qiao P; Amurthur A; Lee JY; Miller JS; Goulian M; Sarkar CA Engineering *Escherichia Coli* for Light-Activated Cytolysis of Mammalian Cells. *ACS Synth. Biol.* 2014, 3, 944–948. [PubMed: 24933444]
- (175). Farzadfard F; Lu TK Genomically Encoded Analog Memory with Precise in Vivo DNA Writing in Living Cell Populations. *Science* 2014, 346, 1256272. [PubMed: 25395541]
- (176). Tang W; Liu DR Rewritable Multi-Event Analog Recording in Bacterial and Mammalian Cells. *Science* 2018, 360, eaap8992. [PubMed: 29449507]
- (177). Engelhard C; Diensthuber RP; Möglich A; Bittl R Blue-Light Reception through Quaternary Transitions. *Sci. Rep* 2017, 7, 1385. [PubMed: 28469162]
- (178). Berntsson O; Diensthuber RP; Panman MR; Björling A; Hughes AJ; Henry L; Niebling S; Newby G; Liebi M; Menzel A; et al. Time-Resolved X-Ray Solution Scattering Reveals the Structural Photoactivation of a Light-Oxygen-Voltage Photoreceptor. *Structure* 2017, 25, 933–938. [PubMed: 28502782]
- (179). Gleichmann T; Diensthuber RP; Möglich A Charting the Signal Trajectory in a Light-Oxygen-Voltage Photoreceptor by Random Mutagenesis and Covariance Analysis. *J. Biol. Chem.* 2013, 288, 29345–29355. [PubMed: 24003219]
- (180). Correa F; Ko WH; Ocasio V; Bogomolni RA; Gardner KH Blue Light Regulated Two-Component Systems: Enzymatic and Functional Analyses of Light-Oxygen-Voltage (LOV)-Histidine Kinases and Downstream Response Regulators. *Biochemistry* 2013, 52, 4656–4666. [PubMed: 23806044]
- (181). Corrêa F; Gardner KH Basis of Mutual Domain Inhibition in a Bacterial Response Regulator. *Cell Chem. Biol.* 2016, 23, 945–955. [PubMed: 27524295]
- (182). Rivera-Cancel G; Motta-Mena LB; Gardner KH Identification of Natural and Artificial DNA Substrates for Light-Activated LOV–HTH Transcription Factor EL222. *Biochemistry* 2012, 51, 10024–10034. [PubMed: 23205774]
- (183). Jayaraman P; Devarajan K; Chua TK; Zhang H; Gunawan E; Poh CL Blue Light-Mediated Transcriptional Activation and Repression of Gene Expression in Bacteria. *Nucleic Acids Res.* 2016, 44, 6994–7005. [PubMed: 27353329]
- (184). Jayaraman P; Yeoh JW; Jayaraman S; Teh AY; Zhang J; Poh CL Cell-Free Optogenetic Gene Expression System. *ACS Synth. Biol.* 2018, 7, 986–994. [PubMed: 29596741]
- (185). Wang X; Chen X; Yang Y Spatiotemporal Control of Gene Expression by a Light-Switchable Transgene System. *Nat. Methods* 2012, 9, 266–269. [PubMed: 22327833]
- (186). Fuerst TR; Niles EG; Studier FW; Moss B Eukaryotic Transient-Expression System Based on Recombinant Vaccinia Virus That Synthesizes Bacteriophage T7 RNA Polymerase. *Proc. Natl. Acad. Sci. U. S. A.* 1986, 83, 8122–8126. [PubMed: 3095828]

- (187). Froehlich AC; Liu Y; Loros JJ; Dunlap JC White Collar-1, a Circadian Blue Light Photoreceptor, Binding to the Frequency Promoter. *Science* 2002, 297, 815–819. [PubMed: 12098706]
- (188). Takahashi F; Yamagata D; Ishikawa M; Fukamatsu Y; Ogura Y; Kasahara M; Kiyosue T; Kikuyama M; Wada M; Kataoka H AUREOCHROME, a Photoreceptor Required for Photomorphogenesis in Stramenopiles. *Proc Natl Acad Sci U S A* 2007, 104, 19625–19630. [PubMed: 18003911]
- (189). Herman E; Sachse M; Kroth PG; Kottke T Blue-Light-Induced Unfolding of the  $\alpha$  Helix Allows for the Dimerization of Aureochrome-LOV from the Diatom *Phaeodactylum Tricornutum*. *Biochemistry* 2013, 52, 3094–3101. [PubMed: 23621750]
- (190). Grusch M; Schelch K; Riedler R; Reichhart E; Differ C; Berger W; Inglés-Prieto Á; Janovjak H Spatio-Temporally Precise Activation of Engineered Receptor Tyrosine Kinases by Light. *EMBO J.* 2014, 33, 1713–1726. [PubMed: 24986882]
- (191). Heintz U; Schlichting I Blue Light-Induced LOV Domain Dimerization Enhances the Affinity of Aureochrome 1a for Its Target DNA Sequence. *Elife* 2016, 5, e11860. [PubMed: 26754770]
- (192). Banerjee A; Herman E; Kottke T; Essen L-O Structure of a Native-like Aureochrome 1a LOV Domain Dimer from *Phaeodactylum Tricornutum*. *Structure* 2016, 24, 171–178. [PubMed: 26688213]
- (193). Liu H; Gomez G; Lin S; Lin S; Lin C Optogenetic Control of Transcription in Zebrafish. *PLoS One* 2012, 7, e50738. [PubMed: 23226369]
- (194). Crefcoeur RP; Yin R; Ulm R; Halazonetis TD Ultraviolet-B-Mediated Induction of Protein-Protein Interactions in Mammalian Cells. *Nat. Commun.* 2013, 4, 1779. [PubMed: 23653191]
- (195). Müller K; Engesser R; Schulz S; Steinberg T; Tomakidi P; Weber CC; Ulm R; Timmer J; Zurbriggen MD; Weber W Multi-Chromatic Control of Mammalian Gene Expression and Signaling. *Nucleic Acids Res.* 2013, 41, e124. [PubMed: 23625964]
- (196). Pathak GP; Spiltoir JI; Höglund C; Polstein LR; Heine-Koskinen S; Gersbach CA; Rossi J; Tucker CL Bidirectional Approaches for Optogenetic Regulation of Gene Expression in Mammalian Cells Using *Arabidopsis* Cryptochrome 2. *Nucleic Acids Res.* 2017, 45, e167. [PubMed: 28431041]
- (197). Reade A; Motta-Mena LB; Gardner KH; Stainier DY; Weiner OD; Woo S TAE1: A Zebrafish-Optimized Optogenetic Gene Expression System with Fine Spatial and Temporal Control. *Development* 2017, 144, 345–355. [PubMed: 27993986]
- (198). Zhao EM; Zhang Y; Mehl J; Park H; Lalwani MA; Toettcher JE; Avalos JL Optogenetic Regulation of Engineered Cellular Metabolism for Microbial Chemical Production. *Nature* 2018, 555, 683–687. [PubMed: 29562237]
- (199). Nihongaki Y; Suzuki H; Kawano F; Sato M Genetically Engineered Photoinducible Homodimerization System with Improved Dimer-Forming Efficiency. *ACS Chem. Biol.* 2014, 9, 617–621. [PubMed: 24428544]
- (200). Zikiyara K; Iwata T; Matsuoka D; Kandori H; Todo T; Tokutomi S Photoreaction Cycle of the Light, Oxygen, and Voltage Domain in FKF1 Determined by Low-Temperature Absorption Spectroscopy. *Biochemistry* 2006, 45, 10828–10837. [PubMed: 16953568]
- (201). Quejada JR; Park S-HE; Awari DW; Shi F; Yamamoto HE; Kawano F; Jung JC; Yazawa M Optimized Light-Inducible Transcription in Mammalian Cells Using Flavin Kelch-Repeat F-box1/GIGANTEA and CRY2/CIB1. *Nucleic Acids Res.* 2017, 45, e172. [PubMed: 29040770]
- (202). Lungu OI; Hallett RA; Choi EJ; Aiken MJ; Hahn KM; Kuhlman B Designing Photoswitchable Peptides Using the AsLOV2 Domain. *Chem. Biol.* 2012, 19, 507–517. [PubMed: 22520757]
- (203). Guntas G; Hallett RA; Zimmerman SP; Williams T; Yumerefendi H; Bear JE; Kuhlman B Engineering an Improved Light-Induced Dimer (iLID) for Controlling the Localization and Activity of Signaling Proteins. *Proc. Natl. Acad. Sci. U. S. A.* 2015, 112, 112–117. [PubMed: 25535392]
- (204). Chan Y-B; Alekseyenko OV; Kravitz EA Optogenetic Control of Gene Expression in *Drosophila*. *PLoS One* 2015, 10, e0138181. [PubMed: 26383635]

- (205). Rademacher A; Erdel F; Trojanowski J; Schumacher S; Rippe K Real-Time Observation of Light-Controlled Transcription in Living Cells. *J Cell Sci* 2017, 130, 4213–4224. [PubMed: 29122982]
- (206). Pathak GP; Strickland D; Vrana JD; Tucker CL Benchmarking of Optical Dimerizer Systems. *ACS Synth. Biol.* 2014, 3, 832–838. [PubMed: 25350266]
- (207). Benedetti L; Barentine AES; Messa M; Wheeler H; Bewersdorf J; De Camilli P Light-Activated Protein Interaction with High Spatial Subcellular Confinement. *Proc. Natl. Acad. Sci. U. S. A.* 2018, 115, E2238–E2245. [PubMed: 29463750]
- (208). Cao J; Arha M; Sudrik C; Bugaj LJ; Schaffer DV; Kane RS Light-Inducible Activation of Target mRNA Translation in Mammalian Cells. *Chem. Commun.* 2013, 49, 8338–8340.
- (209). Niopek D; Benzinger D; Roensch J; Draebing T; Wehler P; Eils R; Di Ventura B Engineering Light-Inducible Nuclear Localization Signals for Precise Spatiotemporal Control of Protein Dynamics in Living Cells. *Nat. Commun.* 2014, 5, 4404. [PubMed: 25019686]
- (210). Niopek D; Wehler P; Roensch J; Eils R; Di Ventura B Optogenetic Control of Nuclear Protein Export. *Nat. Commun.* 2016, 7, 10624. [PubMed: 26853913]
- (211). Yumerefendi H; Dickinson DJ; Wang H; Zimmerman SP; Bear JE; Goldstein B; Hahn K; Kuhlman B Control of Protein Activity and Cell Fate Specification via Light-Mediated Nuclear Translocation. *PLoS One* 2015, 10, e0128443. [PubMed: 26083500]
- (212). Yumerefendi H; Lerner AM; Zimmerman SP; Hahn K; Bear JE; Strahl BD; Kuhlman B Light-Induced Nuclear Export Reveals Rapid Dynamics of Epigenetic Modifications. *Nat. Chem. Biol.* 2016, 12, 399–401. [PubMed: 27089030]
- (213). Masuda S; Nakatani Y; Ren S; Tanaka M Blue Light-Mediated Manipulation of Transcription Factor Activity *In Vivo*. *ACS Chem. Biol.* 2013, 8, 2649–2653. [PubMed: 24063403]
- (214). Polstein LR; Gersbach CA A Light-Inducible CRISPR-Cas9 System for Control of Endogenous Gene Activation. *Nat. Chem. Biol.* 2015, 11, 198–200. [PubMed: 25664691]
- (215). Nihongaki Y; Yamamoto S; Kawano F; Suzuki H; Sato M CRISPR-Cas9-Based Photoactivatable Transcription System. *Chem. Biol.* 2015, 22, 169–174. [PubMed: 25619936]
- (216). Masuda S; Tanaka M PICCORO. *Methods Cell Biol.* 2016, 135, 289–295. [PubMed: 27443931]
- (217). Paonessa F; Criscuolo S; Sacchetti S; Amoroso D; Scarongella H; Pecoraro Bisogni F; Carminati E; Pruzzo G; Maragliano L; Cesca F; et al. Regulation of Neural Gene Transcription by Optogenetic Inhibition of the RE1-Silencing Transcription Factor. *Proc. Natl. Acad. Sci.* 2016, 113, E91–E100. [PubMed: 26699507]
- (218). Huang A; Amourda C; Zhang S; Tolwinski NS; Saunders TE Decoding Temporal Interpretation of the Morphogen Bicoid in the Early *Drosophila* Embryo. *Elife* 2017, 6, e26258. [PubMed: 28691901]
- (219). Polstein LR; Gersbach CA Light-Inducible Spatiotemporal Control of Gene Activation by Customizable Zinc Finger Transcription Factors. *J. Am. Chem. Soc.* 2012, 134, 16480–16483. [PubMed: 22963237]
- (220). Gaj T; Gersbach CA; Barbas CF ZFN, TALEN and CRISPR/Cas-Based Methods for Genome Engineering. *Trends Biotechnol.* 2013, 31, 397–405. [PubMed: 23664777]
- (221). Konermann S; Brigham MD; Trevino AE; Hsu PD; Heidenreich M; Cong L; Platt RJ; Scott DA; Church GM; Zhang F Optical Control of Mammalian Endogenous Transcription and Epigenetic States. *Nature* 2013, 500, 472–476. [PubMed: 23877069]
- (222). Jinek M; Chylinski K; Fonfara I; Hauer M; Doudna JA; Charpentier E A Programmable Dual-RNA-Guided DNA Endonuclease in Adaptive Bacterial Immunity. *Science* 2012, 337, 816–821. [PubMed: 22745249]
- (223). Makarova KS; Wolf YI; Alkhnbashi OS; Costa F; Shah SA; Saunders SJ; Barrangou R; Brouns SJJ; Charpentier E; Haft DH; et al. An Updated Evolutionary Classification of CRISPR-Cas Systems. *Nat. Rev. Microbiol.* 2015, 13, 722–736. [PubMed: 26411297]
- (224). Shmakov S; Smargon A; Scott D; Cox D; Pyzocha N; Yan W; Abudayyeh OO; Gootenberg JS; Makarova KS; Wolf YI; et al. Diversity and Evolution of Class 2 CRISPR-Cas Systems. *Nat. Rev. Microbiol.* 2017, 15, 169–182. [PubMed: 28111461]
- (225). Richter F; Fonfara I; Gelfert R; Nack J; Charpentier E; Möglich A Switchable Cas9. *Curr. Opin. Biotechnol.* 2017, 48, 119–126. [PubMed: 28456061]



- (226). Nihongaki Y; Furuhashi Y; Otabe T; Hasegawa S; Yoshimoto K; Sato M CRISPR-Cas9-Based Photoactivatable Transcription Systems to Induce Neuronal Differentiation. *Nat. Methods* 2017, 10, 963–966.
- (227). Nihongaki Y; Kawano F; Nakajima T; Sato M Photoactivatable CRISPR-Cas9 for Optogenetic Genome Editing. *Nat. Biotechnol.* 2015, 33, 755–760. [PubMed: 26076431]
- (228). Qi LS; Larson MH; Gilbert LA; Doudna JA; Weissman JS; Arkin AP; Lim WA Repurposing CRISPR as an RNA-Guided Platform for Sequence-Specific Control of Gene Expression. *Cell* 2013, 152, 1173–1183. [PubMed: 23452860]
- (229). Konermann S; Brigham MD; Trevino AE; Joung J; Abudayyeh OO; Barcena C; Hsu PD; Habib N; Gootenberg JS; Nishimasu H; et al. Genome-Scale Transcriptional Activation by an Engineered CRISPR-Cas9 Complex. *Nature* 2015, 517, 583–588. [PubMed: 25494202]
- (230). Lo C-L; Choudhury SR; Irudayaraj J; Zhou FC Epigenetic Editing of Ascl1 Gene in Neural Stem Cells by Optogenetics. *Sci. Rep.* 2017, 7, 42047. [PubMed: 28181538]
- (231). Doudna JA; Charpentier E The New Frontier of Genome Engineering with CRISPR-Cas9. *Science* 2014, 346, 1258096. [PubMed: 25430774]
- (232). Richter F; Fonfara I; Bouazza B; Schumacher CH; Bratovi M; Charpentier E; Möglich A Engineering of Temperature- and Light-Switchable Cas9 Variants. *Nucleic Acids Res.* 2016, 44, 10003–10014. [PubMed: 27744350]
- (233). Conrad KS; Bilwes AM; Crane BR Light-Induced Subunit Dissociation by a Light-Oxygen-Voltage Domain Photoreceptor from *Rhodobacter Sphaeroides*. *Biochemistry* 2013, 52, 378–391. [PubMed: 23252338]
- (234). Kawano F; Okazaki R; Yazawa M; Sato M A Photoactivatable Cre-loxP Recombination System for Optogenetic Genome Engineering. *Nat. Chem. Biol.* 2016, 12, 1059–1064. [PubMed: 27723747]
- (235). Jullien N; Sampieri F; Enjalbert A; Herman J Regulation of Cre Recombinase by Ligand-Induced Complementation of Inactive Fragments. *Nucleic Acids Res.* 2003, 31, e131. [PubMed: 14576331]
- (236). Polstein L; Juhas M; Hanna G; Bursac N; Gersbach CA An Engineered Optogenetic Switch for Spatiotemporal Control of Gene Expression, Cell Differentiation, and Tissue Morphogenesis. *ACS Synth. Biol.* 2017, 6, 2003–2013. [PubMed: 28793186]
- (237). Schindler SE; McCall JG; Yan P; Hyrc KL; Li M; Tucker CL; Lee J-M; Bruchas MR; Diamond MI Photo-Activatable Cre Recombinase Regulates Gene Expression *in Vivo*. *Sci. Rep.* 2015, 5, 13627. [PubMed: 26350769]
- (238). Wang H; Vilela M; Winkler A; Tarnawski M; Schlichting I; Yumerefendi H; Kuhlman B; Liu R; Danuser G; Hahn KM LOVTRAP: An Optogenetic System for Photoinduced Protein Dissociation. *Nat. Methods* 2016, 13, 755–758. [PubMed: 27427858]
- (239). Yumerefendi H; Wang H; Dickinson DJ; Lerner AM; Malkus P; Goldstein B; Hahn K; Kuhlman B Light-Dependent Cytoplasmic Recruitment Enhances the Dynamic Range of a Nuclear Import Photoswitch. *Chembiochem A Eur. J. Chem. Biol.* 2018, 10.1002/cbic.201700681.
- (240). Spiltoir JI; Strickland D; Glotzer M; Tucker CL Optical Control of Peroxisomal Trafficking. *ACS Synth. Biol.* 2016, 5, 554–560. [PubMed: 26513473]
- (241). Yu X; Sayegh R; Maymon M; Warpeha K; Klejnot J; Yang H; Huang J; Lee J; Kaufman L; Lin C Formation of Nuclear Bodies of *Arabidopsis* CRY2 in Response to Blue Light Is Associated with Its Blue Light-Dependent Degradation. *Plant Cell* 2009, 21, 118–130. [PubMed: 19141709]
- (242). Lee S; Park H; Kyung T; Kim NY; Kim S; Kim J; Heo W. Do. Reversible Protein Inactivation by Optogenetic Trapping in Cells. *Nat. Methods* 2014, 11, 633–636. [PubMed: 24793453]
- (243). Brangwynne CP Phase Transitions and Size Scaling of Membrane-Less Organelles. *J. Cell Biol.* 2013, 203, 875–881. [PubMed: 24368804]
- (244). Park H; Kim NYN; Lee S; Kim NYN; Kim J; Heo W. Do. Optogenetic Protein Clustering through Fluorescent Protein Tagging and Extension of CRY2. *Nat. Commun* 2017, 8, 30. [PubMed: 28646204]
- (245). Shi F; Kawano F; Park SE; Komazaki S; Hirabayashi Y; Polleux F; Yazawa M Optogenetic Control of Endoplasmic Reticulum–Mitochondria Tethering. *ACS Synth. Biol.* 2018, 7, 2–9. [PubMed: 29172503]

- (246). Kornmann B; Currie E; Collins SR; Schuldiner M; Nunnari J; Weissman JS; Walter P An ER-Mitochondria Tethering Complex Revealed by a Synthetic Biology Screen. *Science* 2009, 325 (5939), 477–481. [PubMed: 19556461]
- (247). Jin X; Riedel-Kruse IH Biofilm Lithography Enables High-Resolution Cell Patterning via Optogenetic Adhesion Expression. *Proc. Natl. Acad. Sci. U. S. A.* 2018, 115, 3698–3703. [PubMed: 29555779]
- (248). Chen F; Wegner SV Blue Light Switchable Bacterial Adhesion as a Key Step toward the Design of Biofilms. *ACS Synth. Biol* 2017, 6, 2170–2174. [PubMed: 28803472]
- (249). Alberts B; Johnson A; Lewis J; Morgan D; Raff M; Roberts K; Walter P *Molecular Biology of the Cell* 6th Ed.; Garland Science, 2014.
- (250). Hodge RG; Ridley AJ Regulating Rho GTPases and Their Regulators. *Nat. Rev. Mol. Cell Biol.* 2016, 17, 496–510. [PubMed: 27301673]
- (251). Hanna S; El-Sibai M Signaling Networks of Rho GTPases in Cell Motility. *Cell. Signal.* 2013, 25, 1955–1961. [PubMed: 23669310]
- (252). Yoo SK; Deng Q; Cavnar PJ; Wu YI; Hahn KM; Huttenlocher A; Takuwa Y; Sugimoto N; Mitchison T; Bourne HR; et al. Differential Regulation of Protrusion and Polarity by PI3K during Neutrophil Motility in Live Zebrafish. *Dev. Cell* 2010, 18, 226–236. [PubMed: 20159593]
- (253). Hayashi-Takagi A; Yagishita S; Nakamura M; Shirai F; Wu YI; Loshbaugh AL; Kuhlman B; Hahn KM; Kasai H Labelling and Optical Erasure of Synaptic Memory Traces in the Motor Cortex. *Nature* 2015, 525, 333–338. [PubMed: 26352471]
- (254). Furuya A; Kawano F; Nakajima T; Ueda Y; Sato M Assembly Domain-Based Optogenetic System for the Efficient Control of Cellular Signaling. *ACS Synth. Biol.* 2017, 6, 1086–1095. [PubMed: 28195693]
- (255). Binz HK; Amstutz P; Pluckthun A Engineering Novel Binding Proteins from Nonimmunoglobulin Domains. *Nat. Biotechnol.* 2005, 23, 1257–1268. [PubMed: 16211069]
- (256). O'Neill PR; Kalyanaraman V; Gautam N Subcellular Optogenetic Activation of Cdc42 Controls Local and Distal Signaling to Drive Immune Cell Migration. *Mol. Biol. Cell* 2016, 27, 1442–1450. [PubMed: 26941336]
- (257). Zimmerman SP; Asokan SB; Kuhlman B; Bear JE Cells Lay Their Own Tracks – Optogenetic Cdc42 Activation Stimulates Fibronectin Deposition Supporting Directed Migration. *J Cell Sci* 2017, 130, 2971–2983. [PubMed: 28754687]
- (258). Strickland D; Lin Y; Wagner E; Hope CM; Zayner J; Antoniou C; Sosnick TR; Weiss EL; Glotzer M TULIPs: Tunable, Light-Controlled Interacting Protein Tags for Cell Biology. *Nat. Methods* 2012, 9, 379–384. [PubMed: 22388287]
- (259). Witte K; Strickland D; Glotzer M Cell Cycle Entry Triggers a Switch between Two Modes of Cdc42 Activation during Yeast Polarization. *Elife* 2017, 6, e26722. [PubMed: 28682236]
- (260). French AR; Sosnick TR; Rock RS Investigations of Human Myosin VI Targeting Using Optogenetically Controlled Cargo Loading. *Proc. Natl. Acad. Sci.* 2017, 114, E1607–E1616. [PubMed: 28193860]
- (261). van Bergeijk P; Adrian M; Hoogenraad CC; Kapitein LC Optogenetic Control of Organelle Transport and Positioning. *Nature* 2015, 518, 111–114. [PubMed: 25561173]
- (262). van Haren J; Ettinger A; Wang H; Hahn K; Wittmann T Local Control of Intracellular Microtubule Dynamics by End Binding Protein 1 (EB1) Photo-Dissociation. *Nat. Cell Biol.* 2018, 20, 252–261. [PubMed: 29379139]
- (263). Duan L; Che D; Zhang K; Ong Q; Guo S; Cui B Optogenetic Control of Molecular Motors and Organelle Distributions in Cells. *Chem. Biol.* 2015, 22, 671–682. [PubMed: 25963241]
- (264). Wood LA; Larocque G; Clarke NI; Sarkar S; Royle SJ New Tools for “hot-Wiring” Clathrin-Mediated Endocytosis with Temporal and Spatial Precision. *J Cell Biol* 2017, 216, 4351–4365. [PubMed: 28954824]
- (265). Nguyen MK; Kim CY; Kim JM; Park BO; Lee S; Park H; Heo W. Do. Optogenetic Oligomerization of Rab GTPases Regulates Intracellular Membrane Trafficking. *Nat. Chem. Biol.* 2016, 12, 431–436. [PubMed: 27065232]
- (266). Chen D; Gibson ES; Kennedy MJ A Light-Triggered Protein Secretion System. *J. Cell Biol.* 2013, 201, 631–640. [PubMed: 23671313]

- (267). Ji C; Fan F; Lou X Vesicle Docking Is a Key Target of Local PI(4,5)P2 Metabolism in the Secretory Pathway of INS-1 Cells. *Cell Rep.* 2017, 20, 1409–1421. [PubMed: 28793264]
- (268). Komander D; Rape M The Ubiquitin Code. *Annu. Rev. Biochem.* 2012, 81, 203–229. [PubMed: 22524316]
- (269). Renicke C; Schuster D; Usherenko S; Essen L-O; Taxis C A LOV2 Domain-Based Optogenetic Tool to Control Protein Degradation and Cellular Function. *Chem. Biol.* 2013, 20, 619–626. [PubMed: 23601651]
- (270). Bongor KM; Rakhit R; Payumo AY; Chen JK; Wandless TJ General Method for Regulating Protein Stability with Light. *ACS Chem. Biol.* 2014, 9, 111–115. [PubMed: 24180414]
- (271). Usherenko S; Stibbe H; Muscó M; Essen L-O; Kostina EA; Taxis C Photo-Sensitive Degron Variants for Tuning Protein Stability by Light. *BMC Syst. Biol.* 2014, 8, 128. [PubMed: 25403319]
- (272). Müller K; Zurbriggen MD; Weber W An Optogenetic Upgrade for the Tet-OFF System. *Biotechnol. Bioeng.* 2015, 112, 1483–1487. [PubMed: 25683779]
- (273). Sun W; Zhang W; Zhang C; Mao M; Zhao Y; Chen X; Yang Y Light-Induced Protein Degradation in Human-Derived Cells. *Biochem. Biophys. Res. Commun.* 2017, 487, 241–246. [PubMed: 28412349]
- (274). Lee D; Hyun JH; Jung K; Hannan P; Kwon H-B A Calcium- and Light-Gated Switch to Induce Gene Expression in Activated Neurons. *Nat. Biotechnol.* 2017, 35, 858–863. [PubMed: 28650460]
- (275). Wang W; Wildes CP; Pattarabanjird T; Sanchez MI; Glober GF; Matthews GA; Tye KM; Ting AY A Light- and Calcium-Gated Transcription Factor for Imaging and Manipulating Activated Neurons. *Nat. Biotechnol.* 2017, 35, 864–871. [PubMed: 28650461]
- (276). Lee D; Creed M; Jung K; Stefanelli T; Wendler DJ; Oh WC; Mignocchi NL; Lüscher C; Kwon H-B Temporally Precise Labeling and Control of Neuromodulatory Circuits in the Mammalian Brain. *Nat. Methods* 2017, 14, 495–503. [PubMed: 28369042]
- (277). Mills E; Chen X; Pham E; Wong S; Truong K Engineering a Photoactivated Caspase-7 for Rapid Induction of Apoptosis. *ACS Synth. Biol.* 2012, 1, 75–82. [PubMed: 23651071]
- (278). Krauss G *Biochemistry of Signal Transduction and Regulation.*; Wiley-VCH, 2014.
- (279). Schröder-Lang S; Schwärzel M; Seifert R; Strünker T; Kateriya S; Looser J; Watanabe M; Kaupp UB; Hegemann P; Nagel G Fast Manipulation of Cellular cAMP Level by Light *in Vivo*. *Nat. Methods* 2007, 4, 39–42. [PubMed: 17128267]
- (280). Raffelberg S; Wang L; Gao S; Losi A; Gärtner W; Nagel G A LOV-Domain-Mediated Blue-Light-Activated Adenylyl (Adenylyl) Cyclase from the Cyanobacterium *Microcoleus Chthonoplastes* PCC 7420. *Biochem. J* 2013, 455, 359–365. [PubMed: 24112109]
- (281). Gasser C; Taiber S; Yeh C-M; Wittig CH; Hegemann P; Ryu S; Wunder F; Möglich A Engineering of a Red-Light-Activated Human cAMP/cGMP-Specific Phosphodiesterase. *Proc. Natl. Acad. Sci. U. S. A.* 2014, 111, 8803–8808. [PubMed: 24889611]
- (282). Ryu M-H; Gomelsky M Near-Infrared Light Responsive Synthetic c-di-GMP Module for Optogenetic Applications. *ACS Synth. Biol* 2014, 3, 802–810. [PubMed: 24926804]
- (283). Folcher M; Oesterle S; Zwicky K; Thekkottil T; Heymoz J; Hohmann M; Christen M; Daoud El-Baba M; Buchmann P; Fussenegger M Mind-Controlled Transgene Expression by a Wireless-Powered Optogenetic Designer Cell Implant. *Nat. Commun.* 2014, 5, 5392. [PubMed: 25386727]
- (284). Cao Z; Livoti E; Losi A; Gärtner W A Blue Light-Inducible Phosphodiesterase Activity in the Cyanobacterium *Synechococcus Elongatus*. *Photochem. Photobiol.* 2010, 86, 606–611. [PubMed: 20408974]
- (285). Ryu M-H; Fomicheva A; Moskvina OV; Gomelsky M Optogenetic Module for Dichromatic Control of c-di-GMP Signaling. *J. Bacteriol.* 2017, 199, e00014–17. [PubMed: 28320886]
- (286). Kim T; Folcher M; Baba MD-E; Fussenegger M A Synthetic Erectile Optogenetic Stimulator Enabling Blue-Light-Inducible Penile Erection. *Angew. Chemie Int. Ed.* 2015, 54, 5933–5938.
- (287). Lindner R; Hartmann E; Tarnawski M; Winkler A; Frey D; Reinstein J; Meinhart A; Schlichting I Photoactivation Mechanism of a Bacterial Light-Regulated Adenylyl Cyclase. *J. Mol. Biol.* 2017, 429, 1336–1351. [PubMed: 28336405]

- (288). Ohki M; Sugiyama K; Kawai F; Tanaka H; Nihei Y; Unzai S; Takebe M; Matsunaga S; Adachi S; Shibayama N; et al. Structural Insight into Photoactivation of an Adenylate Cyclase from a Photosynthetic Cyanobacterium. *Proc. Natl. Acad. Sci.* 2016, 113, 6659–6664. [PubMed: 27247413]
- (289). Ohki M; Sato-Tomita A; Matsunaga S; Iseki M; Tame JRH; Shibayama N; Park S-Y Molecular Mechanism of Photoactivation of a Light-Regulated Adenylate Cyclase. *Proc. Natl. Acad. Sci.* 2017, 114, 8562–8567. [PubMed: 28739908]
- (290). Chen Z; Raffelberg S; Losi A; Schaap P; Gärtner W A Cyanobacterial Light Activated Adenylyl Cyclase Partially Restores Development of a *Dictyostelium Discoideum*, Adenylyl Cyclase a Null Mutant. *J. Biotechnol.* 2014, 191, 246–249. [PubMed: 25128613]
- (291). Avelar GM; Schumacher RI; Zaini PA; Leonard G; Richards TA; Gomes SL A Rhodopsin-Guanylyl Cyclase Gene Fusion Functions in Visual Perception in a Fungus. *Curr. Biol.* 2014, 24, 1234–1240. [PubMed: 24835457]
- (292). Ryu M-H; Kang I-H; Nelson MD; Jensen TM; Lyuksyutova AI; Siltberg-Liberles J; Raizen DM; Gomelsky M Engineering Adenylate Cyclases Regulated by near-Infrared Window Light. *Proc. Natl. Acad. Sci. U. S. A.* 2014, 111, 10167–10172. [PubMed: 24982160]
- (293). Etzl S; Lindner R; Nelson MD; Winkler A Structure-Guided Design and Functional Characterization of an Artificial Red Light-Regulated Guanylate/adenylate Cyclase for Optogenetic Applications. *J. Biol. Chem.* 2018, 293, 9078–9089. [PubMed: 29695503]
- (294). Blain-Hartung M; Rockwell NC; Moreno MV; Martin SS; Gan F; Bryant DA; Lagarias JC Cyanobacteriochrome-Based Photoswitchable Adenylyl Cyclases (cPACs) for Broad Spectrum Light Regulation of cAMP Levels in Cells. *J. Biol. Chem.* 2018, 293, 8473–8483. [PubMed: 29632072]
- (295). Yoshida K; Tsunoda SP; Brown LS; Kandori H A Unique Choanoflagellate Enzyme Rhodopsin Exhibits Light-Dependent Cyclic Nucleotide Phosphodiesterase Activity. *J. Biol. Chem.* 2017, 292, 7531–7541. [PubMed: 28302718]
- (296). Mukherjee S; Jansen V; Jikeli JF; Hamzeh H; Alvarez L; Dombrowski M; Balbach M; Strünker T; Seifert R; Kaupp UB; et al. A Novel Biosensor to Study cAMP Dynamics in Cilia and Flagella. *Elife* 2016, 5, e14052. [PubMed: 27003291]
- (297). O'Banion CP; Priestman MA; Hughes RM; Herring LE; Capuzzi SJ; Lawrence DS Design and Profiling of a Subcellular Targeted Optogenetic cAMP-Dependent Protein Kinase. *Cell Chem. Biol.* 2018, 25, 100–109.e8. [PubMed: 29104065]
- (298). Gomelsky M cAMP, c-di-GMP, c-di-AMP and Now cGMP: Bacteria Use Them All! *Mol. Microbiol.* 2011, 79, 562–565. [PubMed: 21255104]
- (299). Jenal U; Reinders A; Lori C Cyclic di-GMP: Second Messenger Extraordinaire. *Nat. Rev. Microbiol.* 2017, 15, 271–284. [PubMed: 28163311]
- (300). Pu L; Yang S; Xia A; Jin F Optogenetics Manipulation Enables Prevention of Biofilm Formation of Engineered *Pseudomonas Aeruginosa* on Surfaces. *ACS Synth. Biol.* 2018, 7, 200–208. [PubMed: 29053252]
- (301). Burdette DL; Vance RE STING and the Innate Immune Response to Nucleic Acids in the Cytosol. *Nat. Immunol.* 2012, 14, 19–26.
- (302). Sun L; Wu J; Du F; Chen X; Chen ZJ Cyclic GMP-AMP Synthase Is a Cytosolic DNA Sensor That Activates the Type I Interferon Pathway. *Science* 2013, 339, 786–791. [PubMed: 23258413]
- (303). Clapham DE; Yeromin AV; Zhang XH; Yu Y; Safrina O; Penna A; Roos J; Stauderman KA; Cahalan MD; Takemori H; et al. Calcium Signaling. *Cell* 2007, 131, 1047–1058. [PubMed: 18083096]
- (304). Pham E; Mills E; Truong K A Synthetic Photoactivated Protein to Generate Local or Global Ca(2+) Signals. *Chem. Biol.* 2011, 18, 880–890. [PubMed: 21802009]
- (305). Ishii T; Sato K; Kakumoto T; Miura S; Touhara K; Takeuchi S; Nakata T Light Generation of Intracellular Ca(2+) Signals by a Genetically Encoded Protein BACCS. *Nat. Commun.* 2015, 6, 8021. [PubMed: 26282514]
- (306). Nguyen NT; He L; Martinez-Moczygamba M; Huang Y; Zhou Y Rewiring Calcium Signaling for Precise Transcriptional Reprogramming. *ACS Synth. Biol.* 2018, 7, 814–821. [PubMed: 29489336]

- (307). Kyung T; Lee S; Kim JE; Cho T; Park H; Jeong Y-M; Kim D; Shin A; Kim S; Baek J; et al. Optogenetic Control of Endogenous Ca(2+) Channels *in Vivo*. *Nat. Biotechnol.* 2015, 33, 1092–1096. [PubMed: 26368050]
- (308). Ma G; Liu J; Ke Y; Liu X; Li M; Wang F; Han G; Huang Y; Wang Y; Zhou Y Optogenetic Control of Voltage-Gated Calcium Channels. *Angew. Chem. Int. Ed. Engl.* 2018, 57, 7019–7022. [PubMed: 29569306]
- (309). Fukuda N; Matsuda T; Nagai T Optical Control of the Ca<sup>2+</sup> Concentration in a Live Specimen with a Genetically Encoded Ca<sup>2+</sup>-Releasing Molecular Tool. *ACS Chem. Biol.* 2014, 9, 1197–1203. [PubMed: 24625002]
- (310). Aper SJA; Merckx M Rewiring Multidomain Protein Switches: Transforming a Fluorescent Zn<sup>2+</sup> Sensor into a Light-Responsive Zn<sup>2+</sup> Binding Protein. *ACS Synth. Biol* 2016, 5, 698–709. [PubMed: 27031076]
- (311). Chang K-Y; Woo D; Jung H; Lee S; Kim S; Won J; Kyung T; Park H; Kim N; Yang HW; et al. Light-Inducible Receptor Tyrosine Kinases That Regulate Neurotrophin Signalling. *Nat. Commun.* 2014, 5, 4057. [PubMed: 24894073]
- (312). Kim N; Kim JM; Lee M; Kim CY; Chang K-Y; Heo W.Do. Spatiotemporal Control of Fibroblast Growth Factor Receptor Signals by Blue Light. *Chem. Biol.* 2014, 21, 903–912. [PubMed: 24981772]
- (313). Inglés-Prieto Á; Reichhart E; Muellner MK; Nowak M; Nijman SMB; Grusch M; Janovjak H Light-Assisted Small-Molecule Screening against Protein Kinases. *Nat. Chem. Biol.* 2015, 11, 952–954. [PubMed: 26457372]
- (314). Agus V; Janovjak H Optogenetic Methods in Drug Screening: Technologies and Applications. *Curr. Opin. Biotechnol.* 2017, 48, 8–14. [PubMed: 28273648]
- (315). Bugaj LJ; Spelke DP; Mesuda CK; Varedi M; Kane RS; Schaffer DV Regulation of Endogenous Transmembrane Receptors through Optogenetic Cry2 Clustering. *Nat. Commun.* 2015, 6, 6898. [PubMed: 25902152]
- (316). Aoki K; Kumagai Y; Sakurai A; Komatsu N; Fujita Y; Shionyu C; Matsuda M Stochastic ERK Activation Induced by Noise and Cell-to-Cell Propagation Regulates Cell Density-Dependent Proliferation. *Mol. Cell* 2013, 52, 529–540. [PubMed: 24140422]
- (317). Zhang K; Duan L; Ong Q; Lin Z; Varman PM; Sung K; Cui B Light-Mediated Kinetic Control Reveals the Temporal Effect of the Raf/MEK/ERK Pathway in PC12 Cell Neurite Outgrowth. *PLoS One* 2014, 9, e92917. [PubMed: 24667437]
- (318). Krishnamurthy VV; Khamo JS; Mei W; Turgeon AJ; Ashraf HM; Mondal P; Patel DB; Risner N; Cho EE; Yang J; et al. Reversible Optogenetic Control of Kinase Activity during Differentiation and Embryonic Development. *Development* 2016, 143, 4085–4094. [PubMed: 27697903]
- (319). Wend S; Wagner HJ; Müller K; Zurbriggen MD; Weber W; Radziwill G Optogenetic Control of Protein Kinase Activity in Mammalian Cells. *ACS Synth. Biol.* 2014, 3, 280–285. [PubMed: 24090449]
- (320). Chatelle CV; Hövermann D; Müller A; Wagner HJ; Weber W; Radziwill G Optogenetically Controlled RAF to Characterize BRAF and CRAF Protein Kinase Inhibitors. *Sci. Rep.* 2016, 6, 23713. [PubMed: 27025703]
- (321). Melero-Fernandez de Mera RM; Li L-L; Popinigis A; Cisek K; Tuittila M; Yadav L; Serva A; Courtney MJ A Simple Optogenetic MAPK Inhibitor Design Reveals Resonance between Transcription-Regulating Circuitry and Temporally-Encoded Inputs. *Nat. Commun.* 2017, 8, 15017. [PubMed: 28497795]
- (322). Di Paolo G; De Camilli P Phosphoinositides in Cell Regulation and Membrane Dynamics. *Nature* 2006, 443, 651–657. [PubMed: 17035995]
- (323). Idevall-Hagren O; Dickson EJ; Hille B; Toomre DK; De Camilli P Optogenetic Control of Phosphoinositide Metabolism. *Proc. Natl. Acad. Sci. U. S. A.* 2012, 109, E2316–2323. [PubMed: 22847441]
- (324). Kakumoto T; Nakata T Optogenetic Control of PIP3: PIP3 Is Sufficient to Induce the Actin-Based Active Part of Growth Cones and Is Regulated via Endocytosis. *PLoS One* 2013, 8, e70861. [PubMed: 23951027]

- (325). Xu Y; Nan D; Fan J; Bogan JS; Toomre D Optogenetic Activation Reveals Distinct Roles of PIP3 and Akt in Adipocyte Insulin Action. *J. Cell Sci.* 2016, 129, 2085–2095. [PubMed: 27076519]
- (326). Katsura Y; Kubota H; Kunida K; Kanno A; Kuroda S; Ozawa T An Optogenetic System for Interrogating the Temporal Dynamics of Akt. *Sci. Rep.* 2015, 5, 14589. [PubMed: 26423353]
- (327). Mühlhäuser WWD; Hörner M; Weber W; Radziwill G Light-Regulated Protein Kinases Based on the CRY2-CIB1 System. In *Methods in molecular biology* (Clifton, N.J.); 2017; Vol. 1596, pp 257–270.
- (328). Kaur P; Saunders TE; Tolwinski NS Coupling Optogenetics and Light-Sheet Microscopy, a Method to Study Wnt Signaling during Embryogenesis. *Sci. Rep* 2017, 7, 16636. [PubMed: 29192250]
- (329). Liao Z; Kasirer-Friede A; Shattil SJ Optogenetic Interrogation of Integrin  $\alpha$ V $\beta$ 3 Function in Endothelial Cells. *J Cell Sci.* 2017, 130, 3532–3541. [PubMed: 28864764]
- (330). Hörner M; Chatelle C; Mühlhäuser WWD; Stocker DR; Coats M; Weber W; Radziwill G Optogenetic Control of Focal Adhesion Kinase Signaling. *Cell. Signal.* 2018, 42, 176–183. [PubMed: 29074139]
- (331). Locke C; Machida K; Wu Y; Yu J Optogenetic Activation of EphB2 Receptor in Dendrites Induced Actin Polymerization by Activating Arg Kinase. *Biol. Open* 2017, 6, 1820–1830. [PubMed: 29158322]
- (332). Li Y; Lee M; Kim N; Wu G; Deng D; Kim JM; Liu X; Heo W. Do.; Zi Z Spatiotemporal Control of TGF- $\beta$  Signaling with Light. *ACS Synth. Biol.* 2018, 7, 443–451. [PubMed: 29241005]
- (333). Broz P; Monack DM Newly Described Pattern Recognition Receptors Team up against Intracellular Pathogens. *Nat. Rev. Immunol.* 2013, 13, 551–565. [PubMed: 23846113]
- (334). Moser BA; Esser-Kahn AP A Photoactivatable Innate Immune Receptor for Optogenetic Inflammation. *ACS Chem. Biol.* 2017, 12, 347–350. [PubMed: 28000442]
- (335). Taylor RC; Cullen SP; Martin SJ Apoptosis: Controlled Demolition at the Cellular Level. *Nat. Rev. Mol. Cell Biol.* 2008, 9, 231–241. [PubMed: 18073771]
- (336). Hughes RM; Freeman DJ; Lamb KN; Pollet RM; Smith WJ; Lawrence DS Optogenetic Apoptosis: Light-Triggered Cell Death. *Angew. Chemie Int. Ed.* 2015, 54, 12064–12068.
- (337). Smart AD; Pache RA; Thomsen ND; Kortemme T; Davis GW; Wells JA Engineering a Light-Activated Caspase-3 for Precise Ablation of Neurons *in Vivo*. *Proc. Natl. Acad. Sci.* 2017, 114, E8174–E8183. [PubMed: 28893998]
- (338). Lee J; Natarajan M; Nashine VC; Socolich M; Vo T; Russ WP; Benkovic SJ; Ranganathan R Surface Sites for Engineering Allosteric Control in Proteins. *Science* 2008, 322, 438–442. [PubMed: 18927392]
- (339). Gehrig S; Macpherson JA; Driscoll PC; Symon A; Martin SR; MacRae JI; Kleijung J; Fraternali F; Anastasiou D An Engineered Photoswitchable Mammalian Pyruvate Kinase. *FEBS J.* 2017, 284, 2955–2980. [PubMed: 28715126]
- (340). Sancar A Mechanisms of DNA Repair by Photolyase and Excision Nuclease (Nobel Lecture). *Angew. Chemie Int. Ed* 2016, 55, 8502–8527.
- (341). Hollmann F; Taglieber A; Schulz F; Reetz MT A Light-Driven Stereoselective Biocatalytic Oxidation. *Angew. Chemie Int. Ed.* 2007, 46, 2903–2906.
- (342). Taglieber A; Schulz F; Hollmann F; Rusek M; Reetz MT Light-Driven Biocatalytic Oxidation and Reduction Reactions: Scope and Limitations. *Chembiochem A Eur. J. Chem. Biol.* 2008, 9, 565–572.
- (343). Wietek J; Wiegert JS; Adeishvili N; Schneider F; Watanabe H; Tsunoda SP; Vogt A; Elstner M; Oertner TG; Hegemann P Conversion of Channelrhodopsin into a Light-Gated Chloride Channel. *Science* 2014, 344, 409–412. [PubMed: 24674867]
- (344). Berndt A; Lee SY; Ramakrishnan C; Deisseroth K Structure-Guided Transformation of Channelrhodopsin into a Light-Activated Chloride Channel. *Science* 2014, 344, 420–424. [PubMed: 24763591]

- (345). Govorunova EG; Sineshchekov OA; Janz R; Liu X; Spudich JL Natural Light-Gated Anion Channels: A Family of Microbial Rhodopsins for Advanced Optogenetics. *Science* 2015, 349, 647–650. [PubMed: 26113638]
- (346). Schmidt D; Tillberg PW; Chen F; Boyden ES A Fully Genetically Encoded Protein Architecture for Optical Control of Peptide Ligand Concentration. *Nat. Commun.* 2014, 5, 3019. [PubMed: 24407101]
- (347). Cosentino C; Alberio L; Gazzarrini S; Aquila M; Romano E; Cerumenati S; Zuccolini P; Petersen J; Beltrame M; Van Etten JL; et al. Optogenetics. Engineering of a Light-Gated Potassium Channel. *Science* 2015, 348, 707–710. [PubMed: 25954011]
- (348). Dixon RE; Yuan C; Cheng EP; Navedo MF; Santana LF Ca<sup>2+</sup> Signaling Amplification by Oligomerization of L-Type Cav1.2 Channels. *Proc. Natl. Acad. Sci. U. S. A.* 2012, 109, 1749–1754. [PubMed: 22307641]
- (349). Sinnen BL; Bowen AB; Forte JS; Hiester BG; Crosby KC; Gibson ES; Dell'Acqua ML; Kennedy MJ Optogenetic Control of Synaptic Composition and Function. *Neuron* 2017, 93, 646–660.e5. [PubMed: 28132827]
- (350). Sanford L; Palmer A Recent Advances in Development of Genetically Encoded Fluorescent Sensors. *Methods Enzym.* 2017, 589, 1–49.
- (351). Thorn K Genetically Encoded Fluorescent Tags. *Mol. Biol. Cell* 2017, 28, 848–857. [PubMed: 28360214]
- (352). Buckley AM; Petersen J; Roe AJ; Douce GR; Christie JM LOV-Based Reporters for Fluorescence Imaging. *Curr. Opin. Chem. Biol.* 2015, 27, 39–45. [PubMed: 26087123]
- (353). Rodriguez EA; Campbell RE; Lin JY; Lin MZ; Miyawaki A; Palmer AE; Shu X; Zhang J; Tsien RY The Growing and Glowing Toolbox of Fluorescent and Photoactive Proteins. *Trends Biochem. Sci.* 2017, 42, 111–129. [PubMed: 27814948]
- (354). Souslova EA; Mironova KE; Deyev SM Applications of Genetically Encoded Photosensitizer miniSOG: From Correlative Light Electron Microscopy to Immunophotosensitizing. *J. Biophotonics* 2017, 10, 338–352. [PubMed: 27435584]
- (355). Jiang HN; Li Y; Cui ZJ Photodynamic Physiology-Photonanomanipulations in Cellular Physiology with Protein Photosensitizers. *Front. Physiol.* 2017, 8, 191. [PubMed: 28421000]
- (356). Drepper T; Gensch T; Pohl M; T. W. Gadella J; Coppey-Moisan M; Bertrand E; Biskup C; Michiels J; Vanderleyden J; Heberle J; et al. Advanced in Vivo Applications of Blue Light Photoreceptors as Alternative Fluorescent Proteins. *Photochem. Photobiol. Sci.* 2013, 12, 1125–1134. [PubMed: 23660639]
- (357). Wingen M; Potzkei J; Endres S; Casini G; Rupprecht C; Fahlke C; Krauss U; Jaeger K-E; Drepper T; Gensch T; et al. The Photophysics of LOV-Based Fluorescent Proteins – New Tools for Cell Biology. *Photochem. Photobiol. Sci.* 2014, 13, 875–883. [PubMed: 24500379]
- (358). Mukherjee A; Schroeder CM Flavin-Based Fluorescent Proteins: Emerging Paradigms in Biological Imaging. *Curr. Opin. Biotechnol.* 2015, 31, 16–23. [PubMed: 25151058]
- (359). Drepper T; Eggert T; Circolone F; Heck A; Krauß U; Guterl J-K; Wendorff M; Losi A; Gärtner W; Jaeger K-E Reporter Proteins for in Vivo Fluorescence without Oxygen. *Nat. Biotechnol.* 2007, 25, 443–445. [PubMed: 17351616]
- (360). Wingen M; Jaeger K-E; Gensch T; Drepper T Novel Thermostable Flavin-Binding Fluorescent Proteins from Thermophilic Organisms. *Photochem. Photobiol.* 2017, 93, 849–856. [PubMed: 28500719]
- (361). Mukherjee A; Weyant KB; Agrawal U; Walker J; Cann IKO; Schroeder CM Engineering and Characterization of New LOV-Based Fluorescent Proteins from *Chlamydomonas Reinhardtii* and *Vaucheria Frigida*. *ACS Synth. Biol.* 2015, 4, 371–377. [PubMed: 25881501]
- (362). Chapman S; Faulkner C; Kaiserli E; Garcia-Mata C; Savenkov EI; Roberts AG; Oparka KJ; Christie JM The Photoreversible Fluorescent Protein iLOV Outperforms GFP as a Reporter of Plant Virus Infection. *Proc. Natl. Acad. Sci. U. S. A.* 2008, 105, 20038–20043. [PubMed: 19060199]
- (363). Seago J; Juleff N; Moffat K; Berryman S; Christie JM; Charleston B; Jackson T An Infectious Recombinant Foot-and-Mouth Disease Virus Expressing a Fluorescent Marker Protein. *J. Gen. Virol.* 2013, 94 (Pt 7), 1517–1527. [PubMed: 23559477]

- (364). Christie JM; Gawthorne J; Young G; Fraser NJ; Roe AJ LOV to BLUF: Flavoprotein Contributions to the Optogenetic Toolkit. *Mol. Plant* 2012, 5, 533–544. [PubMed: 22431563]
- (365). Christie JM; Hitomi K; Arvai AS; Hartfield KA; Mettlen M; Pratt AJ; Tainer JA; Getzoff ED Structural Tuning of the Fluorescent Protein iLOV for Improved Photostability. *J. Biol. Chem.* 2012, 287, 22295–22304. [PubMed: 22573334]
- (366). Mukherjee A; Walker J; Weyant KB; Schroeder CM; Stahl U Characterization of Flavin-Based Fluorescent Proteins: An Emerging Class of Fluorescent Reporters. *PLoS One* 2013, 8, e64753. [PubMed: 23741385]
- (367). Khrenova MG; Nemukhin AV; Domratcheva T Theoretical Characterization of the Flavin-Based Fluorescent Protein iLOV and Its Q489K Mutant. *J. Phys. Chem. B* 2015, 119, 5176–5183. [PubMed: 25830816]
- (368). Landete JM; Peirotn Á; Medina M; Arques JL Short Communication: Labeling *Listeria* with Anaerobic Fluorescent Protein for Food Safety Studies. *J. Dairy Sci.* 2017, 100, 113–117. [PubMed: 27837972]
- (369). Choi CH; DeGuzman JV; Lamont RJ; Yilmaz Ö; Berche P Genetic Transformation of an Obligate Anaerobe, *P. gingivalis* for FMN-Green Fluorescent Protein Expression in Studying Host-Microbe Interaction. *PLoS One* 2011, 6, e18499. [PubMed: 21525983]
- (370). Eichhof I; Ernst JF Oxygen-Independent FbFP: Fluorescent Sentinel and Oxygen Sensor Component in *Saccharomyces Cerevisiae* and *Candida Albicans*. *Fungal Genet. Biol.* 2016, 92, 14–25. [PubMed: 27126475]
- (371). Immethun CM; DeLorenzo DM; Focht CM; Gupta D; Johnson CB; Moon TS Physical, Chemical, and Metabolic State Sensors Expand the Synthetic Biology Toolbox for *Synechocystis Sp.* PCC 6803. *Biotechnol. Bioeng.* 2017, 114, 1561–1569. [PubMed: 28244586]
- (372). Wang SE; Brooks AES; Cann B; Simoes-Barbosa A The Fluorescent Protein iLOV Outperforms eGFP as a Reporter Gene in the Microaerophilic Protozoan *Trichomonas vaginalis*. *Mol. Biochem. Parasitol.* 2017, 216, 1–4. [PubMed: 28602728]
- (373). Buckley AM; Jukes C; Candlish D; Irvine JJ; Spencer J; Fagan RP; Roe AJ; Christie JM; Fairweather NF; Douce GR Lighting Up *Clostridium Difficile*: Reporting Gene Expression Using Fluorescent Lov Domains. *Sci. Rep.* 2016, 6, 23463. [PubMed: 26996606]
- (374). Elgamoudi BA; Ketley JM Lighting up My Life: A LOV-Based Fluorescent Reporter for *Campylobacter Jejuni*. *Res. Microbiol.* 2018, 169, 108–114. [PubMed: 29113919]
- (375). Ravikumar Y; Nadarajan SP; Lee C-S; Jung S; Bae D-H; Yun H FMN-Based Fluorescent Proteins as Heavy Metal Sensors Against Mercury Ions. *J. Microbiol. Biotechnol.* 2016, 26, 530–539. [PubMed: 26699753]
- (376). Ravikumar Y; Nadarajan SP; Lee C; Yun H Engineering an FMN-Based iLOV Protein for the Detection of Arsenic Ions. *Anal. Biochem.* 2017, 525, 38–43. [PubMed: 28245978]
- (377). Chang X-P; Gao Y-J; Fang W-H; Cui G; Thiel W Quantum Mechanics/Molecular Mechanics Study on the Photoreactions of Dark- and Light-Adapted States of a Blue-Light YtvA LOV Photoreceptor. *Angew. Chemie Int. Ed* 2017, 56, 9341–9345.
- (378). Losi A; Gärtner W; Raffelberg S; Cella Zancchi F; Bianchini P; Diaspro A; Mandalari C; Abbruzzetti S; Viappiani C; Schwarzel M; et al. A Photochromic Bacterial Photoreceptor with Potential for Super-Resolution Microscopy. *Photochem. Photobiol. Sci.* 2013, 12, 231–235. [PubMed: 23047813]
- (379). Gregor C; Sidenstein SC; Andresen M; Sahl SJ; Danzl JG; Hell SW Novel Reversibly Switchable Fluorescent Proteins for RESOLFT and STED Nanoscopy Engineered from the Bacterial Photoreceptor YtvA. *Sci. Rep.* 2018, 8, 2724. [PubMed: 29426833]
- (380). van der Steen JB; Hellingwerf KJ Activation of the General Stress Response of *Bacillus Subtilis* by Visible Light. *Photochem. Photobiol.* 2015, 91, 1032–1045. [PubMed: 26189730]
- (381). Potzkei J; Kunze M; Drepper T; Gensch T; Jaeger K-E; Buechs J Real-Time Determination of Intracellular Oxygen in Bacteria Using a Genetically Encoded FRET-Based Biosensor. *BMC Biol.* 2012, 10, 28. [PubMed: 22439625]
- (382). Rupprecht C; Wingen M; Potzkei J; Gensch T; Jaeger K-E; Drepper T A Novel FbFP-Based Biosensor Toolbox for Sensitive in Vivo Determination of Intracellular pH. *J. Biotechnol.* 2017, 258, 25–35. [PubMed: 28501596]

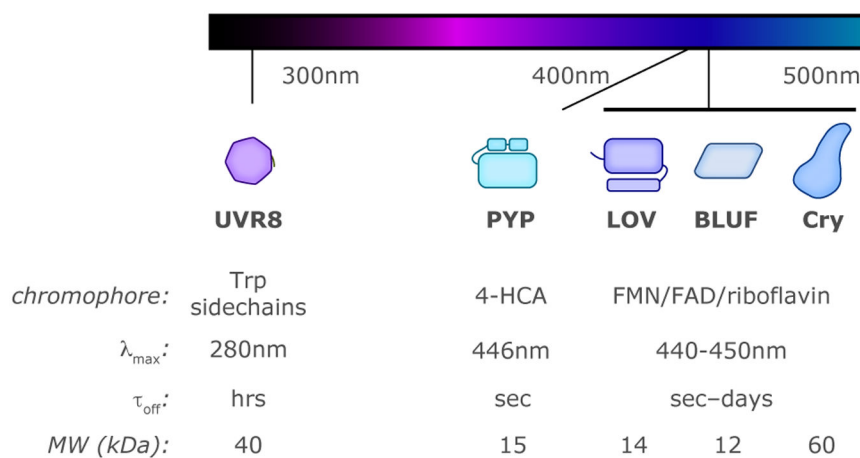


- (383). Simon J; Losi A; Zhao K-H; Gärtner W FRET in a Synthetic Flavin- and Bilin-Binding Protein. *Photochem. Photobiol.* 2017, 93, 1057–1062. [PubMed: 28055118]
- (384). Baier J; Maisch T; Maier M; Engel E; Landthaler M; Bäuml W Singlet Oxygen Generation by UVA Light Exposure of Endogenous Photosensitizers. *Biophys. J.* 2006, 91, 1452–1459. [PubMed: 16751234]
- (385). Bourdeaux F; Hammer CA; Vogt S; Schweighöfer F; Nöll G; Wachtveitl J; Grininger M Flavin Storage and Sequestration by *Mycobacterium Tuberculosis* Dodecin. *ACS Infect. Dis.* 2018, *in press*, 10.1021/acscinfecdis.7b00237.
- (386). Scheurer M; Brisker-Klaiman D; Dreuw A Molecular Mechanism of Flavin Photoprotection by Archaeal Dodecin: Photoinduced Electron Transfer and  $Mg^{2+}$ -Promoted Proton Transfer. *J. Phys. Chem. B* 2017, 121, 10457–10466. [PubMed: 29069901]
- (387). Baptista MS; Cadet J; Di Mascio P; Ghogare AA; Greer A; Hamblin MR; Lorente C; Nunez SC; Ribeiro MS; Thomas AH; et al. Type I and Type II Photosensitized Oxidation Reactions: Guidelines and Mechanistic Pathways. *Photochem. Photobiol.* 2017, 93, 912–919. [PubMed: 28084040]
- (388). Brunk GR; Martin KA; Nishimura AM A Study of Solvent Effects on the Phosphorescence Properties of Flavins. *Biophys. J.* 1976, 16, 1373–1384. [PubMed: 990392]
- (389). Bregnhøj M; Blázquez-Castro A; Westberg M; Breitenbach T; Ogilby PR Direct 765 nm Optical Excitation of Molecular Oxygen in Solution and in Single Mammalian Cells. *J. Phys. Chem. B* 2015, 119, 5422–5429. [PubMed: 25856010]
- (390). Westberg M; Bregnhøj M; Etzerodt M; Ogilby PR Temperature Sensitive Singlet Oxygen Photosensitization by LOV-Derived Fluorescent Flavoproteins. *J. Phys. Chem. B* 2017, 121, 2561–2574. [PubMed: 28257211]
- (391). Shu X; Lev-Ram V; Deerinck TJ; Qi Y; Ramko EB; Davidson MW; Jin Y; Ellisman MH; Tsien RY A Genetically Encoded Tag for Correlated Light and Electron Microscopy of Intact Cells, Tissues, and Organisms. *PLoS Biol.* 2011, 9, e1001041. [PubMed: 21483721]
- (392). Kottke T; Heberle J; Hehn D; Dick B; Hegemann P Phot-LOV1: Photocycle of a Blue-Light Receptor Domain from the Green Alga *Chlamydomonas Reinhardtii*. *Biophys. J.* 2003, 84, 1192–1201. [PubMed: 12547798]
- (393). Caplan J; Niethammer M; Taylor RM; Czymmek KJ The Power of Correlative Microscopy: Multi-Modal, Multi-Scale, Multi-Dimensional. *Curr. Opin. Struct. Biol.* 2011, 21, 686–693. [PubMed: 21782417]
- (394). Hauser M; Wojcik M; Kim D; Mahmoudi M; Li W; Xu K Correlative Super-Resolution Microscopy: New Dimensions and New Opportunities. *Chem. Rev.* 2017, 117, 7428–7456. [PubMed: 28045508]
- (395). Hirabayashi Y; Tapia JC; Polleux F Correlated Light-Serial Scanning Electron Microscopy (CoLSSEM) for Ultrastructural Visualization of Single Neurons *in Vivo*. *bioRxiv* 2017, 10.1101/148585.
- (396). Lee D; Huang T-H; De La Cruz A; Callejas A; Lois C Methods to Investigate the Structure and Connectivity of the Nervous System. *Fly (Austin)*. 2017, 11, 224–238. [PubMed: 28277925]
- (397). Follain G; Mercier L; Osmani N; Harlepp S; Goetz JG Seeing Is Believing – Multi-Scale Spatio-Temporal Imaging towards *in Vivo* Cell Biology. *J. Cell Sci.* 2017, 130, 23–38. [PubMed: 27505891]
- (398). Ellisman MH; Deerinck TJ; Shu X; Sosinsky GE Picking Faces out of a Crowd: Genetic Labels for Identification of Proteins in Correlated Light and Electron Microscopy Imaging. *Methods Cell Biol.* 2012, 111, 139–155. [PubMed: 22857927]
- (399). Rodríguez-Pulido A; Cortajarena AL; Torra J; Ruiz-González R; Nonell S; Flors C Assessing the Potential of Photosensitizing Flavoproteins as Tags for Correlative Microscopy. *Chem. Commun.* 2016, 52, 8405–8408.
- (400). Ruiz-González R; Cortajarena AL; Mejias SH; Agut M; Nonell S; Flors C Singlet Oxygen Generation by the Genetically Encoded Tag miniSOG. *J. Am. Chem. Soc.* 2013, 135, 9564–9567. [PubMed: 23781844]

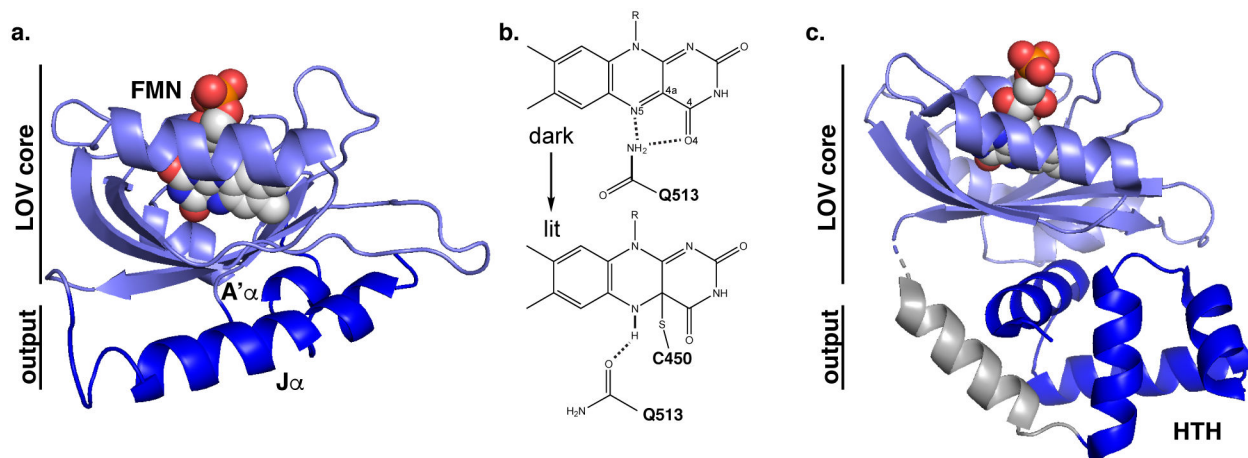
- (401). Pimenta FM; Jensen RL; Breitenbach T; Etzerodt M; Ogilby PR Oxygen-Dependent Photochemistry and Photophysics of “MiniSOG,” a Protein-Encased Flavin. *Photochem. Photobiol.* 2013, 89, 1116–1126. [PubMed: 23869989]
- (402). Westberg M; Holmegaard L; Pimenta FM; Etzerodt M; Ogilby PR Rational Design of an Efficient, Genetically Encodable, Protein-Encased Singlet Oxygen Photosensitizer. *J. Am. Chem. Soc.* 2015, 137, 1632–1642. [PubMed: 25575190]
- (403). Torra J; Burgos-Caminal A; Endres S; Wingen M; Drepper T; Gensch T; Ruiz-González R; Nonell S; Drepper T; Gensch T; et al. Singlet Oxygen Photosensitisation by the Fluorescent Protein Pp2FbFP L30M, a Novel Derivative of *Pseudomonas Putida* Flavin-Binding Pp2FbFP. *Photochem. Photobiol. Sci.* 2015, 14, 280–287. [PubMed: 25375892]
- (404). Ruiz-González R; Bresolí-Obach R; Gulías Ò; Agut M; Savoie H; Boyle RW; Nonell S; Giuntini F NanoSOSG: A Nanostructured Fluorescent Probe for the Detection of Intracellular Singlet Oxygen. *Angew. Chemie Int. Ed* 2017, 56, 2885–2888.
- (405). Xu S; Chisholm AD Highly Efficient Optogenetic Cell Ablation in *C. Elegans* Using Membrane-Targeted miniSOG. *Sci. Rep.* 2016, 6, 21271. [PubMed: 26861262]
- (406). Makhijani K; To T-L; Ruiz-González R; Lafaye C; Royant A; Shu X Precision Optogenetic Tool for Selective Single- and Multiple-Cell Ablation in a Live Animal Model System. *Cell Chem. Biol.* 2017, 24, 110–119. [PubMed: 28065655]
- (407). Westberg M; Bregnhøj M; Etzerodt M; Ogilby PR No Photon Wasted: An Efficient and Selective Singlet Oxygen Photosensitizing Protein. *J. Phys. Chem. B* 2017, 121, 9366–9371. [PubMed: 28892628]
- (408). Rodríguez-Pulido A; Torra J; Mejías SH; Cortajarena AL; Ruiz-González R; Nonell S; Flors C Fluorescent Flavoprotein Heterodimers: Combining Photostability with Singlet Oxygen Generation. *ChemPhotoChem* 2018, *in press*, 10.1002/cptc.201800002.
- (409). Serebrovskaya EO; Lukyanov KA Chromophore-Assisted Light Inactivation: A Powerful Tool to Study Protein Functions. In *Singlet Oxygen: Applications in Biosciences and Nanosciences, Volume 2*; 2016; pp 185–203.
- (410). Sano Y; Watanabe W; Matsunaga S Chromophore-Assisted Laser Inactivation – towards a Spatiotemporal–functional Analysis of Proteins, and the Ablation of Chromatin, Organelle and Cell Function. *J. Cell Sci.* 2014, 127, 1621–1629. [PubMed: 24737873]
- (411). Lin JY; Sann SB; Zhou K; Nabavi S; Proulx CD; Malinow R; Jin Y; Tsien RY Optogenetic Inhibition of Synaptic Release with Chromophore-Assisted Light Inactivation (CALI). *Neuron* 2013, 79, 241–253. [PubMed: 23889931]
- (412). Hermann A; Liewald JF; Gottschalk A A Photosensitive Degron Enables Acute Light-Induced Protein Degradation in the Nervous System. *Current Biology.* 2015, pp R749–R750. [PubMed: 26325132]
- (413). Zhou K; Stawicki T; Goncharov A; Jin Y Position of UNC-13 in the Active Zone Regulates Synaptic Vesicle Release Probability and Release Kinetics. *Elife* 2013, 2, e01180. [PubMed: 24220508]
- (414). Noma K; Jin Y Optogenetic Mutagenesis in *Caenorhabditis Elegans*. *Nat. Commun.* 2015, 6, 8868. [PubMed: 26632265]
- (415). Wojtovich A; Wei A; Sherman T; Foster T Chromophore-Assisted Light Inactivation of Mitochondrial Electron Transport Chain Complex II in *Caenorhabditis Elegans*. *Sci. Rep.* 2016, 6, 29695. [PubMed: 27440050]
- (416). Sweeney ST; Hidalgo A; de Belle JS; Keshishian H Hydroxyurea Ablation of Mushroom Bodies in *Drosophila*. *Cold Spring Harb. Protoc.* 2012, 2012, 231–234. [PubMed: 22301647]
- (417). Sweeney ST; Hidalgo A; de Belle JS; Keshishian H Genetic Systems for Functional Cell Ablation in *Drosophila*. *Cold Spring Harb. Protoc.* 2012, 2012, 950–956. [PubMed: 22949708]
- (418). Sweeney ST; Hidalgo A; de Belle JS; Keshishian H Embryonic Cell Ablation in *Drosophila* Using Lasers. *Cold Spring Harb. Protoc.* 2012, 2012, 691–693. [PubMed: 22661443]
- (419). Leinwand SG; Chalasani SH Neuropeptide Signaling Remodels Chemosensory Circuit Composition in *Caenorhabditis Elegans*. *Nat. Neurosci.* 2013, 16, 1461–1467. [PubMed: 24013594]

- (420). Fry AL; Laboy JT; Norman KR VAV-1 Acts in a Single Interneuron to Inhibit Motor Circuit Activity in *Caenorhabditis Elegans*. Nat. Commun. 2014, 5, 5579. [PubMed: 25412913]
- (421). Qi YB; Garren EJ; Shu X; Tsien RY; Jin Y Photo-Inducible Cell Ablation in *Caenorhabditis Elegans* Using the Genetically Encoded Singlet Oxygen Generating Protein miniSOG. Proc. Natl. Acad. Sci. U. S. A. 2012, 109, 7499–7504. [PubMed: 22532663]
- (422). Williams DC; El Bejjani R; Ramirez PM; Coakley S; Kim SA; Lee H; Wen Q; Samuel A; Lu H; Hilliard MA; et al. Rapid and Permanent Neuronal Inactivation *In Vivo* via Subcellular Generation of Reactive Oxygen with the Use of KillerRed. Cell Rep. 2013, 5, 553–563. [PubMed: 24209746]
- (423). Gao S; Guan SA; Fouad AD; Meng J; Huang Y-C; Li Y; Alcaire S; Hung W; Kawano T; Lu Y; et al. Excitatory Motor Neurons Are Local Central Pattern Generators in an Anatomically Compressed Motor Circuit for Reverse Locomotion. eLife 2018, 7, e29915. [PubMed: 29360035]
- (424). Ryumina AP; Serebrovskaya EO; Shirmanova MV; Snopova LB; Kuznetsova MM; Turchin IV; Ignatova NI; Klementieva NV; Fradkov AF; Shakhov BE; et al. Flavoprotein miniSOG as a Genetically Encoded Photosensitizer for Cancer Cells. Biochim. Biophys. Acta - Gen. Subj 2013, 1830, 5059–5067.
- (425). Barnett M; Baran T; Foster T; Wojtovich A The Genetically-Encoded Photosensitizer Mini Singlet Oxygen Generator Produces Superoxide. Free Radic. Biol. Med. 2017, 112, 61–62.
- (426). Barnett ME; Baran TM; Foster TH; Wojtovich AP Quantification of Light-Induced miniSOG Superoxide Production Using the Selective Marker, 2-Hydroxyethidium. Free Radic. Biol. Med. 2018, 116, 134–140. [PubMed: 29353158]
- (427). Mironova KE; Proshkina GM; Ryabova AV; Stremovskiy OA; Lukyanov SA; Petrov RV; Deyev SM Genetically Encoded Immunophotosensitizer 4D5scFv-miniSOG Is a Highly Selective Agent for Targeted Photokilling of Tumor Cells *in Vitro*. Theranostics 2013, 3, 831–840. [PubMed: 24312153]
- (428). Proshkina GM; Shilova ON; Ryabova AV; Stremovskiy OA; Deyev SM A New Anticancer Toxin Based on HER2/neu-Specific DARPIn and Photoactive Flavoprotein miniSOG. Biochimie 2015, 118, 116–122. [PubMed: 26319592]
- (429). Consentino L; Lambert S; Martino C; Jourdan N; Bouchet P-E; Witczak J; Castello P; El-Esawi M; Corbineau F; d'Harlingue A; et al. Blue-light Dependent Reactive Oxygen Species Formation by *Arabidopsis* Cryptochrome May Define a Novel Evolutionarily Conserved Signaling Mechanism. New Phytol. 2015, 206, 1450–1462. [PubMed: 25728686]
- (430). Jourdan N; Martino CF; El-Esawi M; Witczak J; Bouchet P-E; D'Harlingue A; Ahmad M Blue-Light Dependent ROS Formation by *Arabidopsis* Cryptochrome-2 May Contribute toward Its Signaling Role. Plant Signal. Behav 2015, 10, e1042647. [PubMed: 26179959]
- (431). El-Esawi M; Arthaut L-D; Jourdan N; D'Harlingue A; Link J; Martino CF; Ahmad M Blue-Light Induced Biosynthesis of ROS Contributes to the Signaling Mechanism of *Arabidopsis* Cryptochrome. Sci. Rep. 2017, 7, 13875. [PubMed: 29066723]
- (432). Massey V The Chemical and Biological Versatility of Riboflavin. Biochem. Soc. Trans. 2000, 28, 283–296. [PubMed: 10961912]
- (433). Mayhew SG The Effects of pH and Semiquinone Formation on the Oxidation-Reduction Potentials of Flavin Mononucleotide. A Reappraisal. Eur. J. Biochem. 1999, 265, 698–702. [PubMed: 10504402]
- (434). Hemmerich P; Veeger C; Wood HCS Progress in the Chemistry and Molecular Biology of Flavins and Flavocoenzymes. Angew. Chemie Int. Ed. English 1965, 4, 671–687.
- (435). Wilson GS Determination of Oxidation-Reduction Potentials. 1978, 54, 396–410.
- (436). Nöll G; Hauska G; Hegemann P; Lanzl K; Nöll T; von Sanden-Flohe M; Dick B Redox Properties of LOV Domains: Chemical versus Photochemical Reduction, and Influence on the Photocycle. ChemBioChem 2007, 8, 2256–2264. [PubMed: 17990262]
- (437). Draper RD; Ingraham LL A Potentiometric Study of the Flavin Semiquinone Equilibrium. Arch. Biochem. Biophys. 1968, 125, 802–808. [PubMed: 5671043]
- (438). Losi A Flavin-Based Blue-Light Photosensors: A Photobiophysics Update. Photochem. Photobiol. 2007, 83, 1283–1300. [PubMed: 18028200]

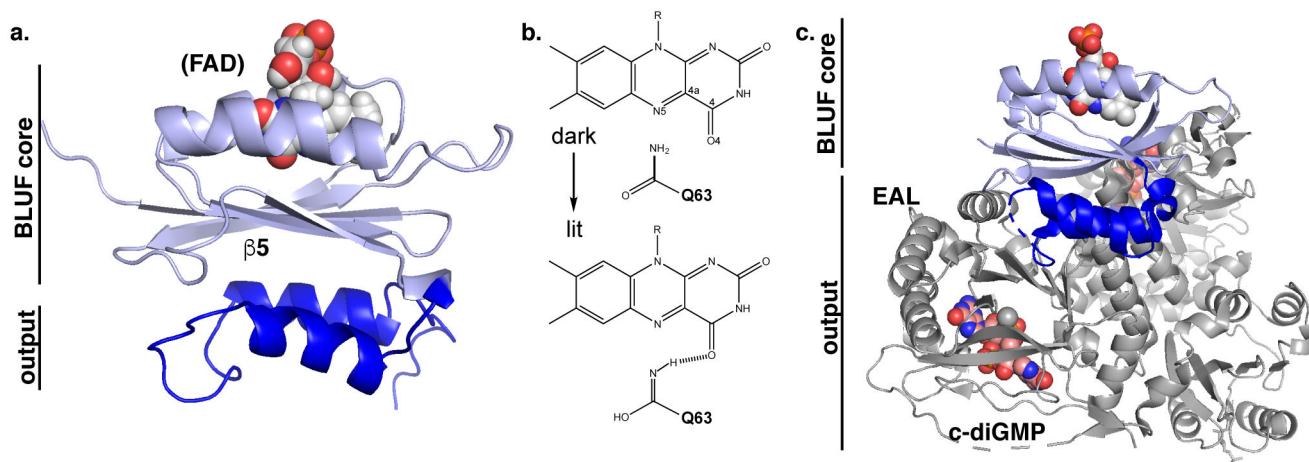
- (439). Chaves I; Pokorny R; Byrdin M; Hoang N; Ritz T; Brettel K; Essen L-O; van der Horst GTJ; Batschauer A; Ahmad M The Cryptochromes: Blue Light Photoreceptors in Plants and Animals. *Annu. Rev. Plant Biol.* 2011, 62, 335–364. [PubMed: 21526969]
- (440). Ahmad M Photocycle and Signaling Mechanisms of Plant Cryptochromes. *Curr. Opin. Plant Biol.* 2016, 33, 108–115. [PubMed: 27423124]
- (441). Hwang C; Sinskey AJ; Lodish HF Oxidized Redox State of Glutathione in the Endoplasmic Reticulum. *Science* 1992, 257, 1496–1502. [PubMed: 1523409]
- (442). López-Mirabal HR; Winther JR Redox Characteristics of the Eukaryotic Cytosol. *Biochim. Biophys. Acta - Mol. Cell Res* 2008, 1783, 629–640.
- (443). Arents JC; Perez MA; Hendriks J; Hellingwerf KJ On the Midpoint Potential of the FAD Chromophore in a BLUF-Domain Containing Photoreceptor Protein. *FEBS Lett.* 2011, 585, 167–172. [PubMed: 21110976]
- (444). Balland V; Byrdin M; Eker APM; Ahmad M; Brettel K What Makes the Difference between a Cryptochrome and DNA Photolyase? A Spectroelectrochemical Comparison of the Flavin Redox Transitions. *J. Am. Chem. Soc.* 2009, 131, 426–427. [PubMed: 19140781]
- (445). Lin C; Robertson DE; Ahmad M; Raibekas AA; Jorns MS; Dutton PL; Cashmore AR Association of Flavin Adenine Dinucleotide with the *Arabidopsis* Blue Light Receptor CRY1. *Science* 1995, 269, 968–970. [PubMed: 7638620]
- (446). Gindt YM; Schelvis JPM; Thoren KL; Huang TH Substrate Binding Modulates the Reduction Potential of DNA Photolyase. *J. Am. Chem. Soc.* 2005, 127, 10472–10473. [PubMed: 16045318]
- (447). Lokhandwala J; Hopkins HC; Rodriguez-Iglesias A; Dattenböck C; Schmoll M; Zoltowski BD Structural Biochemistry of a Fungal LOV Domain Photoreceptor Reveals an Evolutionarily Conserved Pathway Integrating Light and Oxidative Stress. *Structure* 2015, 23, 116–125. [PubMed: 25533487]
- (448). Magerl K; Stambolic I; Dick B; Balland V; Getzoff ED; Ritz T; Brettel K; Nonell S; Tonge PJ; Meech SR; et al. Switching from Adduct Formation to Electron Transfer in a Light–oxygen–voltage Domain Containing the Reactive Cysteine. *Phys. Chem. Chem. Phys.* 2017, 19, 10808–10819. [PubMed: 28271102]
- (449). Ortiz-Guerrero JM; Polanco MC; Murillo FJ; Padmanabhan S; Elías-Arnanz M Light-Dependent Gene Regulation by a Coenzyme B<sub>12</sub>-Based Photoreceptor. *Proc. Natl. Acad. Sci. U. S. A.* 2011, 108, 7565–7570. [PubMed: 21502508]
- (450). Wilson A; Punginelli C; Gall A; Bonetti C; Alexandre M; Routaboul JM; Kerfeld CA; van Grondelle R; Robert B; Kennis JT; et al. A Photoactive Carotenoid Protein Acting as Light Intensity Sensor. *Proc Natl Acad Sci U S A* 2008, 105, 12075–12080. [PubMed: 18687902]
- (451). Mukherjee A; Weyant KB; Walker J; Schroeder CM Directed Evolution of Bright Mutants of an Oxygen-Independent Flavin-Binding Fluorescent Protein from *Pseudomonas Putida*. *J. Biol. Eng.* 2012, 6, 20. [PubMed: 23095243]
- (452). Möglich A; Moffat K Structural Basis for Light-Dependent Signaling in the Dimeric LOV Domain of the Photosensor YtvA. *J. Mol. Biol.* 2007, 373, 112–126. [PubMed: 17764689]
- (453). Rullan M; Benzinger D; Schmidt GW; Miliás-Argeitis A; Khammash M An optogenetic platform for real-time, single-cell interrogation of stochastic transcriptional regulation. *Mol. Cell* 2018, 70, 745–756. [PubMed: 29775585]



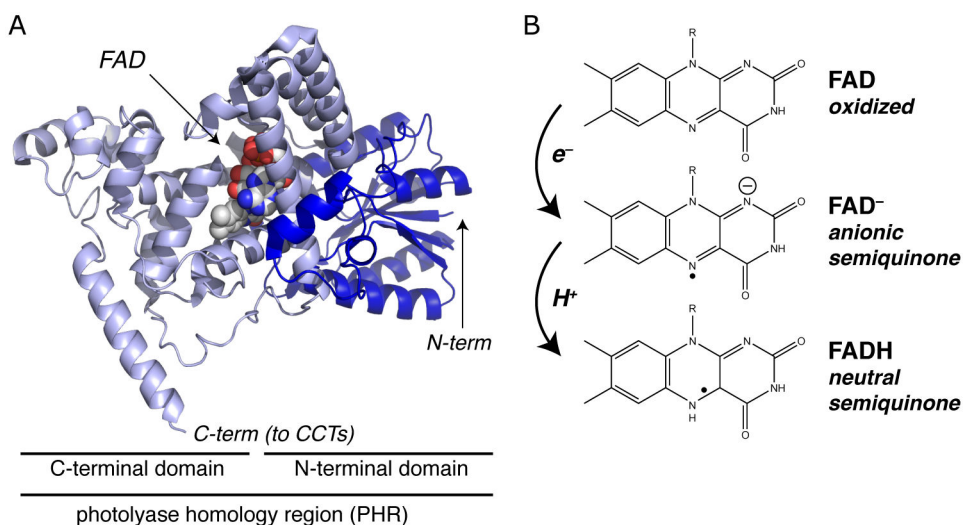
**Figure 1.** Overview of the five types of soluble blue-/UV-light-sensitive photosensory proteins and protein domains utilized in optogenetic applications. Typical characteristics for members of each family are listed, including chromophores, wavelength of maximum sensitivity ( $\lambda_{\max}$ ), typical time constants for thermal reversion of photoactivated state ( $\tau_{\text{off}}$ ) and molecular weight (MW) of minimal sensory fragment minus effectors.



**Figure 2.** Fundamental aspects of photoactivation of LOV domains. (A) Structure of *AsLOV2*,<sup>19,20</sup> showing the location of the LOV  $\alpha/\beta$  “core” domain surrounding the FMN chromophore and effector A'α and Jα helices on adjacent faces of the  $\beta$ -sheet. (B) Simplified LOV photocycle, demonstrating the effect of blue light to interconvert between noncovalent protein complex with oxidized flavin and covalently-attached, reduced flavin. Residue numberings apply to *AsLOV2*. (C) Example of a more complex LOV-effector arrangement within EL222,<sup>21</sup> a LOV-helix-turn-helix (HTH) protein, where an effector helix (more distantly located within the primary structure) from within the HTH domain structurally and functionally replaces the Jα helix of *AsLOV2*.

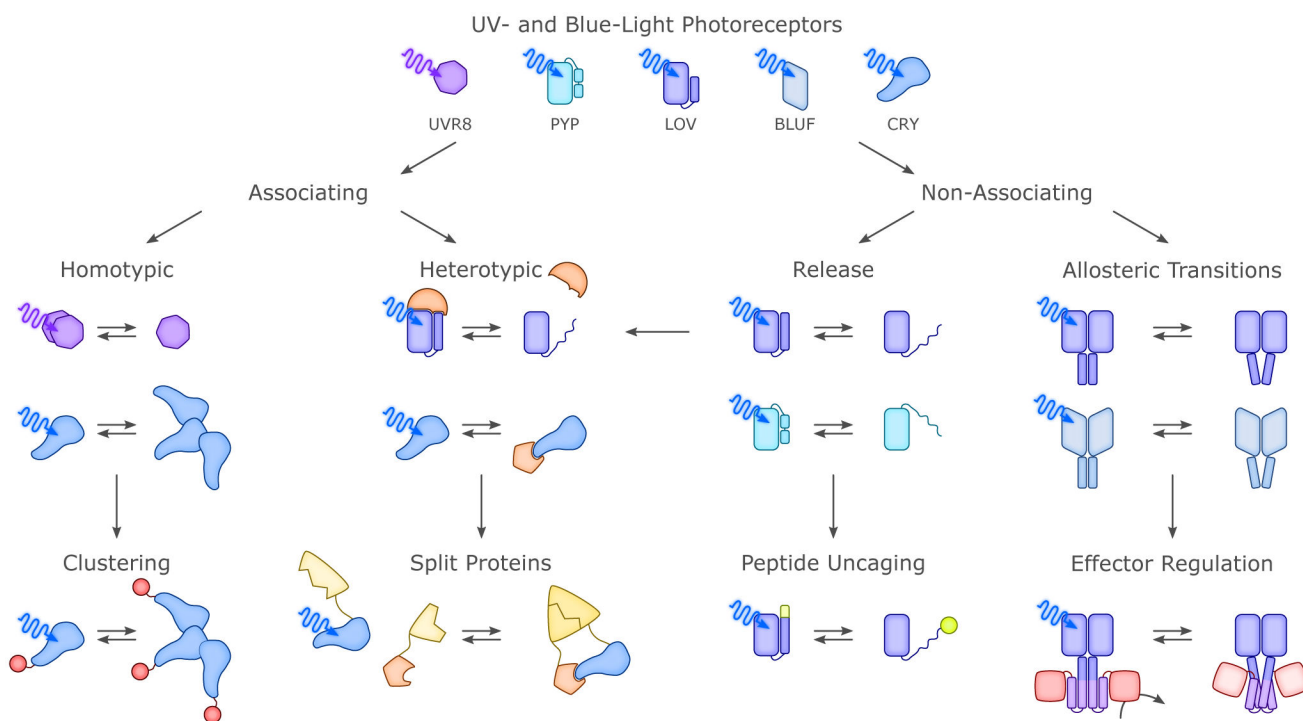


**Figure 3.** Fundamental aspects of photoactivation of BLUF domains. (A) Structure of the BLUF domain of *Klebsiella pneumoniae* BlrP1,<sup>30,31</sup> exemplifying location of the BLUF  $\alpha/\beta$  “core” domain surrounding the FAD chromophore and effector C-terminal helices. (B) Simplified BLUF photocycle, showing how photochemically-driven effects including altered hydrogen-bonding of a nearby glutamine lead to altered protein/FAD interactions. (C) Example of a more complex BLUF-effector arrangement within full-length BlrP1,<sup>31</sup> a BLUF-EAL enzyme involved in c-di-GMP breakdown.

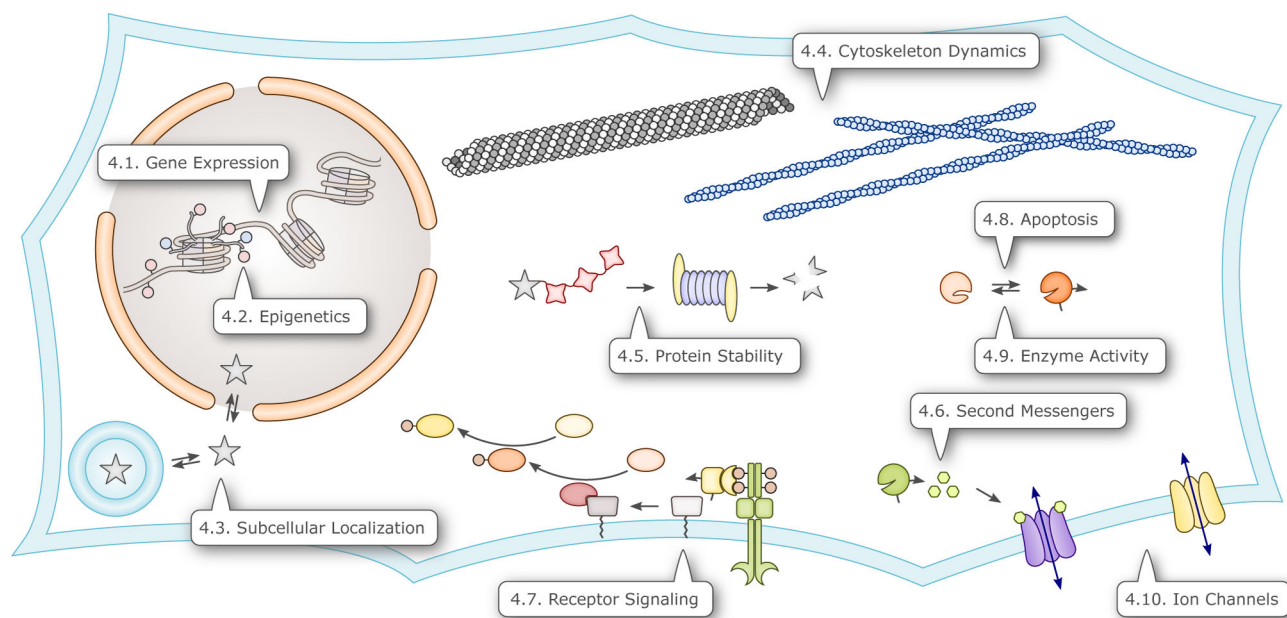


**Figure 4.** Fundamental aspects of photoactivation of cryptochromes. (A) Structure of the photolyase homology region (PHR) of *A. thaliana* CRY1,<sup>44</sup> showing the location of the bound FAD chromophore within the highly-helical C-terminal domain. The locations of the N- and C-termini are also indicated, as these have been implicated in CIB1 binding and homooligomerization<sup>45</sup> in the homologous *A. thaliana* CRY2 (*AtCRY2*) protein widely used for optogenetic applications. CCT = CRY C-Terminal region. (B) Simplified cryptochrome photocycle, showing the oxidized FAD chromophore present in the inactive dark-adapted state and photochemically-generated anionic and neutral semiquinone states.

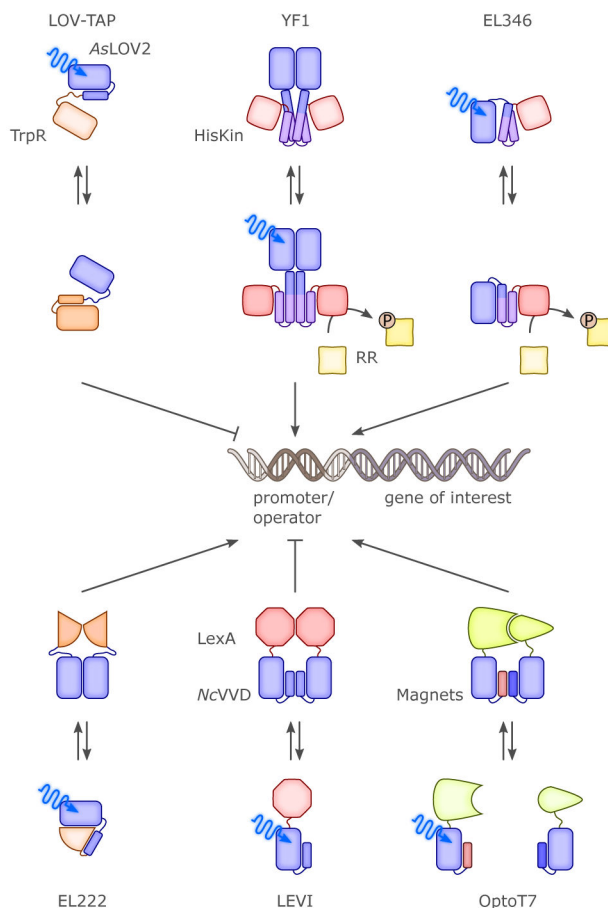




**Figure 5.** Allosterity and engineering of UV-light- and BL-sensitive photoreceptors. Despite the rich diversity of these photoreceptors, their signal transduction mechanisms largely fall into but a few classes. In case of the associating photoreceptors, the transition between dark-adapted and light-adapted states entails a change in oligomeric state, either in homotypic or heterotypic manner. Light-modulated oligomerization has proven a particularly versatile approach for engineering novel optogenetic actuators as detailed in section 4. Among the non-associating photoreceptors, we identify light-modulated order-disorder transitions, as exemplified by the Ja helix unfolding in *AsLOV2*,<sup>19</sup> and changes in tertiary and quaternary structure as prevalent mechanisms. Both types of mechanisms have lent themselves to the engineering of novel photoreceptors (cf. sec. 4.).

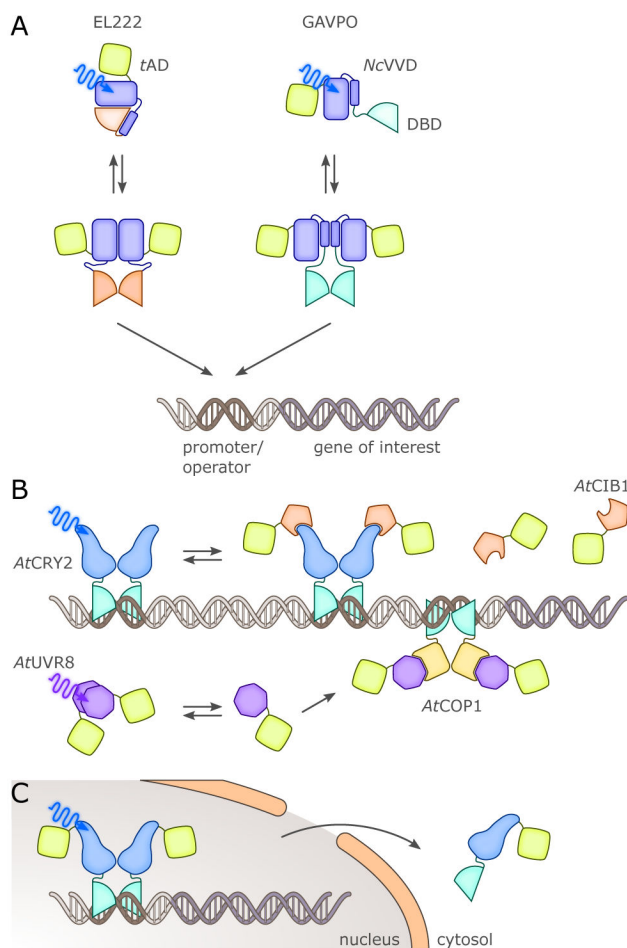


**Figure 6.** Overview of cellular processes that have been optogenetically controlled via photoreceptors sensitive to UV and blue light. The callouts direct to the sections that discuss the corresponding applications.



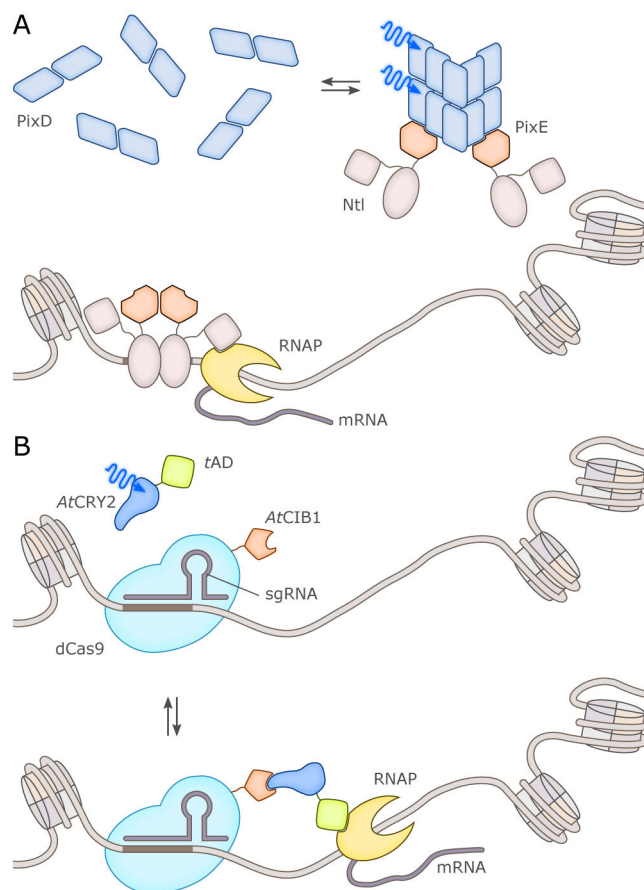
**Figure 7.**

Several optogenetic systems achieved BL control over transcription in prokaryotes. In LOV-TAP<sup>104</sup>, the *E. coli* Trp repressor and the AsLOV2 were fused such that mutually exclusive folding of a shared  $\alpha$  helix resulted; BL exposure allowed the repressor to correctly fold and bind to DNA. The homodimeric YF1<sup>105</sup> and the monomeric EL346<sup>163</sup> are LOV histidine kinases that phosphorylate cognate response regulators in BL-dependent manner; when phosphorylated, the response regulators bind DNA and activate transcription. In EL222,<sup>21</sup> BL absorption by a LOV photosensor prompts dimerization and DNA binding of an associated helix-turn-helix effector, leading to transcriptional activation. The LEVI approach<sup>164</sup> is based on the NcVivid LOV sensor; BL-induced homodimerization rescues the repressional activity of the truncated LexA repressor. Based on the Magnets system for BL-induced heterodimerization<sup>165</sup>, BL-activated split variants of the phage T7 polymerase were engineered.<sup>166,167</sup>

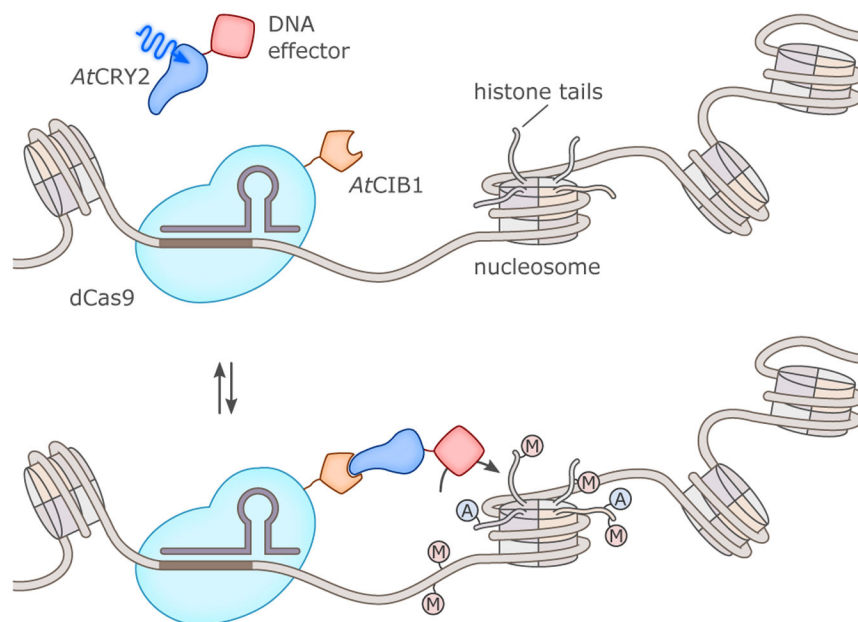


**Figure 8.**

BL-dependent control of transgene transcription in eukaryotes was realized with single-chain constructs (panels A and C) and with split transcription factors (TF) (panel B). (A) The bacterial LOV receptor EL222 was linked to a eukaryotic *trans*-activating domain (*tAD*) to achieve light-dependent control of transgenes in eukaryotic cells.<sup>92</sup> The GAVPO approach makes use of the homodimerization reaction *NcVivid* undergoes upon BL exposure.<sup>185</sup> By linking a DNA-binding domain (DBD) and a *tAD* to *NcVivid*, a chimeric TF was obtained that in darkness is monomeric and unable to bind to the DNA operator sequence. BL induced dimerization, DNA binding and transcriptional activation. (B) In several studies, split-TF systems were generated, as exemplarily shown for two specific scenarios. (top) Several approaches relied on linking *AtCRY2* to a DBD such that upon BL application a *tAD*, linked to *AtCIB1*, could be recruited to induce gene expression.<sup>51,193</sup> (bottom) Conceptually similar approaches were realized for *AtUVR8* which forms a homodimer in the dark but dissociates upon UV-light exposure.<sup>194,195</sup> In its monomerized form, *AtUVR8* can then bind to *AtCOP1*. By linking the two proteins to a DBD and *tAD*, respectively, UV-light-dependent control of transcription was achieved. (C) *AtCRY2* was fused with both a DBD and a *tAD* to yield a single-chain TF.<sup>196</sup> BL induced nuclear clearing of this TF, accompanied by downregulation of transcription.

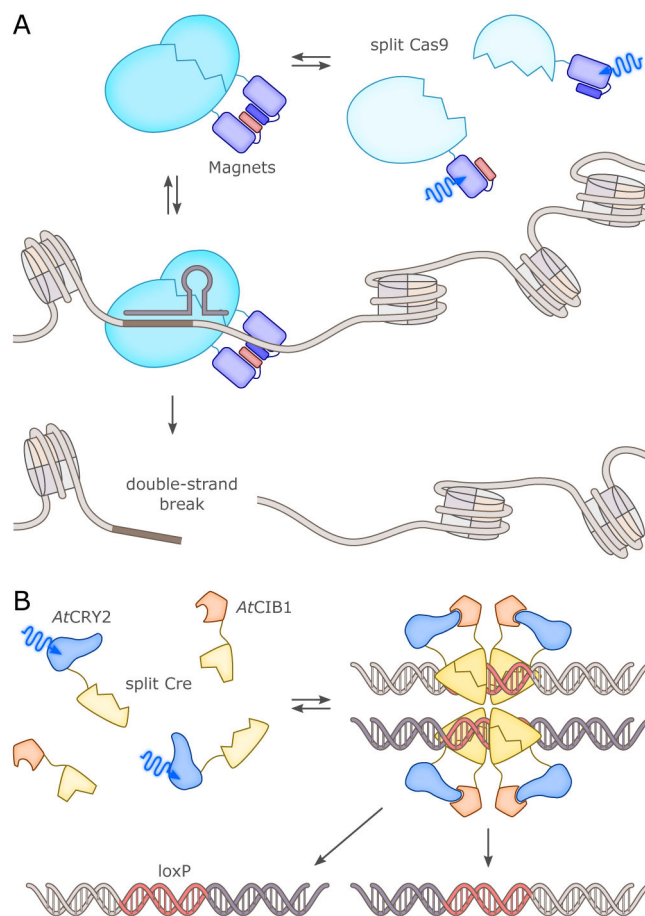


**Figure 9.** BL-dependent expression from endogenous eukaryotic promoters. (A) In the PICCORO approach,<sup>213</sup> an endogenous transcription factor, e.g., Ntl, was fused to the PixE protein which in the dark associates with the homodecameric BLUF photoreceptor PixD. Upon BL absorption, PixD disassembled into homodimers and dissociated from the PixE-Ntl fusion protein, thus allowing Ntl to bind its endogenous operator site and activate transcription. (B) Programmable DNA-binding proteins, e.g., the TALEs or the cleavage-deficient dCas9, allow to specifically designate endogenous promoters. Transcriptional activation of these promoters was achieved by BL-dependent recruitment of a trans-activating domain (*tAD*), for example via the *AtCRY2:AtCIB1* pair.<sup>214,215</sup>

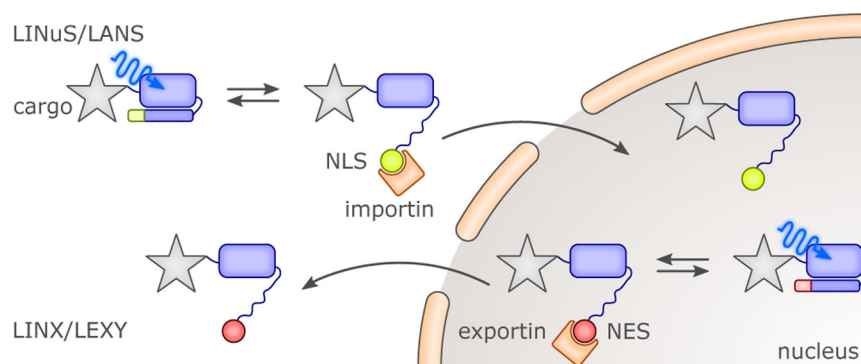


**Figure 10.**

Optogenetic control of epigenetics. TALE proteins and cleavage-deficient dCas9 serve as inert DNA-binding modules that can be programmed to specifically locate to unique target sites in eukaryotic genomes.<sup>230</sup> Linkage of dCas9 with *AtCIB1* allows BL-dependent recruitment of DNA effector enzymes that are covalently coupled to *AtCRY2*. Suitable effectors include DNA and histone methylases, histone (de)acetylases as well as chromatin remodeling enzymes. For example, acetylation and methylation (indicated by 'A' and 'M', respectively) serve as epigenetic marks and modulate transcriptional activity. For clarity, histone N-terminal tails are only drawn for one nucleosome unit.

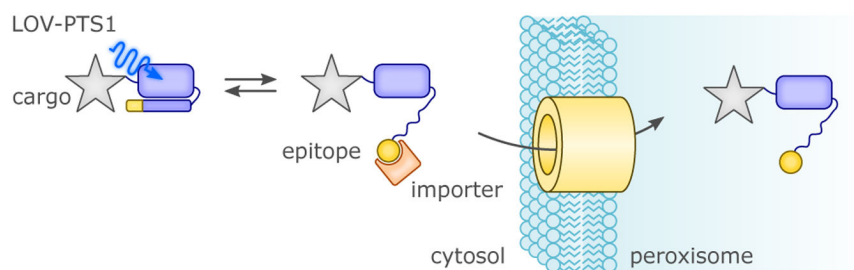


**Figure 11.** Optogenetic control of DNA recombination. (A) The programmable DNA endonuclease Cas9 was split into two parts which could be reassembled in BL-dependent manner via the Magnets LOV receptors.<sup>227</sup> The reconstituted Cas9 enzyme mediated double-strand breaks at defined genomic sites, thus triggering non-homologous end joining and homology-directed repair. (B) Light-regulated recombination was also achieved by splitting the Cre recombinase into two fragments which were linked with *AtCRY2* and *AtCIB1*, respectively.<sup>51,53,234</sup> BL induced fragment assembly and restoration of activity, thereby enabling recombination at loxP sites.



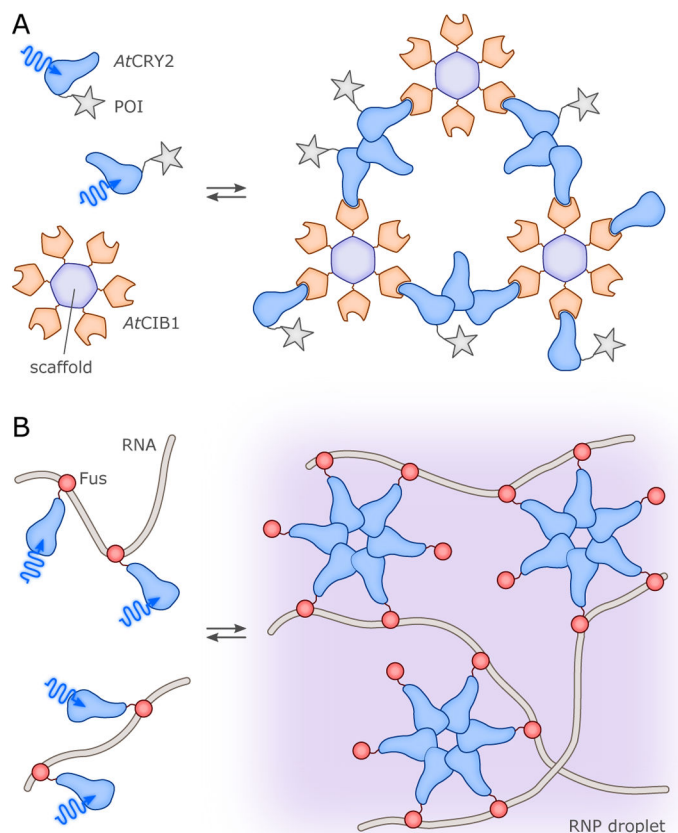
**Figure 12.** BL control of nuclear import and export processes was achieved in the LINuS<sup>209</sup>/LANS<sup>211</sup> and LINX<sup>212</sup>/LEXY<sup>210</sup> approaches by embedding corresponding trafficking signal peptides in the J $\alpha$  helix of the *AsLOV2* photosensor. BL-induced unfolding prompted exposure of the signal peptides and caused nuclear import and export, respectively, of cargo proteins.





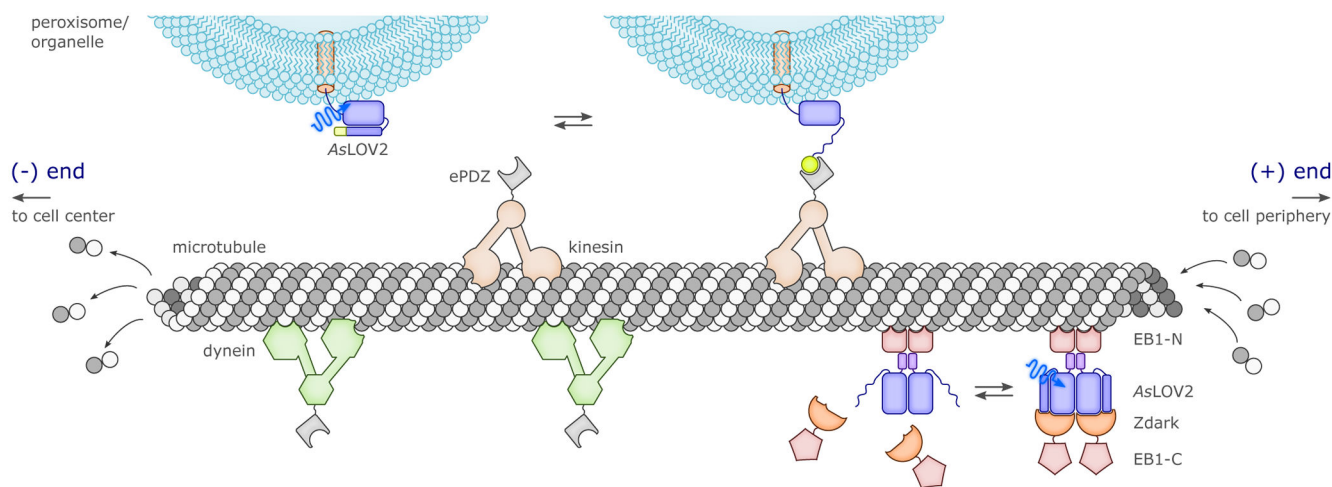
**Figure 13.**

The LOV-PTS1 strategy<sup>240</sup> is based on the *AsLOV2* photosensor to which a peroxisomal trafficking epitope was appended. BL-induced J $\alpha$  unfolding relieved caging of the epitope and promoted peroxisomal import of cargo proteins.



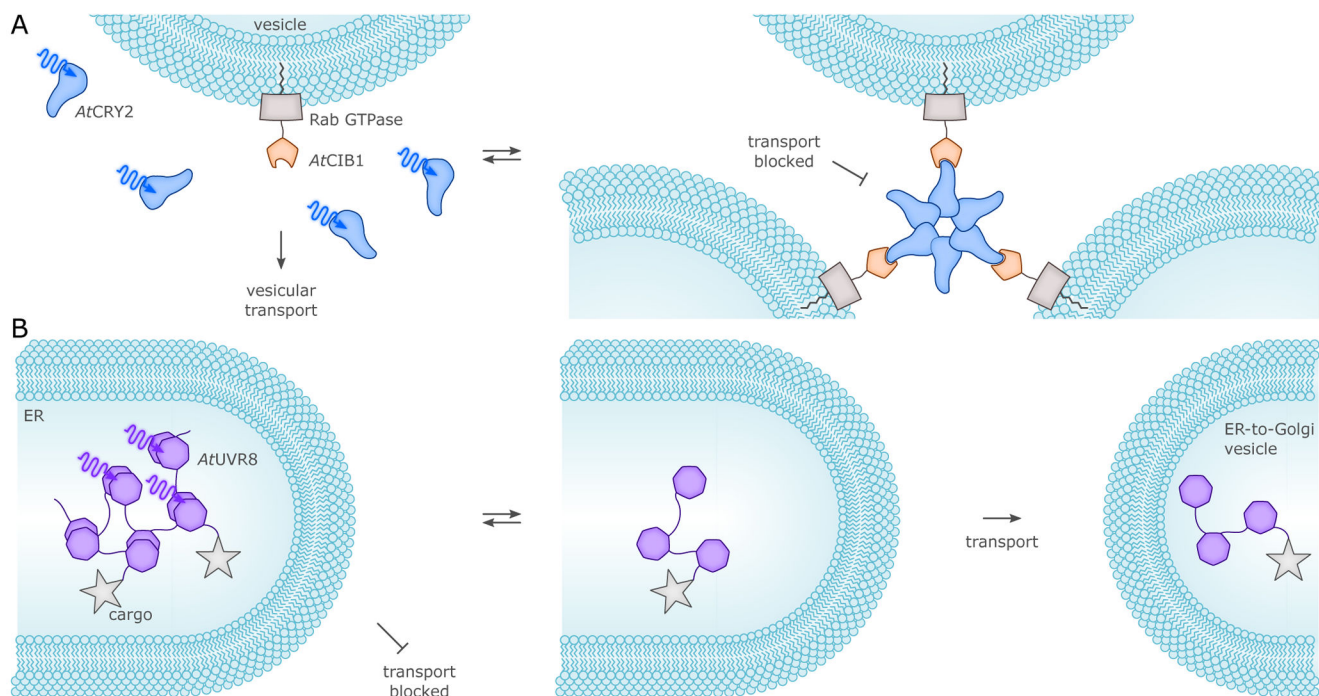
**Figure 14.** Optically induced compartments. (A) In the LARIAT method,<sup>242</sup> *AtCIB1* is conjugated to a multimeric scaffold protein such that upon BL-induced association with *AtCRY2* clusters formed. Proteins of interest (POI) can be sequestered into said clusters either via direct coupling to *AtCRY2* or via adapter proteins. For clarity, not all *AtCRY2* molecules are shown with attached POI. The related LINC approach<sup>52</sup> does away with *AtCIB1* and instead exploits the ability of *AtCRY2* to form homooligomers upon BL absorption. (B) The BL-induced clustering of *AtCRY2* also underpins a strategy for optogenetically controlling ribonucleoprotein (RNP) droplets.<sup>66</sup> To this end, *AtCRY2* was fused to the unstructured RNA-binding protein FUS to allow light-induced liquid-liquid phase transition and formation of RNP droplets.





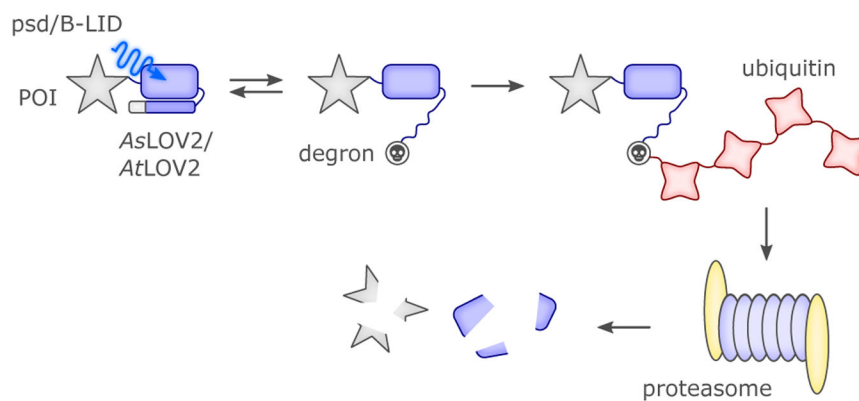
**Figure 16.**

Optogenetic control of microtubule stability and transport. Using the TULIP system for BL-induced heterodimerization,<sup>258</sup> kinesin motors could be recruited to desired organelles, e.g., peroxisomes, which were then transported to the (+) end of microtubules.<sup>261</sup> The principal concept extends to dyneins which move to the (-) end and to myosins which move along actin filaments (not shown). The polymerization dynamics of microtubules was modulated by using a split version of the end-binding protein EB1.<sup>262</sup> In darkness, the two halves of split-EB1 were held together via the *AsLOV2*:Zdark interaction but BL prompted *AsLOV2* Ja unwinding and dissociation of the EB1 fragments.

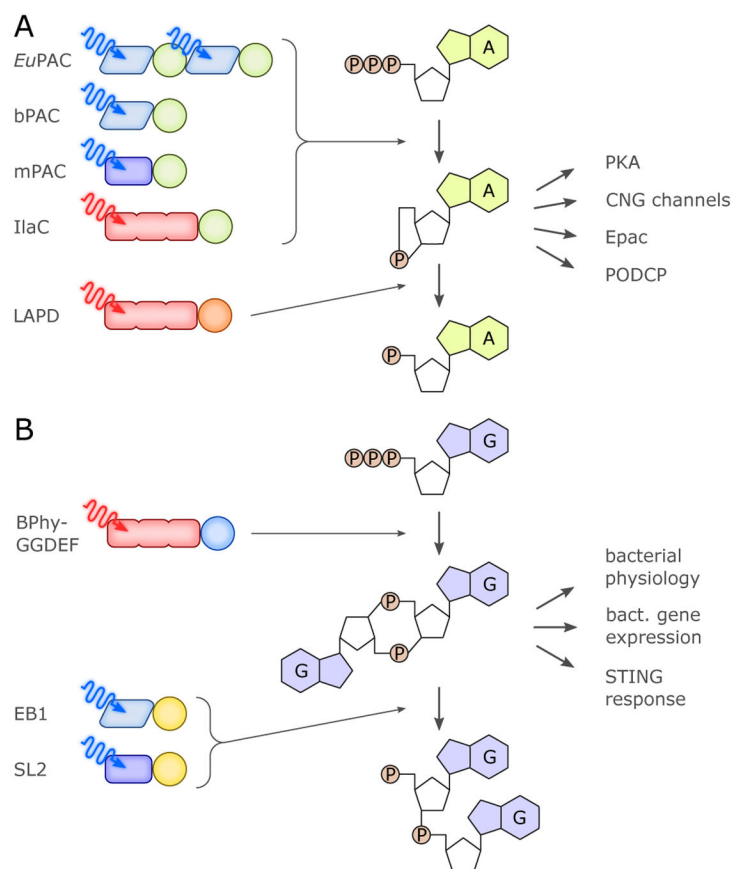


**Figure 17.**

Optogenetic control of vesicular transport. (A) *AtCIB1* was linked to different Rab GTPases that orchestrate vesicular transport.<sup>265</sup> BL induced *AtCRY2* to form clusters and to bind *AtCIB1*, thereby gumming up the vesicular transport machinery. (B) The secretory export of cargo proteins could be modulated in UV-light-dependent manner by linking them to one or several copies of the homodimeric *AtUVR8*.<sup>266</sup> Formation of higher-order assemblies resulted in retention in the endoplasmic reticulum. UV light prompted *AtUVR8* dissociation and resolution of these assemblies, and transport of the cargo ensued.

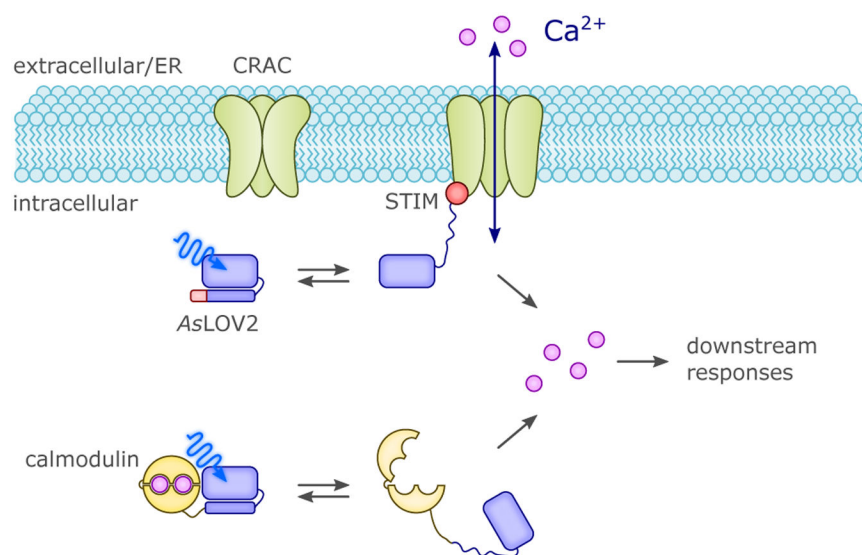


**Figure 18.** The intracellular half life of POIs was optogenetically regulated with the psd<sup>271</sup> and B-LID<sup>270</sup> strategies. BL stimulated unfolding of the J $\alpha$  helix of *At*LOV2 or *As*LOV2, thereby increasing the exposure of an embedded degron epitope. The cellular ubiquitin/proteasome machinery then degraded the POI and the attached LOV2 module.



**Figure 19.**

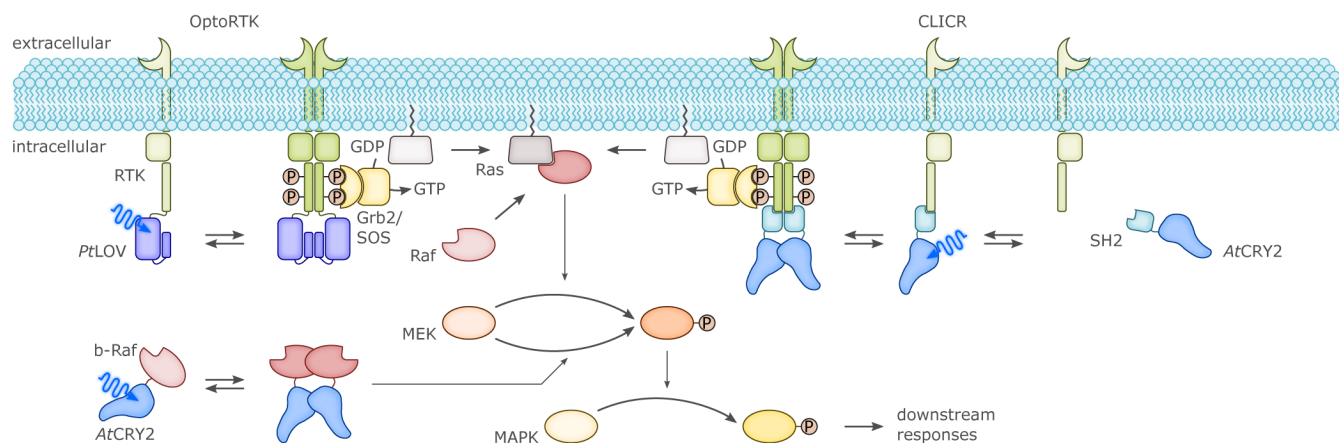
Optogenetic actuators for controlling cyclic-nucleotide second messengers. (A) A palette of photoactivated adenylate cyclases (PACs) responsive to BL<sup>93,94,279,280</sup> or red light catalyze the formation of cAMP or cGMP. In eukaryotic cells, cAMP binds to and thus activates CNG channels, PKA, Epac and popeye-domain-containing proteins (PODCP).<sup>278</sup> The red-light-activated PDE LAPD mediates the hydrolytic breakdown of cAMP and cGMP.<sup>281</sup> (B) C-di-GMP is a versatile second messenger involved in numerous physiological adaptations of bacteria. Red-light-activated GGDEF enzymes produce c-di-GMP and achieve optogenetic control over physiology and gene expression in bacteria.<sup>282,283</sup> In eukaryotes, c-di-GMP triggers the STING response as part of the vertebrate innate immune system. BL-activated EAL enzymes<sup>31,284,285</sup> catalyze the hydrolysis of c-di-GMP. For clarity, all photoreceptors in panels (A) and (B) are drawn as monomers although they are active as homodimers. BLUF, LOV and bacteriophytochrome photosensors are denoted as parallelograms, rectangles and tripartite shapes, respectively; colored circles denote cyclases and phosphodiesterases specific for cyclic nucleotides.



**Figure 20.**

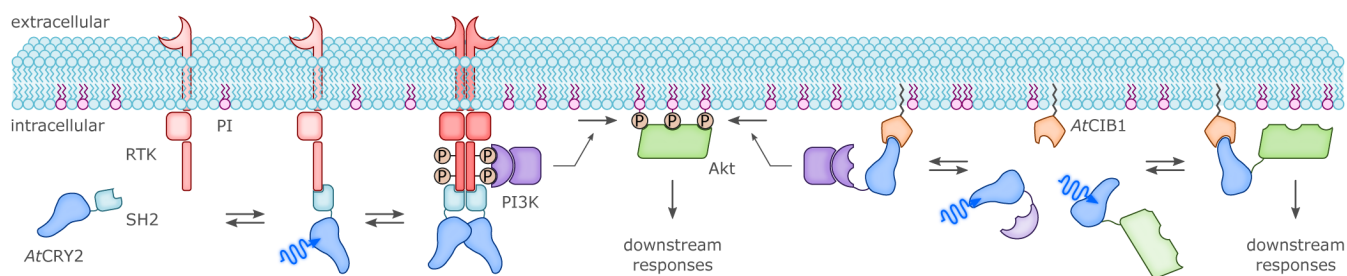
Intracellular calcium concentrations could be perturbed with BL-sensitive photoreceptors. On the one hand, the opening of Ca<sup>2+</sup>-specific CRAC channels in the plasma membrane or the endoplasmic/sarcoplasmic reticulum was gated via interactions with the STIM peptide.<sup>124,304,305</sup> When interleaved with Ja of AsLOV2, the exposure of STIM could be controlled by BL exposure. Alternatively, the STIM epitope was fused to *AtCRY2* such that BL-induced clustering resulted in translocation to the membrane and CRAC gating (not shown<sup>307</sup>). A different strategy was pursued in the construction of a fusion protein between the AsLOV2 photosensor and the calcium-binding calmodulin.<sup>309</sup> BL prompted Ja unfolding, destabilization of the calmodulin module and release of bound Ca<sup>2+</sup> ions.





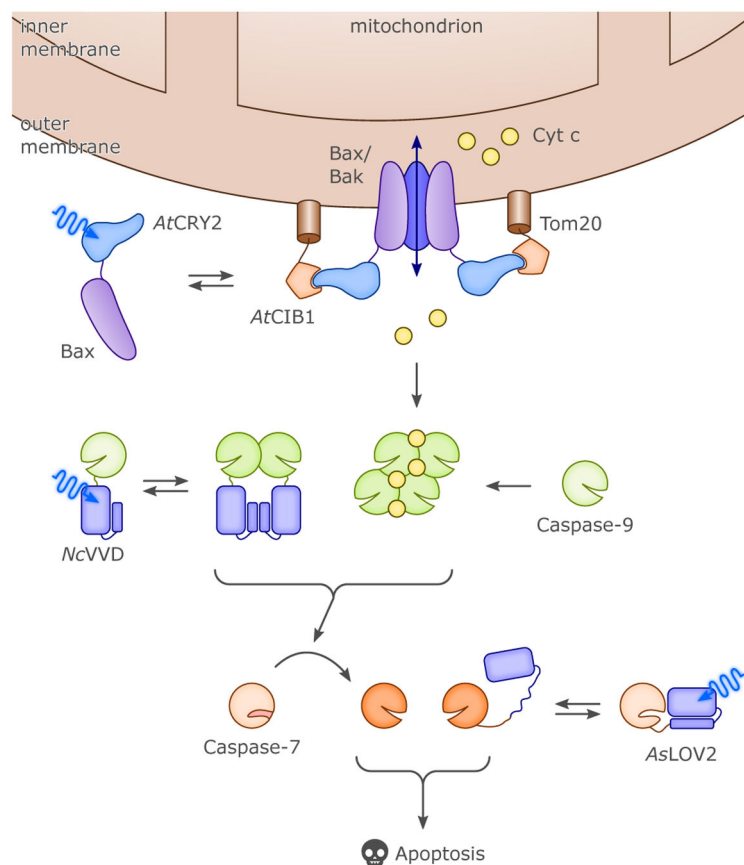
**Figure 21.**

Receptor tyrosine kinase (RTK) signaling was subjected to BL-dependent optogenetic control as exemplarily illustrated for the MAPK/ERK pathway. In several approaches, <sup>190,311,312</sup> OptoRTKs were constructed by appending an associating photoreceptor, e.g., the LOV domain of *P. tricornutum* aureochrome, to the intracellular C terminus of an RTK. BL then induced homodimerization of the chimeric receptor and activation of the downstream signaling cascade. In the CLICR strategy,<sup>315</sup> endogenous RTKs could be activated upon BL exposure via an adapter protein consisting of *AtCRY2* and an SH2 domain that specifically binds to the C termini of RTKs. The MAPK/ERK pathway was also targeted at lower tiers. <sup>316,317</sup> On the one hand, the Raf kinase can be activated by recruiting it in BL-dependent manner to the plasma membrane (not shown). On the other hand, the B-Raf isoform can be activated away from the membrane in the cytosol by homodimerization or association with the isoform c-Raf. To optogenetically control these processes, the BL-dependent oligomerization of *AtCRY2* or its interaction with *AtCIB1* was harnessed.



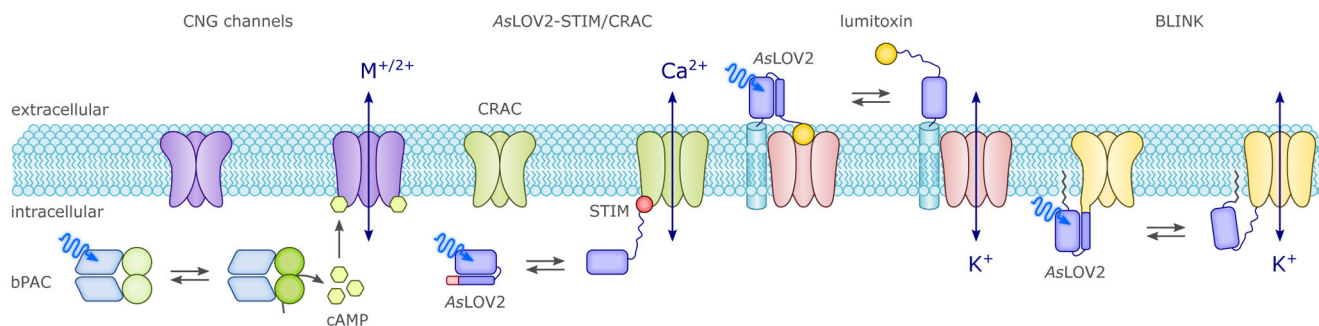
**Figure 22.**

Optogenetic control of phosphatidylinositol signaling. In the CLICR strategy,<sup>315</sup> endogenous receptor tyrosine kinases (RTKs) were put under BL control via *AtCRY2*-mediated clustering, and the PI3K/Akt signal pathway could be optogenetically manipulated. Once activated by the RTK, the PI3K kinase phosphorylates phosphatidylinositol (PI) to produce the phosphoinositides PIP<sub>2</sub> and PIP<sub>3</sub>. In turn, the Akt kinase binds to PIP<sub>3</sub>, is thereby activated and elicits downstream responses. Optogenetic intervention in the pathway was also accomplished at the level of PI3K via *AtCRY2:AtCIB1*-mediated membrane recruitment and concomitant activation.<sup>323,324</sup> Likewise, the Akt kinase could be directly controlled by translocating it to the membrane upon BL exposure, again using the *AtCRY2:AtCIB1* system.<sup>325–327</sup>



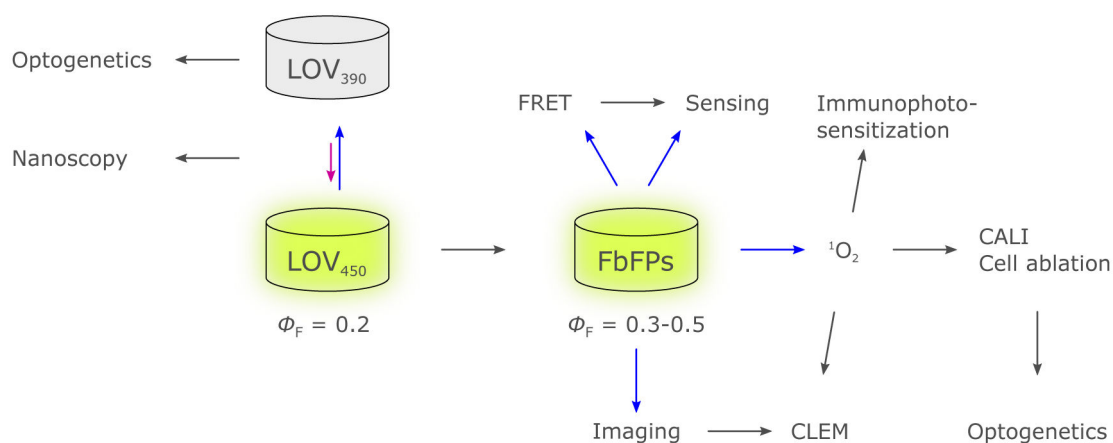
**Figure 23.**

Apoptosis, the programmed cell death, was optogenetically controlled at several tiers with BL-responsive photoreceptors. Covalent fusion of Bax with *AtCRY2* allowed its BL-regulated recruitment to *AtCIB1* which was connected to the Tom20 protein residing in the outer membrane of the mitochondrion.<sup>336</sup> Oligomerization and assembly with Bak contributed to pore formation and outflow of cytochrome c from the mitochondrial intermembrane compartment; in the cytosol, cytochrome c promoted oligomerization and activation of the initiator caspase-9. In an alternative approach, the activity of caspase-9 was directly controlled via coupling to the *NcVivid* photosensor which undergoes BL-induced homodimerization.<sup>215</sup> Activated caspase-9 proteolytically activated downstream executioner caspases, e.g., caspase-7. The latter could be subjected to direct BL control by linkage to the *AsLOV2* photosensor such that steric hindrance of the active site resulted.<sup>277</sup> BL promoted *AsLOV2*  $\text{J}\alpha$  unfolding and restored catalytic activity of caspase-7. Executioner caspases then acted on numerous downstream targets to elicit apoptosis.



**Figure 24.**

Optogenetic regulation of membrane potential and ion flux. BL-sensitive photoreceptors mediate optogenetic perturbation of membrane potential and thus supplement the light-gated channelrhodopsins. Several PACs catalyze the formation of cAMP and cGMP upon BL exposure,<sup>93,94,279,280</sup> cf. Fig. 19, and can be combined with CNG channels to optogenetically control ion flux across the plasma membrane. Depending upon CNG channel, different mono- and divalent cations ( $M^{+/2+}$ ) are specifically conducted. The gating of CRAC channels was optogenetically controlled by embedding a stimulatory peptide derived from the STIM protein into the Ja helix of AsLOV2, cf. Fig. 20.<sup>124,304,305</sup> In the lumitoxin method,<sup>346</sup> the AsLOV2 photosensor was anchored to the outer leaflet of the plasma membrane and connected to a peptide toxin that blocked potassium channels. Light-induced Ja unfolding granted enhanced diffusional space to the toxin, resulting in its dissociation from the channel and relieve of inhibition. In the BLINK receptor,<sup>347</sup> the AsLOV2 photosensor was fused via its C-terminal Ja helix to the N terminus of a minimal potassium channel. BL exposure resulted in an increased potassium conductance of BLINK.

**Figure 25.**

Overview of the properties and biophysical applications of flavin-binding fluorescent proteins (FbFPs). Constitutively fluorescent FbFPs are engineered from wild-type LOV domains, by substituting the active-site cysteine to abrogate canonical LOV photochemistry, and by introducing other mutations to increase the fluorescence quantum yield  $\Phi_F$ . They can be used for imaging in fluorescence microscopy, as donors in FRET and as fluorescence-based sensors.<sup>350–353</sup> The photochromicity of cysteine-retaining LOV domains can be exploited in cellular super-resolution microscopy (nanoscopy),<sup>157–159</sup> while formation of the thioadduct in LOV domains underlies conventional optogenetic applications. In addition, FbFPs can function as genetically-encoded photosensitizers for  $^1\text{O}_2$ , with a range of further applications.<sup>354,355</sup> Blue and purple arrows indicate excitation with blue or violet light, respectively.

Table 1

Photophysical parameters of FbFPs

Protein <sup>a</sup>	$\Phi_F$	Brightness/ $M^{-1} \text{ cm}^{-1}$	Abs <sub>max</sub> /nm	Fluo <sub>max</sub> /nm
<i>Bs</i> FbFP <sup>357,359</sup>	0.39	5,420	449	495
<i>Ec</i> FbFP <sup>357,359,366</sup>	0.39; 0.44; 0.34	6,380; 4,250	448	496
<i>Pp</i> 2FbFP <sup>357,359,366</sup>	0.17; 0.22	2,125; 3,120	449	495
<i>Pp</i> 2FbFP-F37S <sup>b,451</sup>	0.30	4,260 <sup>c</sup>	450	497
<i>Pp</i> 2FbFP-F37T <sup>451</sup>	0.24	3,400 <sup>c</sup>	450	498
<i>Pp</i> 2FbFP-Q116V <sup>357</sup>	0.26	3,930	439	485
<i>Pp</i> 2FbFP-Y112L <sup>357</sup>	0.30	4,200	449	496
<i>Pp</i> 2FbFP-L30M	0.25 <sup>403</sup>	3,550 <sup>c</sup>	448	494
<i>Pp</i> 1FbFP <sup>357</sup>	0.27	3,750	450	496
<i>Ds</i> FbFP <sup>357</sup>	0.35	5,000	449	498
iLOV <sup>128,362,366</sup>	0.32; 0.33; 0.34	4,880; 4,250	447	493
iLOV-Q489K <sup>128</sup>	0.35	5,630	440	489
miniSOG <sup>357,391</sup>	0.41; 0.37	5,820	447	497
phiLOV2.1 <sup>365</sup>	0.20	2,500	450	496
<i>Mt</i> FbFP <sup>360</sup>	0.22	3,340	448	498
<i>Te</i> FbFP <sup>360</sup>	0.13	1,850	445	494
YNP1FbFP <sup>360</sup>	0.31	4,120	446	496
YNP2FbFP <sup>360</sup>	0.33	4,690	449	497
YNP3FbFP <sup>360</sup>	0.20	2,840	449	498
YNP3FbFP-Y116F <sup>360</sup>	0.26	3,590	449	498
YNP4FbFP <sup>360</sup>	0.33	4,720	446	496
VfLOV <sup>361</sup>	0.23	2,875	450	498
CrLOV <sup>361</sup>	0.51	6,375	450	498
rsLOV1 <sup>379</sup>	0.17	1,850	450	498
rsLOV2 <sup>379</sup>	0.31	3,530	450	498
phiSOG <sup>408</sup>	0.36	4800 <sup>d</sup>	449	498
phiSOG-Q103V <sup>408</sup>	0.35	4670 <sup>d</sup>	444	497

<sup>a</sup>: Organism labels: *Bs* = *Bacillus subtilis*; *Ec* = *Escherichia coli*; *Pp* = *Pseudomonas putida*; *Ds* = *Dinoreoseobacter shibae*; *Mt* = *Meiothermus ruber*; *Te* = *Thermosynechococcus elongatus*; YNP = metagenomic sequences; *Vf* = *Vaucheria frigida*; *Cr* = *Chlamydomonas reinhardtii*

<sup>b</sup>: phenylalanine in this position is conserved in the LOV series.<sup>90</sup> This residue, localized on helix Ca, is in hydrophobic contact with the chromophore.<sup>77,452</sup>

<sup>c</sup>: calculated using the absorption coefficient of *Pp*2FbFP,  $\epsilon_{450} = 14,200 \text{ M}^{-1} \text{ cm}^{-1}$ , reference<sup>357</sup>

<sup>d</sup>: calculated using and absorption coefficient  $\epsilon_{450} = 13,350 \text{ M}^{-1} \text{ cm}^{-1}$ , i.e. average between miniSOG and phiLOV2.1.<sup>357,365,391</sup>